Manuscript Details

Manuscript number	PALAEO_2018_498_R1
Title	Speleothem U/Th age constraints for the Last Glacial conditions in the Apuan Alps, northwestern Italy.
Article type	Research Paper

Abstract

During the Quaternary several glaciations occurred in the mountain regions around the Mediterranean and, in recent years, new ages have better constrained their timing. However, this is not the case for the Apuan Alps, a high-rainfall mountain chain adjacent to the Mediterranean Sea. Here, in spite of the widespread evidence for glaciers, the complete lack of geochronological information hinders our understanding of glaciation history. In this paper, we utilize speleothem ages to better constrain the timing of these glacial features. We re-examine 293 uranium-thorium ages from 19 speleothems collected in five caves at different elevations. After a period of very low growth between 160 and 132 ka, the analysed speleothems grew almost continuously to ~75 ka, this period was followed by intermittent growth with lower deposition rate and presence of hiatuses until ~12.5 /12 ka. This is consistent with an ice coverage persisting over the Apuan Alps, inhibiting or interrupting the growth of speleothems via the limited availability of groundwater and the scarcity/absence of soils. This interval is much greater than the time interval that has previously been attributed to the existence of glaciers on the Apuan Alps, which has been assumed to be restricted to Marine Isotope Stage (MIS) 2. Instead, ice cover probably also appeared in the Apuan Alps during MIS 4. The phase of restarting of growth, which may implies the definitive or substantial glacier melts seem to predate the Holocene.

Keywords	Glacier; Pleniglacial; MIS2; MIS3; MIS4; Italy
Manuscript region of origin	Europe

Corresponding Author	Ilaria Isola
Corresponding Author's Institution	Istituto Nazionale di Geofisica e Vulcanologia
Order of Authors	Ilaria Isola, Adriano Ribolini, Giovanni Zanchetta, Monica Bini, Eleonora Regattieri, Russ Drysdale, John Hellstrom, Petra Bajo, Paolo Montagna, Edwige Pons-Branchu
Suggested reviewers	Carlo Giraudi, Philip. Hughes, Ana Moreno, palacios david, Andrea Zerboni

Submission Files Included in this PDF

File Name [File Type]

cover_let.docx [Cover Letter]

Response to reviewers.docx [Response to Reviewers]

Isola_et_al_2018_changes_marked.docx [Revised Manuscript with Changes Marked]

Highlights_.docx [Highlights]

Isola_et_al_2018_revised.docx [Manuscript File]

Figure1.jpg [Figure]

Figure2.jpg [Figure]

Figure3.jpg [Figure]

Figure4.jpg [Figure]

Figure5.jpg [Figure]

Table_S1.docx [Table]

Table_S2.docx [Table]

To view all the submission files, including those not included in the PDF, click on the manuscript title on your EVISE Homepage, then click 'Download zip file'.

Dear Editor,

We would like to submit to Palaeogeography, Palaeoclimatology, Palaeoecology the research manuscript titled: "**Speleothem U/Th age constraints for the Last Glacial conditions in the Apuan Alps, northwestern Italy.**"

by Isola I., Ribolini A., Zanchetta G., Bini M., Regattieri E., Drysdale R.N., Hellstrom J.C., Bajo P., Montagna P., Edwige Pons-Branchu

The Apuan Alps, are a high-rainfall mountain chain in northwestern Italy, adjacent to the Mediterranean Sea. Until now, in spite of the widespread evidence of glaciation, the complete lack of geochronological information hinders our understanding of glaciations history and their significance in the framework of the Quaternary cold periods in the Mediterranean area.
We re-examine 293 uranium-thorium ages from 19 speleothems collected in five caves at different elevations in the Apuan Alps, and we use periods of very low or absent speleothems growth as proxy for a chronologic constraint of glaciers presence. According to this timing we can state that unfavorable conditions for speleothems deposition (low temperature) persisted on the Apuan Alps, not only during the MIS 2, but also during the MIS 4. This is consistent with evidence from the Alps and other mountain areas around the world, of a major phase of glaciation during MIS 4.

Hoping this will be of interest for the journal

Sincerely

Ilaria Isola

Comments from the editors and reviewers:
-Reviewer 1

- This is an outstanding contribution that presents important new findings on the nature of glaciations during the last two cold stages (Middle and Late Pleistocene). The paper utilises existing and new U-series data from speleothems in the Apuan Alps in Italy. The findings are very significant because the authors have identified hiatuses corresponding to periods of ice growth/ice cover in both the last two glacial cycles. I have a few minor points to make below which should help strength the paper even further.

Specific Comments
- Introduction. You should cite the recent paper by Baroni et al. 2018 which reports cosmogenic exposure ages from glacial sites very near your area.
Baroni et al. 2018. Last glacial maximum glaciers in the Northern Apennines reflect primarily the influence of southerly storm-tracks in the western Mediterranean. Quaternary Science Reviews, Volume 197, 1 October 2018, Pages 352-367.

Right. We included the citation

- Line 122. Please provide a brief definition of the LGM. This is defined as the interval 26.5-20/19 ka (Clark et al. 2009) or 27.5-23.3 ka (Hughes and Gibbard 2015), both definitions within MIS 2. The latter reference is in the reference list but it is not cited in the text.

Clark, P.U., Dyke, A.S., Shakun, J.D., Carlson, A.E., Clark, J., Wohlfarth, B., Mitrovica, J.X., Hostetler, S.W., McCabe, A.M., 2009. The Last Glacial Maximum. Science 325, 710-714.
Hughes, P.D., Gibbard, P.L. 2015. A stratigraphical basis for the Last Glacial Maximum (LGM). *Quaternary International* 383, 174-185.

We added the suggested definitions and the references

- Lines 127-129. You note “The presence of these older, cemented deposits, attributed to “Riss glaciation” (i.e. penultimate glaciation), has long been debated but no conclusive results have been forthcoming due to the absence of chronological constraints (Federici, 2005)”. In this section it might be worth citing the work elsewhere in the Apennines that has shown similar types of older cemented moraines have been dated conclusively using U-series to the Riss by Kotarba et al. (2001).
Kotarba, A., Hercman, H., Dramis, F., 2001. On the age of Campo Imperatore glaciations, Gran Sasso massif, central Italy. Geografia Fisica e Dinamica Quaternaria 24, 65-69.

Yes. We added this part

- Line 292. (Hughes et al., 2015). This is not cited in the reference list. Do you mean Hughes and Gibbard 2015, which is in the reference list?

Yes. We changed accordingly

- Section 5, Results. In the abstract you state that there was “very low growth between 160 and 135 ka”. But in the results it is not as clear-cut as this. I wondered why you chose the age of 135 ka in the abstract?

It is a misprint. We changed accordingly to the main text

- On this note it is interesting to compare your findings with the lake core evidence from Ioannina where Wilson et al. 2015 found that lake levels started to rise at 132-131 ka, which is c. 3 ka before the start of the interglacial recorded in pollen records. This accords with your timing of the deglaciation of the Apuan Alps indicated in the speleothem records, especially with “speleothem growth at Corchia, after a period of low values, becomes significant between ca.132 and 80 ka”.

Wilson, G.P., et al. 2015**.** Reconciling diverse lacustrine and terrestrial system response to penultimate deglacial warming in Southern Europe. *Geology* 43, 819-822.

Right. We added this part

- The fact that speleothems appear to start growing again after c. 13 ka is significant. What does this mean for our understanding of climate during the Younger Dryas in Mediterranean? I presume it means that your caves were not ice covered at that time. But again, I presume that this does not preclude there being small glaciers present in the highest cirques during the Younger Dryas?

Yes. It is possible that little glaciers persisted in the higher and more favorable positions, but unfortunately we aren’t able to demonstrate this

- Lines 377-379. You note that your hiatuses in speleothem growth are “consistent with evidence of a phase of glaciation during MIS 4 from the Alps and other peri-Mediterranean mountain ranges”. There is now more evidence with ages of 30-40 ka from moraines in southern Greece (Pope et al. 2017) and indeed from Turkey (Sarıkaya et al. 2014) and mean moraines ages of ~50 ka from the High Atlas, Morocco (Hughes et al. 2018). This might need some minor alterations to Figure 5c. It all supports the findings that you present, so this is clearly a good thing for your paper and makes your findings very convincing that your signal of ice growth is relevant right across the Mediterranean mountains.

Hughes, P.D., Fink, D., Rodés, Á., Fenton, C.R., 2018. ^{10}Be and ^{36}Cl exposure ages and palaeoclimatic significance of glaciations in the High Atlas, Morocco. *Quaternary Science Reviews* 180, 193-213.
Pope, R.J., Hughes, P.D., Skourtsos, E., 2017. Glacial history of Mt Chelmos, Peloponnesus, Greece. In: Hughes, P.D., Woodward, J.C. (Eds.) Quaternary glaciation in the Mediterranean Mountains. Geological Society of London Special Publications 433, 211-236. https://doi.org/10.1144/SP433.11
Sarıkaya et al. 2014. An early advance of glaciers on Mount Akdağ, SW Turkey, before the global Last Glacial Maximum; insights from cosmogenic nuclides and
glacier modelling. Quaternary Science Reviews 88, 96-109.

Right. We added all the suggested data in figure 5

-**Reviewer 2**

-
The manuscript by Isola et al. explores an innovative approach to establish the existence and extent of glaciers in the northern Apennines (Apuane Alps) during the Upper Pleistocene. Authors consider a large dataset of U/Th dating on speleothems and correlate the phase of interruption of speleothems growth with phases of glacier expansion or, at least, of diffuse permafrost occurrence. The same data well fit also with inferred surface temperatures. I think the paper is robust and deserves to be published in Palaeo3, but it requires some minor to moderate changes before it can be accepted.

General comments:
- In the introduction you discuss the importance of humidity as a trigger of speleothem growth and you cite present-day desert environments. I think that in the case of desert environments you may cite also the case of spring tufa, which occurrence significantly correlates with wet phases.

We added a sentence about tufa and associated references

- The presentation of the procedure followed to obtain MAAT is in the discussion session; I suggest to move this part in the Methods section.

We moved this part in the Method section as suggested

- The correlation between speleothems growth and occurrence of glaciers is convincing and well supported by data, but I would like to explore an alternative explanation for the lack of speleothems at least during MIS 3 and MIS4. I agree that during MIS2 glaciers were present on the Apuan Alps, as confirmed by many geomorphological observations, but their existence during the MIS3–4 periods is less supported by geomorphological data. As you propose, the absence of speleothem is related to a decrease in soil metabolism and a general lack of water. These two preconditions required by speleothems formation are limited in the case of (i) topographic surfaces covered by ice, (ii) soils freezing (permafrost), and (iii) increased environmental aridity. You did not consider the latter factor, but aridity is well attested in North Italy (namely in the Po Plain) during MIS3–4 and before MIS2. Aridity is suggested by extensive loess accumulation. I think that aridity affected also central Italy, and the Apuan Alps may have suffered a phase of cooling as well as aridification. I strongly suggest discussing this possibility in the Discussion session and possibly adding the age of loess formation (proxy for aridity) in Figure 2 or Figure 5. More in general I suggest that speleothem inhibition occurred in both glacial and periglacial conditions.
- Lines 288–298: the discussion on what happened in the Lateglacial is very interesting, as this period is poorly understood. Also in this case, I would suggest considering the possibility that environmental aridity, and not necessarily glacial expansion, tuned speleothems growth. In fact, a number of records indicate the formation of Lateglacial loess along the valleys of the Alps and the Apennines, also not far from the Apuan Alps. The age of these loess sequences seems to correlate with the phases of reduced speleothems growth.

Generally speaking we agree that an increased environmental aridity can inhibit the speleothems growth, but the Apuan Alps has a geographic position so favorable for rainfall, that only a really very strong aridity can produce the affect recorded by the described speleothems. We introduced a new part about this in the Discussion section.

Minor changes:
- line 57: ‘soil development’ I would say ‘soil formation’
Yes. We changed accordingly

- Figure 1: can you add the main circulation systems to the inset?

We added arrows showing the main winds direction

- Figure 2: add indications of all MIS, not only MIS1/Holocene.

We added an upper bar with all the indications

- Lines 278–283: do you relate this to a proper phase of fluvial activity of to a general phase of slope instability?

As it is explained in the txt we think that this phase is related to snow\ice melting and the great availability of debris due to weathering process

- lines 412–415: can you find any correlations with the Alps?

We added information about the Alps in the Discussion section

Speleothem U/Th age constraints for the Last Glacial conditions in the Apuan Alps, northwestern Italy.

Isola I.[1], Ribolini A.[2], Zanchetta G.[1,2], Bini M.[1,2], Regattieri E.[2,3], Drysdale R.N.[4,5], Hellstrom J.C.[6] , Bajo P.[6], Montagna P.[7], Edwige Pons-Branchu[8]

[1]Istituto Nazionale di Geofisica e Vulcanologia, Pisa Italy

[2]Dipartimento di Scienze della Terra, University of Pisa

[3]Istituto di Geoscienze e Georisorse-CNR, Pisa

[4]School of Geography, University of Melbourne, Victoria 3010, Australia

[5]Environnements, Dynamiques et Territoires de la Montagne, UMR CNRS, Universite´ de Savoie-Mont Blanc, France

[6]School of Earth Sciences, University of Melbourne, Victoria 3010, Australia

[7]Istituto di Scienze Marine (ISMAR-CNR), Bologna, Italy

[8]Laboratoire des Sciences du Climat et de l'Environnemen, LSCE/IPSL, CEA-CNRS-UVSQ, Université Paris-Saclay, Gif-sur-Yvette, France

Corresponding author: Ilaria Isola Ilaria.isola@ingv.it

Istituto Nazionale di Geofisica e Vulcanologia,via delle Faggiola 32, 56126 Pisa Italy

Abstract

During the Quaternary several glaciations occurred in the mountain regions around the Mediterranean and, in recent years, new ages have better constrained their timing. However, this is not the case for the Apuan Alps, a high-rainfall mountain chain adjacent to the Mediterranean Sea. Here, in spite of the widespread evidence for glaciers, the complete lack of geochronological

information hinders our understanding of glaciation history. In this paper, we utilize speleothem ages to better constrain the timing of these glacial features. We re-examine 293 uranium-thorium ages from 19 speleothems collected in five caves at different elevations. After a period of very low growth between 160 and ~~135~~ 132 ka, the analysed speleothems grew almost continuously to ~75 ka, this period was followed by intermittent growth with lower deposition rate and presence of hiatuses until ~12.5 /12 ka. This is consistent with an ice coverage persisting over the Apuan Alps, inhibiting or interrupting the growth of speleothems via the limited availability of groundwater and the scarcity/absence of soils. This interval is much greater than the time interval that has previously been attributed to the existence of glaciers on the Apuan Alps, which has been assumed to be restricted to Marine Isotope Stage (MIS) 2. Instead, ice cover probably also appeared in the Apuan Alps during MIS 4. The phase of restarting of growth, which may implies the definitive or substantial glacier melts seem to predate the Holocene.

Keywords: Glacier; Pleniglacial; MIS2; MIS3; MIS4; Italy

1. Introduction

Speleothems (i.e. cave carbonate deposits) are multi-proxy paleoclimate archives, which can be accurately dated back to several hundred thousand years before present thanks to U-Th isotope systematic (Edwards et al. 1987; Hellstrom, 2006). Most of the paleoclimate research conducted using speleothems focused on the interpretation of stable isotope and trace element proxy records (e.g. Dykoski et al., 2005; Bar-Matthews et al., 1996; Wang et al., 2008; Regattieri et al., 2016). However, speleothems need certain conditions to grow continuously, such as the presence of liquid water, CO_2 and high Ca concentrations in drip waters (e.g. Atkinson et al., 1986; Gascoyne 1992; Genty et al., 2001). This generally implies relatively wet climate conditions, surface temperature above 0 °C and a well-developed soil above the cave (Gordon et al., 1989; Genty et al., 2001,2005). For instance, in desert environments, phases of speleothem growth are important indicators of past

humid periods (Burns et al., 2001; Fleitmann et al., 2011; Vaks et al., 2006, 2007, 2010), as well as tufa, which occurrence significantly correlates with wetter phases (Smith et al., 2004; Cremaschi et al., 2015a). Similarly, the growth of speleothems in permafrost or glacier-dominated environments, often marks interruptions of cold conditions (i.e. Berstad et al., 2002; Spötl and Mangini, 2006; Pons-Branchu et al., 2010; Vaks et al., 2013). This is potentially consistent with degradation of permafrost and the formation of large ice-free surfaces, favoring water infiltration and soil ~~development~~ formation (Varks et al., 2013). Growth hiatuses within a single or multiple speleothems have been interpreted as evidences of particularly dry and/or cold conditions (e.g. Hodges et al., 2008; Genty et al., 2003, Baldini, 2002; Moreno et al., 2010; Mayer et al. 2012, Stoll et al., 2013), even if the nature and duration of hiatuses in speleothems cannot be unambiguously correlated to climatic conditions. However, stacking multiple speleothem records can give more robust information about the relationship between growth cessations and climate (e.g. Stoll et al., 2013).

During glacial periods, depressed external air temperatures at high latitudes and/or high altitudes sites may cause extensive freezing at the surface above a cave, strongly limiting water infiltration (Berstad et al., 2002; Genty et al., 2003,2005; Ayalon et al., 2013) and totally inhibiting soil activity (McDermott, 2004). This implies a strong reduction in the CO_2 transfer to the epikarst, a prerequisite for bedrock dissolution and speleothem growth. Therefore, development of glacial conditions (i.e. the presence of glaciers) in the water-infiltering area over a cave (catchment area from here onwards) would be a factor for reduced or ceased speleothem growth. In such conditions, the only possibility for the deposition of calcite can be related to sulphide oxidation if liquid water is present (Atkinson 1983; Gascoyne and Nelson, 1983; Spötl and Mangini, 2007).

In the Mediterranean region there are numerous mountains where geomorphological and geological evidence for the presence of glaciers has been dated (Baroni et al., 2018; Finsinger and Ribolini 2001; Perez-Alberti et al., 2004; Federici et al., 2008; 2012; 2017; Kuhlemann et al., 2008; Hughes et al., 2004, 2011, 2013; Giraudi et al., 2011 Giraudi and Giaccio, 2017; Ribolini al., 2011,

2018; Serrano et al. 2012; Hughes and Woodward, 2017 and references therein, Gromig et al., 2018; Hannah et al., 2017; Akçar et al., 2017; Çiner et al., 2017; Sarikaya and Çiner, 2017). However, for some regions, it is still challenging to identify the glacial cycles to which this evidence belongs. This is particularly true for the Apuan Alps, a mid-latitude (44°N) mountain chain in northwestern Italy where, despite the recognition of numerous glacial features, no precise chronological data exist so far.

In this paper, we use periods of speleothem deposition as an indicator of ice-free conditions in cave catchment areas, and periods of very low or absent stalagmite growth as proxy for constraining the chronology of glacier presence in the Apuan Alps. To achieve this, we use previously published and new U/Th ages of speleothems from five different caves located at different altitudes (Fig. 1).

2. Site description

The Apuan Alps is a NW-SE-oriented mountain range rising abruptly to about 2000 m a.s.l. from the narrow coastal plain bordered by the Ligurian Sea (Fig. 1). The atmospheric circulation is dominated by the important cyclogenesis centre of the Gulf of Genoa (Trigo et al., 2002) and by the humid westerly air masses of North Atlantic provenance (e.g. Reale and Lionello, 20132014; Fig. 1). These sources of moisture impact on the Apuan Alps mountain chain, which acts as a natural barrier by forcing an adiabatic rise of air masses, resulting in high precipitation (> 2,500 mm/yr Rapetti and Vittorini, 1994; Piccini et al., 2008). As with most of the Apennine chain, winter rainfall amount, which is the main period of recharge of Apuan caves (Piccini et al., 2008), is strongly regulated by the North Atlantic Oscillation (NAO), with a negative correlations observed between NAO index and winter precipitation (López-Moreno et al., 2011).

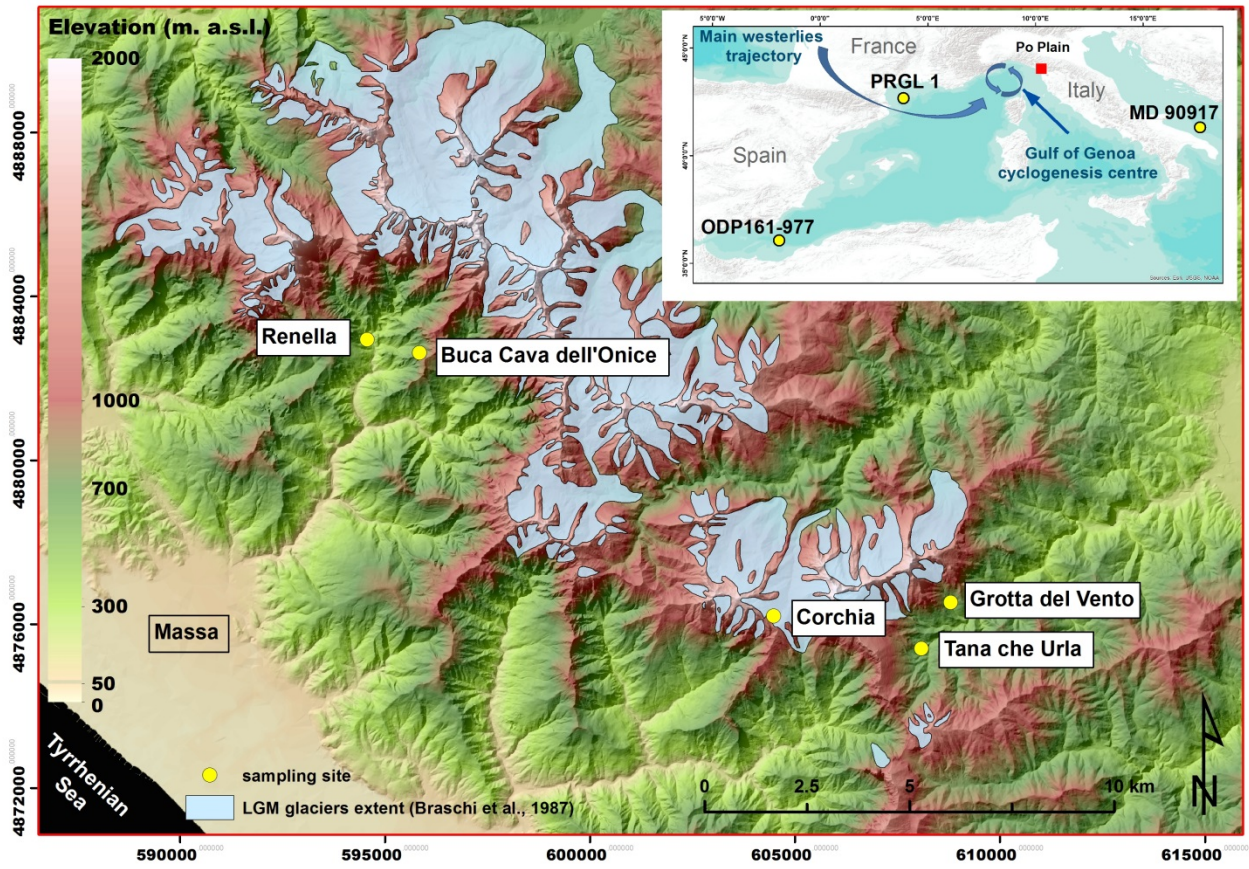

Fig. 1. Glacier extent (light blue) during the LGM according to the reconstruction of Braschi et al. (2001). Sampled sites are shown in yellow.

Two main tectono-metamorphic regional events have determined the structural setting of the Apuan Alps (e.g. Carmignani and Kligfield, 1990; Molli and Vaselli, 2006), where extensive areas of carbonate lithologies outcrop (Mesozoic marbles and metadolostones). The actions of glacial, fluvial and karst processes led to an Alpine-like landscape, where exokarst landforms and Quaternary cave systems are particularly developed (Piccini, 1998, 2003, 2011).

The Apuan Alps is one of the first places amongst the larger Apennine chain where glacial landforms have been described (Cocchi, 1872; Stopani, 1872). Following these pioneering studies, in the second half of nineteenth and throughout the twentieth century, further qualitative evidence of glacial landforms were reported (De Stefani, 1874,1875,1890; Merciai, 1912; Paci, 1935; Zaccagna, 1937; Tongiorgi and Trevisan, 1940; Beneo, 1945; Masini, 1970; Federici, 1981; 2005; Braschi al., 1987; Putzolu, 1995, Baroni et al. 2013; 2015). Most of these glacial features are now

under risk of destruction due to marble quarrying (Bini, 2005). Despite only traces of small glaciers have been reported on the seaward side of the mountain chain (i.e. erosional landforms and a few scattered glacial deposits, Federici, 1981), features associated with at least nine glaciers have been identified on the northern side. These include lateral and terminal moraines, cirques and polished surfaces. Different phases of expansion have been described and, in some cases, the glacier termini reached exceptionally low elevations (~600 a.s.l.) considering the latitude (Braschi et al., 1987; Jaurand, 1998). The best-preserved glacial features, with relatively unweathered, incoherent detrital materials, are traditionally attributed to the Last Glacial Maximum (LGM) by all previous authors on the basis of their fresh appearance and by analogy with the Apennines and Alpine landforms. The temporal definition of LGM itself is not univocal, depending on the considered references, e.g. Clark at al. (2009) defined the LGM as the duration of sea-level lowstand during the interval 26.5-20/19 ka, while Hughes and Gibbard (2015) as the event between the top (end) of Greenland Interstadial 3 and the base (onset) of Greenland Interstadial 2, spanning the interval 27.540-23.340 ka (Greenland Stadial 3). In both cases within MIS2.

Inner terminal moraines have been interpreted as the Late-Glacial readvance/stillstand phases (Braschi et al., 1987; Federici, 2005). Cemented glacial deposits, rarely outcropping, have been attributed to a pre-LGM glacial event according to their appearance, altitude and stratigraphic position (Braschi et al. 1987). The presence of these older, cemented deposits, attributed to “Riss glaciation” (i.e. penultimate glaciation), has long been debated but no conclusive results have been forthcoming due to the absence of chronological constraints (Federici, 2005), moreover, Kotarba et al. (2001) have dated in the Apennines, similar types of older cemented moraines to the Riss, using U-series.

3. Cave descriptions

143 In the Apuan Alps karst massif, about 2000 cave entrances are now mapped with a composite
144 length of cave development of ~500 km (http://www.speleotoscana.it). About 80 caves are carved
145 below the areas potentially covered by glaciers during the Last Glacial expansion, as reconstructed
146 by Braschi et al. (1987). Despite most of the Apuan caves are mainly vertical with active drainage
147 systems, many kilometres of passages are relict and nowadays host carbonate (usually calcite)
148 concretions. Here we focus on speleothems from five caves located at different elevations (Fig. 1).
149 The largest and highest cave is Antro del Corchia (CC), a large complex cave system (~60 km
150 long ~1200 m deep) mainly developed in the Upper Triassic-Liassic marble, dolomitic marble and
151 metadolostone of the Mt Corchia syncline confined by the non-karstifiable, low-permeable rocks of
152 the Paleozoic basement (Piccini et al., 2008).
153 Tana che Urla (TCU) is a small resurgence cave with a permanent stream (~600 m of total length
154 of which almost half is submerged; +45 m of total difference in height), developed at the contact
155 between Paleozoic schist basement and Triassic metadolostone (Regattieri et al., 2012). The
156 entrance is located at ~620 m a.s.l. on the south-eastern side of Panie Massif and functions as an
157 overflow spring during intense rainfall and snowmelt.
158 Grotta Del Vento (GDV) is an almost fossil phreatic cave (~4.5 km total length and over 450 m
159 of elevation change) developed at the contact between the Paleozoic schist basement and Triassic
160 metadolostone. The entrance is located at ~630 m a.s.l. on the south-eastern side of the Panie Massif
161 (Piccini et al., 2003).
162 Buca della Renella (RL) is a small, shallow cave at the confluence of Canale Regolo and the
163 Frigido River (Drysdale et al. 2006; Zhornyak et al., 2011). The entrance is located at ~275 m a.s.l.,
164 only a few metres above the stream confluence. The cave, predominantly horizontal (~200 m
165 length), is carved in Triassic metadolostone close to the contact with the Paleozoic phyllite.
166 Buca Cava dell'Onice (BCO) is a fossil small cave (85 m long and 65 m deep), carved in Lower
167 Jurassic cherty metalimestone. The entrance is located in the northwest side of Mt. Castagnolo at
168 ~700 m a.s.l.

169

170 **4. Methods**

171

172 We consider 19 speleothems (ages in supplementary material, Table 1), collected from the five
173 caves described above. Nine stalagmites and two cores drilled from flowstones have been collected
174 from the "Galleria delle Stalattiti" of the Corchia Cave. This part of the cave is a near-horizontal
175 chamber carved at ~840 m a.s.l., vertically overlain by ~400 m of rock. The chamber lies hundreds
176 of metres above the present groundwater table and is characterised by a mean annual air
177 temperature of 7.8 °C (Piccini et al., 2008). Five speleothems have already been described in
178 previous papers (CC1, CC5, CC7, CC26, CC27 and CC28, Drysdale et al., 2004, 2005, 2007, 2009;
179 Zanchetta et al., 2007; Bajo et al., 2017; Isola et al., 2018). We present new ages for stalagmites
180 CC4, CC7, CC22, CC27, CC53, and two flowstone cores CD4 and CD20.

181 At TCU two cores have been drilled from the same flowstone in the main gallery, about 100 m
182 from the entrance. The mean air temperature is 10.2 °C (Regattieri et al., 2014a). Speleothem
183 stratigraphy, chronology and geochemistry have been discussed by Regattieri et al. (2012, 2014a,
184 2016).

185 Two cores have been drilled from different flowstones located in the middle level of GDV
186 (Piccini et al., 2003).

187 At RL, three samples have been collected in different stratigraphic levels from a fan-like
188 flowstone deposited at the margin of an epiphreatic passage in the inner part of the cave (average air
189 temperature ca. 12 °C) and their stratigraphy and chronology have been discussed by Drysdale et al.
190 (2006) and Zhornyak et al. (2011).

191 Only one stalagmite (BCO1) has been collected in BCO, in a fossil gently dipping gallery, about
192 30 m from the entrance.

193 All ages from Corchia, Tana Che Urla and Renella have been obtained following the same
194 procedure at the University of Melbourne (Victoria, Australia). Briefly, uranium and thorium

isotopes were analysed using a Nu Instruments Multicollector Inductively Coupled Plasma–Mass Spectrometer (MC-ICP-MS), according to the analytical method and corrections (where necessary) described by Hellstrom (2003, 2006).

Age-depth models and speleothems growth rates were obtained from a Monte Carlo-derived method (described in Drysdale et al. 2005 and Scholz et al. 2012). Dating methods for Grotta del Vento are discussed by Piccini et al. (2003).

BCO1 $^{230}Th/^{234}U$ ages were determined at LSCE from 9 subsamples collected along the growth axis of the stalagmite. Subsamples were crushed in an agate pestle and aliquots of typically ~400 mg were rinsed twice with MilliQ, dissolved in diluted HCl (~10%) and equilibrated with a mixed ^{236}U-^{233}U-^{229}Th spike that was calibrated against a Harwell Uraninite solution (HU-1) assumed to be at secular equilibrium. Uranium and thorium were purified and separated using Eichrom UTEVA® and pre-filter resins in nitric media following a procedure modified from Pons-Branchu et al. (2005) and Douville et al. (2010). The isotopes of uranium and thorium were analysed by solution multi-collector ICPMS using a ThermoScientific Neptune^{Plus} hosted at the Laboratoire des Sciences du Climat et de l'Environnement (LSCE, Gif-sur-Yvette, France) following the procedure described by Pons-Branchu et al. (2014). Based on the measured atomic ratios, the $^{230}Th/^{234}U$ ages were calculated through iterative age estimation (Ludwig and Titterington, 1994) using the ^{230}Th, ^{234}U and ^{238}U decay constants of Cheng et al. (2013) and Jaffey et al. (1971). An initial $^{230}Th/^{232}Th$ activity ratio of 0.9±50% was used for correction of the non-radiogenic, detrital ^{230}Th fraction.

In order to highlight the higher and lower periods of speleothems deposition rate, we calculate the growth rate for all the considered speleothems from Corchia Cave and for speleothems from lower altitude caves, cumulated at 1000-yr intervals. Uncertainties in the growth rates were obtained using the standard errors propagation.

It is worth estimating potential changes in air temperature at the altitude of the different infiltration areas of the four caves (we ignore BCO because the sole sampled stalagmite covers only

MIS 5), in order to understand causes of any leads and lags in speleothem growth phases in the context of likely glacier development. The following calculations represent a first-order estimate that can be used to underpin the interpretations proposed below.

Speleothem growth patterns described above were compared with sea-surface temperature (SST) series from three Mediterranean cores: ODP 161-977 (Martrat et al., 2014) spanning all over the considered period; PRGL1 (Cortina et al., 2015), the nearest core to the Apuan Alps; and MD 90917 (Siani et al 2013), a high-resolution dataset covering the last ~25 kyr (cores locations are shown in Fig. 1). As these cores (ODP 161-977, PRGL1) provide SST data based on Alkenone unsaturation indices (Müller at al., 1998; Conte et al., 2006) and planktonic foraminifera assemblages (Siani et al 2013), they do not reflect exactly the same temperature signal. SST records in the Alboran Sea (ODP191-977) are more related to spring-summer conditions (Martrat et al., 2004, 2014), while the SST records from the Gulf of Lyon reflects a winter-spring temperature signal showing a colder imprint than other more southern SST records (Rigual-Hernández et al., 2013, Cortina et al., 2015). Finally, planktonic foraminifera assemblages coincide with the most productive period during the spring and the synchronous bloom of *G. bulloides* in the Mediterranean Sea (Pujol and Vergnaud-Grazzini, 1995; Siani et al., 2013). In performing the ocean-cave comparisons, we make several assumptions. First, we assume that the difference in mean annual SST (MASST) between the selected marine cores and the MASST offshore of the Apuan Alps (Locarnini et al., 2010) was constant through time; second, that the difference between the MASST and the Mean Annual Air Temperature (MAAT) measured along the coast facing the Apuan Alps (http://www.autorita.bacinoserchio.it/) was constant through time; third, we adopt an air temperature lapse rate of 0.6 °C/100 m (as calculated for the area by Rapetti and Vittorini, 2012) to estimate the MAAT in the speleothem catchment areas of four of the studied caves. For the elevations of the water recharge area feeding the caves, two values are considered: the elevation of the surface above the cave on the vertical of the sampling sites (C1, supplementary material Table 2) and the average between this point and the highest point of the drainage basin (C2,

supplementary material 2). The first is the most conservative value representing the minimum elevation of recharge area while the second is probably more realistic because takes into account the whole hydrographic basin upvalley the cave. A more refined estimate of MAAT could incorporate also the effects of sea-level lowering during glaciations and tectonic uplift (estimates to be 0.6 mm/yr; Fellin et al. 2007; Piccini 2011) of the Apuan Alps. However, both effects introduce negligible temperature variations. Indeed, the maximum increase in relative elevation of the infiltration area above the contemporary sea level is during the LGM (e.g. ca. 100-120 m for the LGM, Lambeck and Bard 2000; Lambeck et al., 2014), corresponding to a total temperature variation (ΔT) of about -0.6°C, while the lowest, during MIS6, corresponds to ΔT of about +0.1°C.

5. Results

For the 19 speleothems considered, the dataset comprises 293 U/Th ages (supplementary material Table 1). In Figure 2, the ages are plotted vs the elevation of the sampling sites.

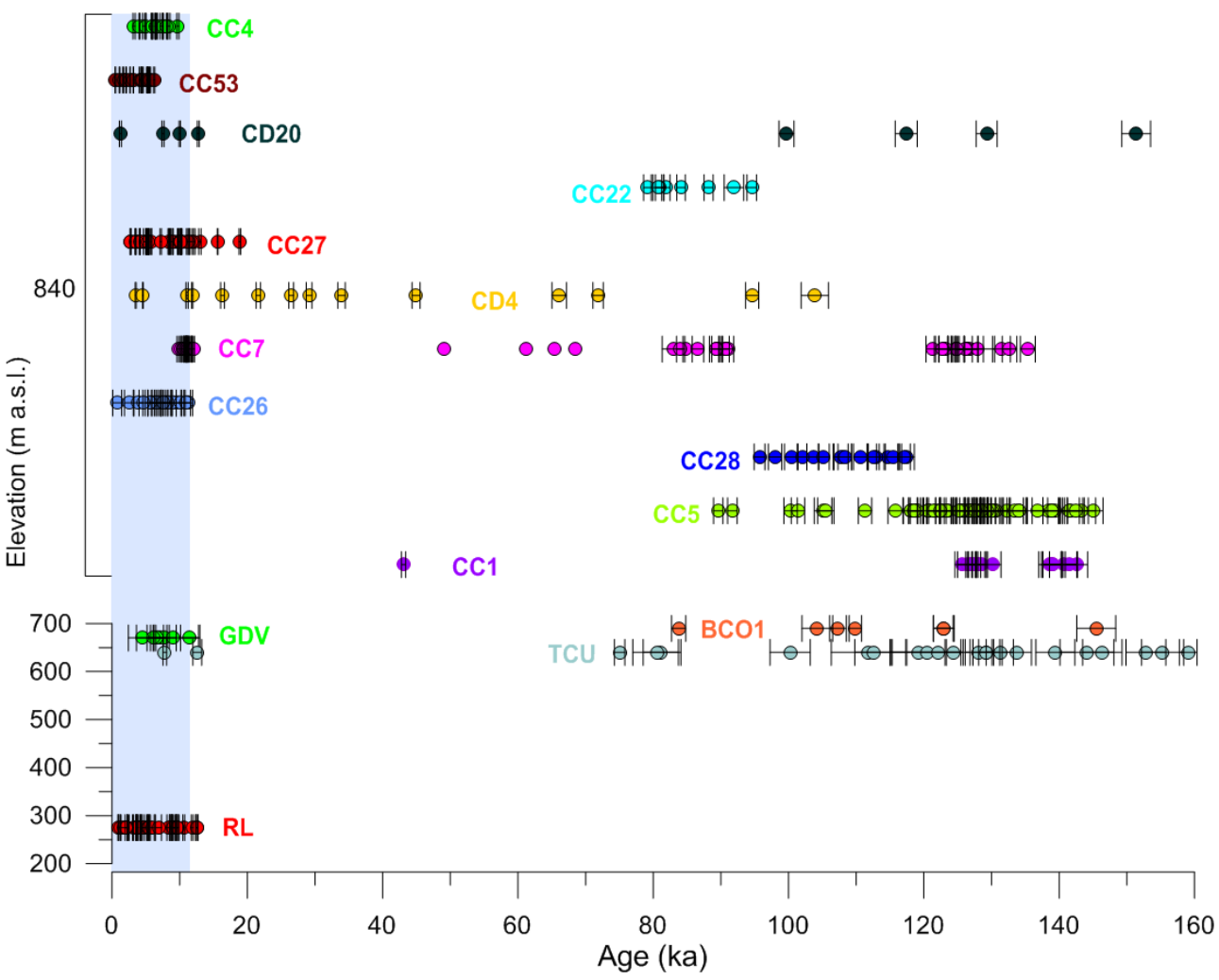
CC4
CC53
CD20
CC22
CC27
840
CD4
CC7
CC26
CC28
CC5
CC1
700
600
500
400
300
200
GDV
TCU
BCO1
RL
Elevation (m a.s.l.)
0
20
40
60
80
100
120
140
160
Age (ka)

259

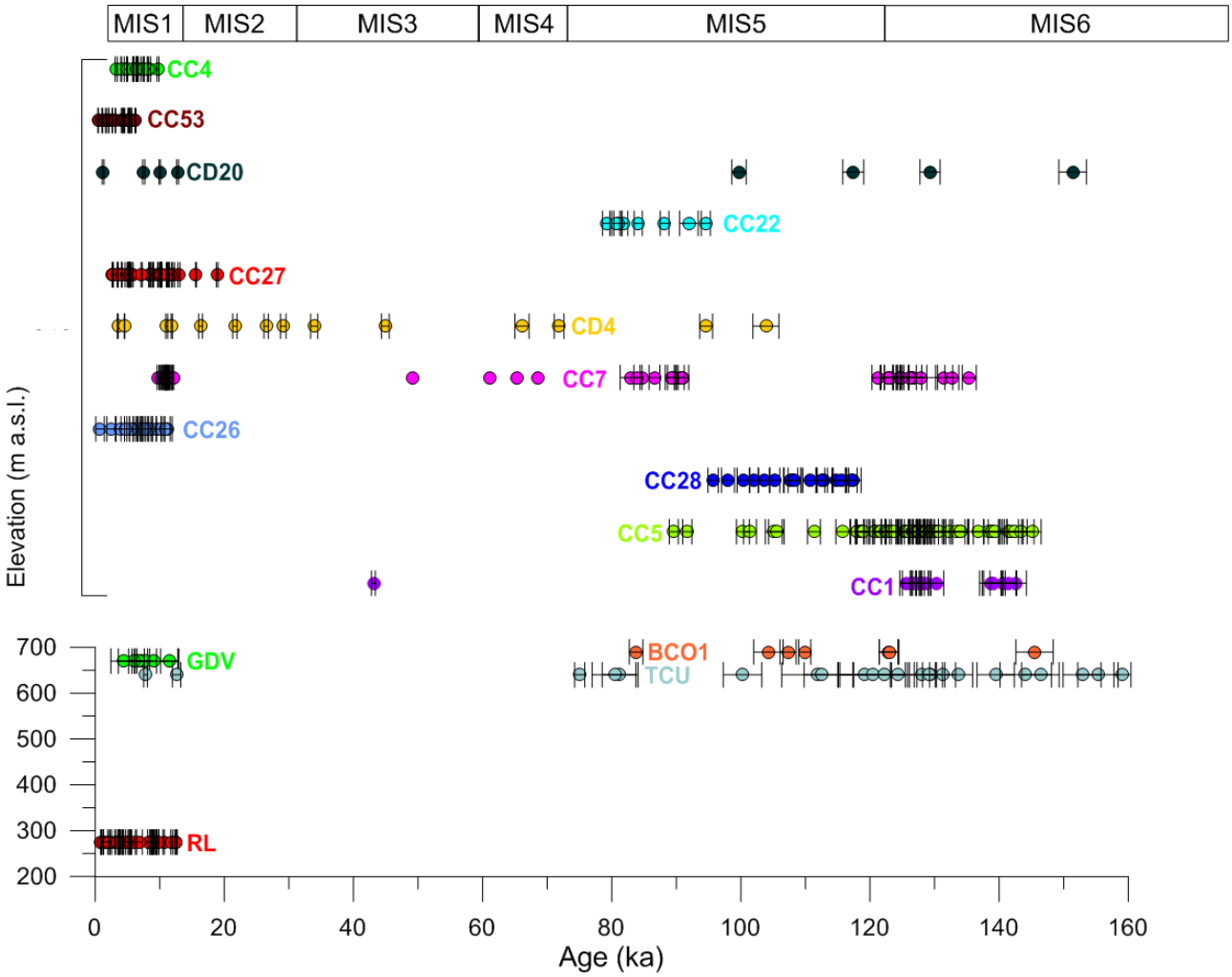

Fig. 2. 293 U/Th ages from 19 Apuan speleothems over the past 160 ka (2σ error bars) vs the elevation of sampling sites. Details on dating can be found in the original papers (Drysdale et al., 2004; 2009; Regattieri et al., 2012, 2014a, 2014b; Piccini et al, 2003; Drysdale et al., 2006; Zhornyak et al 2011, Isola et al., 2018). ~~The Holocene is shown in light blue shading.~~

Despite some differences, there are many common features. All caves show a major episodes of calcite deposition during the Holocene and the latest Late Glacial. Available samples from RL and GDV do not show phases of growth older than this period and the studied concretions cover, or are stratigraphically located over, thick fluvial deposits. TCU shows continuous deposition between ca. 160 and 121 ka (Regattieri et al., 2014a), followed by a discontinuous deposition to ca. 75 ka, after which there is a long hiatus from ca. 75 to 12.5 ka. The most relevant record is represented by

Corchia Cave, showing almost continuous calcite deposition from ca. 145 to 79 ka. A long lag of growth, with only very reduced phases of calcite deposition is evident during the Pleniglacial. The stalagmite from BCO has an intermittent growth phase throughout MIS 5, confirming a speleothems deposition phase during this period in the Apuan Alps. No information about other periods including the Holocene are available for this site until now, but we cannot exclude further growing phases, in fact, a single speleothem cannot be considered representative of the whole speleothems growth history of this cave.

More interesting than the simple ages distribution is the cumulative growth curve which takes into account the propagation of age errors for Corchia cave speleothems and for the other studied caves located at lower altitudes (Fig. 3). It is evident that speleothem growth at Corchia, after a period of low values, becomes significant between ca.132 and 80 ka (curve b in figure 3), after which it decreases abruptly until ca. 60 ka, and then almost stops for ca. 44 kyr. Continuous growth resumes at ca. 15 ka and increases later at ca. 12 ka.

The growth of speleothems belonging to the lower-altitude caves evidently decreases after 130 ka, reaching a local minimum at ca. 100 ka. An increase of composite growth rate is then observed around 80 ka, followed by an interruption in calcite deposition up to 13 ka.

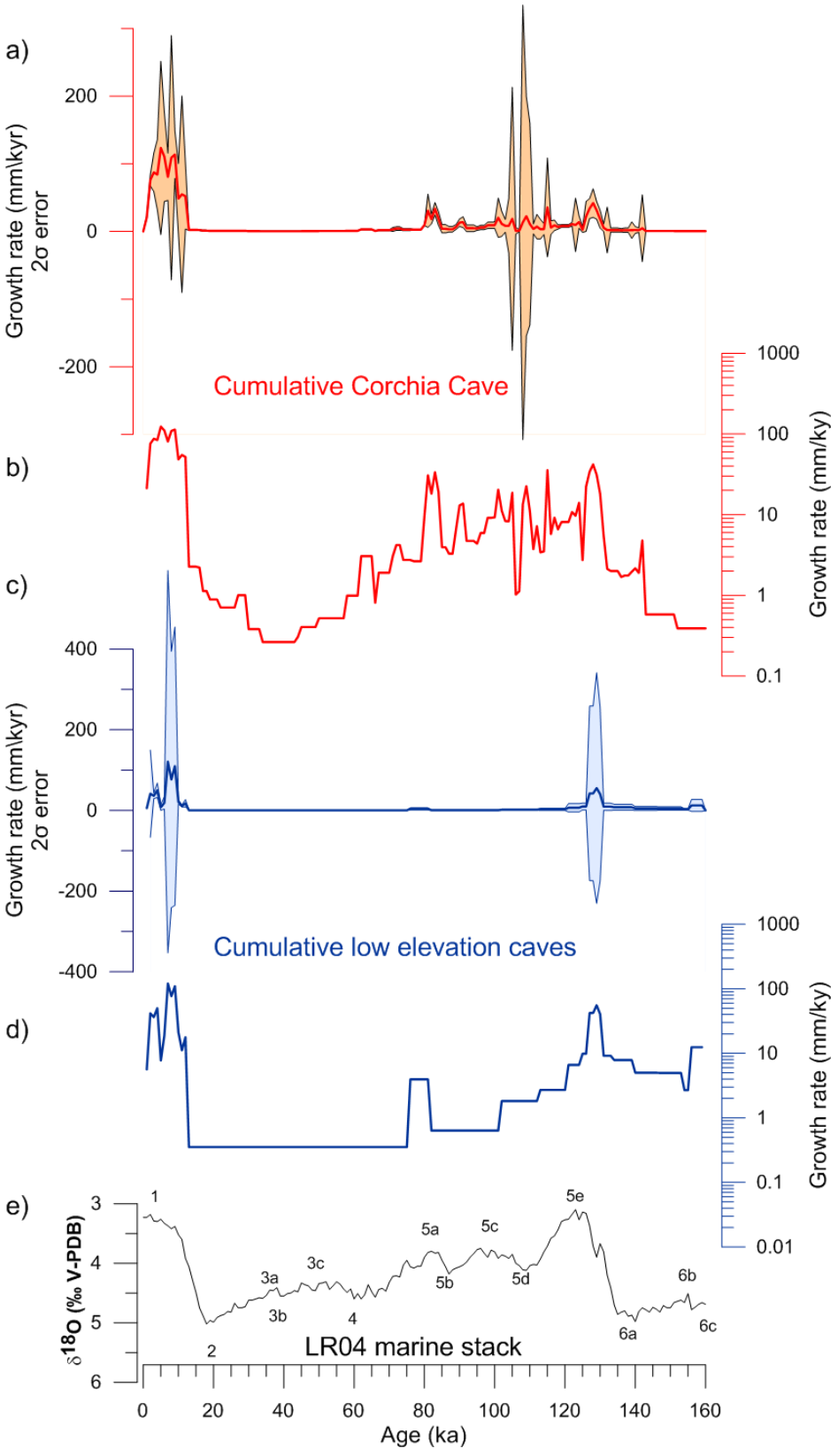

Fig. 3. Cumulative growth curves (i.e. the total speleothem growth calculated for all the considered speleothems and binned into 1000-yr intervals) for Corchia Cave speleothems (red lines a and b) and for the caves located at lower altitude (blue lines, c and d), the associated errors in shaded

strips. Note the linear (b and d) and the logarithmic (a and c) scales in the vertical axes. Shown in black (e) is the LR04 stack (Lisiecki and Raymo 2005) from benthic foraminifera $\delta^{18}O$ data. Numbers indicate Marine Isotope Substages.

Figure 4 shows the estimation of MAAT as described above. Due to the very similar geographic location (fig. 1), GDV and TCU temperature estimates are almost indistinguishable in all the reconstructions (blue and black lines in Fig. 4). The MAAT curves obtained for each cave using MD90917 data (~ 0.6 - 24 ka interval), including the two different infiltrating elevations (C1 and C2), are shown respectively in Figure 4a and b. The MAAT curves obtained using ODP 161-977 data (~ 0.06 - 120 ka interval) are shown respectively in figure 4c and d. The MAAT curves obtained using PRGL1 data (~ 29 - 120 ka interval) are shown respectively in Figure 4e and f. In the C1 cases (Fig. 4a, c, e) only the CC series displays excursions where MAAT is <0°C. In the C2 scenario (Fig. 4b, d, f), GDV and TCU areas also show periods when MAAT is <0°C. As expected, the temperature above RL is the mildest.

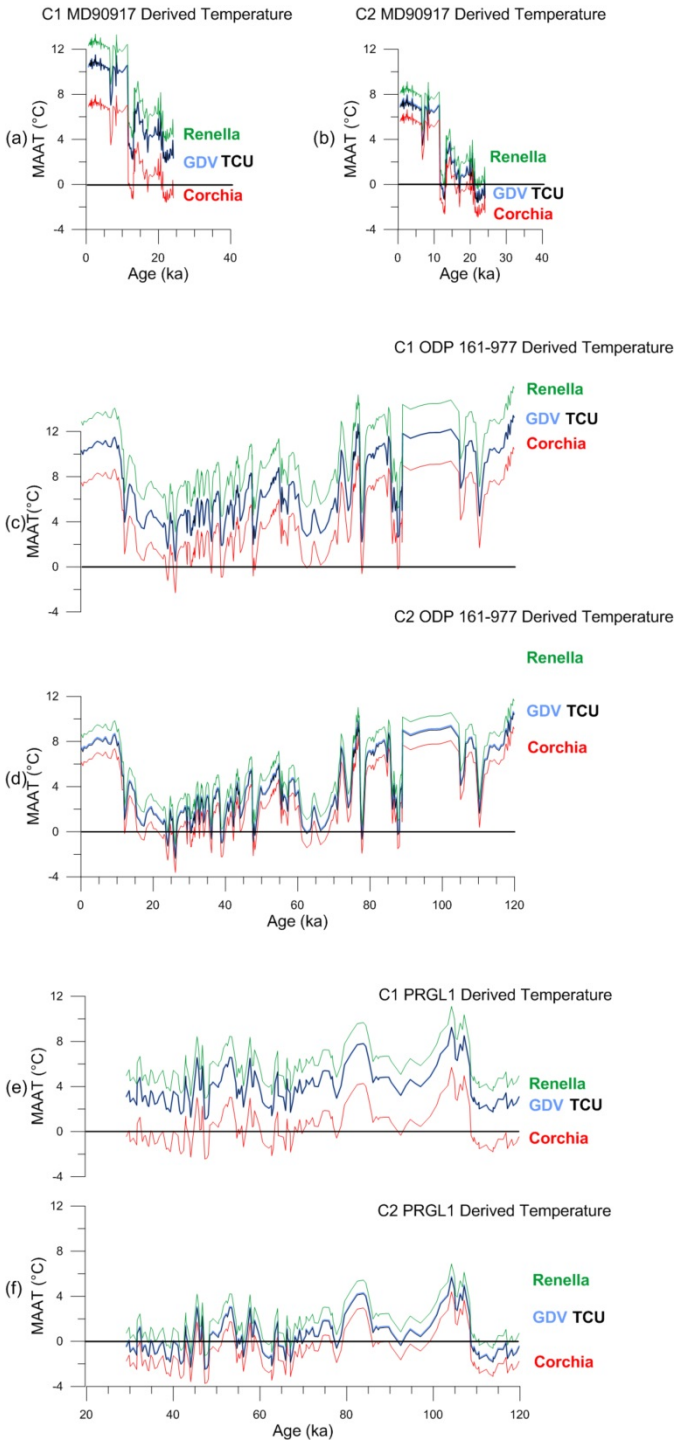

Fig. 4. MAAT curves derived for all the caves from MD90917: (a) C1 (see the text for explanation), (b) C2; from ODP 161-977, (c) C1 and (d) C2 ; and from PRGL1, (e) C1 and (f) C2. Black horizontal lines indicate the 0°C MAAT.

6. Discussion

According to the presented data, there is a long interval during the Pleniglacial where calcite deposition at CC and TCU caves slows down or is absent (fig. 3). This interval roughly corresponds to an extensive loess deposition in the Po Plain (Fig. 1 and 5; Cremaschi et al., 2015b; Zarboni et al., 2015). This marks a wide phase of aridity in northern Italy that might have involved also the Apuan Alps, but probably with different effects. Nowadays the mean annual precipitation in Po Plain does not exceed 1000 mm (www.arpalombardia.it), while the Apuan Alps are characterized by higher precipitations exceeding 2500mm/yr (Rapetti and Vittorini, 1994; Piccini et al., 2008). The different geographic position underpinning the actual rainfall regime, certainly played a role in the past too, mitigating the drought effect in the Apuan Alps. Moreover, it is very difficult to explain in a dry regime, the strong fluvial activity suggested, in the low elevation caves, by the presence of thick fluvial deposits, stratigraphically older than the phase of speleothems regrowth (about 12.5 ka). The resumption of calcite deposition is ~~instead,~~ almost coeval in all caves, with evidence of sustained growth slightly preceding the beginning of the Holocene, instead, the period of deposition decrease, at the end of MIS5, is not coeval between TCU and CC. However, the CC dataset is more extensive because the number of analyzed speleothems.

Moreover, this cave is very close to areas of the catchment occupied by glaciers in the Last Glacial (Fig.1). Specifically, the recharge basin of the "Galleria delle Stalattiti", mainly consisting of the higher slopes of the northern side of Monte Corchia, was covered by a glacier according to Braschi et al. (1987). The most obvious process responsible for the strong reduction of speleothem growth at the "Galleria delle Stalattiti" would thus be a persistent ice cover. This long interval of extremely reduced or absent calcite deposition covers most of MIS4-MIS2, a time span more extensive than the classical attribution of Apuan glacial activity to the only Last Glacial Maximum (Federici, 2005; Jaurand 1998). This hypothesis is supported by evidence of moraines formed during MIS3 and MIS4 glacier expansions in the Central Apennines (Giraudi et al. 2011; Giraudi and Giaccio, 2015, 2017). In this regard, the Corchia speleothems cumulative growth curve delimits for the first time the temporal interval of possible glacier existence over the Apuan Alps or

338 temperature lower enough to inhibit speleothem growth at higher altitudes. Although the
339 chronological constraints are indirect because they do not refer to moraine ages, there is
340 considerable robustness in the speleothem-age dataset. However, cessation of speleothem growth
341 can be related to combined effect of low air temperature, soil-CO_2 deficiency and reduction of
342 dripping. These conditions might have been present without invoking continuous ice covering of the
343 slopes, i.e. where permafrost inhibits water infiltration and following dryer cave conditions. In the
344 nearby Apennine chain, landforms diagnostic of permanently frozen ground are rare and essentially
345 limited to the southern latitudes, where higher elevations are reached (Kotarba et al., 2001; Giraudi
346 et al., 2011; Oliva et al., 2018).

347 The absence of speleothem growth in the other caves during the glacial period cannot be directly
348 related to the reconstructed ice cover (Braschi et al. 1987) because of their lower altitudes. A recent
349 geomorphology synthesis of the Apuan Alps (Baroni et al., 2015) does not report glacial deposits
350 indicative of a glacial cover of the lower caves.

351 At RL and GDV, the presence of thick fluvial deposits stratigraphically older than the phase of
352 speleothem growth (about 12.5 ka) suggests strong fluvial activity during the glacial period, which
353 would inhibit speleothem growth (Zhornyak et al., 2011). This strong activity might be related to
354 seasonal snow/ice melting and abundant availability of loose material coming from physical
355 weathering. A similar explanation is also valid for the long deposition hiatus at TCU (about 12.6-75
356 ka). A continuous glacier cover nearby is unlikely throughout this period.

357 ~~Speleothem growth, which was possible for most of MIS5, decreases or ceases during MIS4~~
358 ~~(Fig. 3)~~

359 It is noteworthy that both CC and TCU show speleothem deposition during part of MIS6,
360 suggesting that temperatures over the Apuan Alps during this period were not as low as those for
361 MIS2-4. The transition between the penultimate glacial and the last interglacial, is marked by the
362 abrupt increase of speleothems growth about 132 ka, as already described for CC by Drysdale et al.,
363 (2009) and for TCU by Regattieri et al. (2014a) and in agreement with other proxies like the more

364 umid-temperate vegetation in Southern Europe (Sanchez –Goñi et al., 1999), or the high level in
365 Ioannina Lake (Wilson et al., 2015). Then, speleothem growth, which was possible for most of
366 MIS5, decreases or ceases during the interval MIS2-4 (Fig. 3).

367 The almost coeval resumption of calcite deposition in all the investigated caves requires further
368 discussion. At CC, some U/Th ages indicate that a small growth phase also occurs at the beginning
369 of the Late Glacial, but significant growth did not occur before ca. 12 ka. However, given the
370 southern latitude and the relatively low altitude of the Apuan Alps, it is hard to argue that glaciers
371 still existed during the middle part of the Lateglacial (Hughes ~~et al~~and Gibbard, 2015). Based on
372 deglacial trends in CC speleothem carbon isotope composition, Drysdale et al. (2004) and Zanchetta
373 et al. (2007) have suggested that soil development at CC is delayed after glacial periods due to
374 intense erosive processes active at high altitudes during the first phases of climatic amelioration,
375 under conditions of increasing rainfall. After the definitive ice melting at the end of MIS2, cold but
376 ice-free conditions and delayed soil development would have retarded significant speleothem
377 growth, which did not accelerate until ca. 12 ka. The fundamental elements of this hypothesis are
378 supported by Bajo et al. (2017), who also invoked near-closed-system conditions and sulphuric-acid
379 dissolution as additional processes to carbonate-acid dissolution (from soil-sourced CO_2) to explain
380 the unusually high carbon isotope composition of CC26 stalagmite during late Late Glacial and the
381 beginning of Holocene. However, an implication of this study is that growth was unsuitable before
382 ca. 12 ka, in spite of the possibility of sulphuric-acid dissolution substituting for carbonic-acid
383 dissolution, thus suggesting that speleothem growth was inhibited by cold climate conditions. From
384 the same stalagmite, Regattieri et al. (2014b) concluded, based on the presence of an aragonite layer
385 at the base of the CC26 succession and on trace element/Ca ratios (Ba, Sr, Mg) changes, that the
386 start of growth of CC26 was related to a re-opening of a dripping point due to the replenishing of
387 the cave plumbing system previously interrupted by reduced recharge.

388 Whilst we cannot detail the point at which resumption of speleothem growth occurred in CC
389 during the Late Glacial, conditions generally favoring speleothem growth seem to have occurred

when the plumbing system was newly recharged significantly even if ice cover should have already disappeared. It is probably not obvious that these conditions did not concomitantly occur in upper and lower altitude caves. Studying the transition between MIS6 and MIS5 at TCU Regattieri et al. (2014a) suggested that the delay in soil development as inferred for CC is not supported for TCU, due to its lower altitude. This may suggest that an earlier resumption of speleothem growth would be anticipated at lower altitude compared to CC. Data collected until now agree with this hypothesis (Fig. 3). We suggest that significant resumption of calcite deposition at CC can occur only when soil development and drip recharge are restored to a certain level.

~~. It is worth estimating potential changes in air temperature at the altitude of the different infiltration areas of the four caves (we ignore BCO because the sole sampled stalagmite covers only MIS 5), in order to understand causes of any leads and lags in speleothem growth phases in the context of likely glacier development. The following calculations represent a first-order estimate that can be used to underpin the interpretations proposed below.~~

~~Speleothem growth patterns described above were compared with sea-surface temperature (SST) series from three Mediterranean cores: ODP 161-977 (Martrat et al., 2014) spanning all over the considered period; PRGL1 (Cortina et al., 2015), the nearest core to the Apuan Alps; and MD 90917 (Siani et al 2013), a high-resolution dataset covering the last ~25 kyr (cores locations are shown in Fig. 1). As these cores (ODP 161-977, PRGL1) provide SST data based on Alkenone unsaturation indices (Müller at al., 1998; Conte et al., 2006) and planktonic foraminifera assemblages (Siani et al 2013), they do not reflect exactly the same temperature signal. SST records in the Alboran Sea (ODP191-977) are more related to spring-summer conditions (Martrat et al., 2004, 2014), while the SST records from the Gulf of Lyon reflects a winter-spring temperature signal showing a colder imprint than other more southern SST records (Rigual-Hernández et al., 2013, Cortina et al., 2015). Finally, planktonic foraminifera assemblages coincide with the most productive period during the spring and the synchronous bloom of *G. bulloides* in the Mediterranean Sea (Pujol and Vergnaud-Grazzini, 1995; Siani et al., 2013). In performing the~~

ocean-cave comparisons, we make several assumptions. First, we assume that the difference in mean annual SST (MASST) between the selected marine cores and the MASST offshore of the Apuan Alps (Locarnini et al., 2010) was constant through time; second, that the difference between the MASST and the Mean Annual Air Temperature (MAAT) measured along the coast facing the Apuan Alps (http://www.autorita.bacinoserchio.it/) was constant through time; third, we adopt an air temperature lapse rate of 0.6 °C/100 m (as calculated for the area by Rapetti and Vittorini, 2012) to estimate the MAAT in the speleothem catchment areas of four of the studied caves. For the elevations of the water recharge area feeding the caves, two values are considered: the elevation of the surface above the cave on the vertical of the sampling sites (C1, supplementary material Table 2) and the average between this point and the highest point of the drainage basin (C2, supplementary material 2). The first is the most conservative value representing the minimum elevation of recharge area while the second is probably more realistic because takes into account the whole hydrographic basin upvalley the cave. A more refined estimate of MAAT could incorporate also the effects of sea-level lowering during glaciations and tectonic uplift (estimates to be 0.6 mm/yr; Fellin et al. 2007; Piccini 2011) of the Apuan Alps. However, both effects introduce negligible temperature variations. Indeed, the maximum increase in relative elevation of the infiltration area above the contemporary sea level is during the LGM (e.g. ca. 100-120 m for the LGM, Lambeck and Bard 2000; Lambeck et al., 2014), corresponding to a total temperature variation (ΔT) of about -0.6°C, while the lowest, during MIS6, corresponds to ΔT of about +0.1°C.

Figure 4 shows the estimation of MAAT as described above. Due to the very similar geographic location (fig. 1), GDV and TCU temperature estimates are almost indistinguishable in all the reconstructions (blue and black lines in Fig. 4). The MAAT curves obtained for each cave using MD90917 data (~ 0.6 - 24 ka interval), including the two different infiltrating elevations (C1 and C2), are shown respectively in Figure 4a and b. The MAAT curves obtained using ODP 161-977 data (~ 0.06 - 120 ka interval) are shown respectively in figure 4c and d. The MAAT curves obtained using PRGL1 data (~ 29 - 120 ka interval) are shown respectively in Figure 4e and f. In

the C1 cases (Fig. 4a, c, e) only the CC series displays excursions where MAAT is <0°C. In the C2 scenario (Fig. 4b, d, f), GDV and TCU areas also show periods when MAAT is <0°C. As expected, the temperature above RL is the mildest.

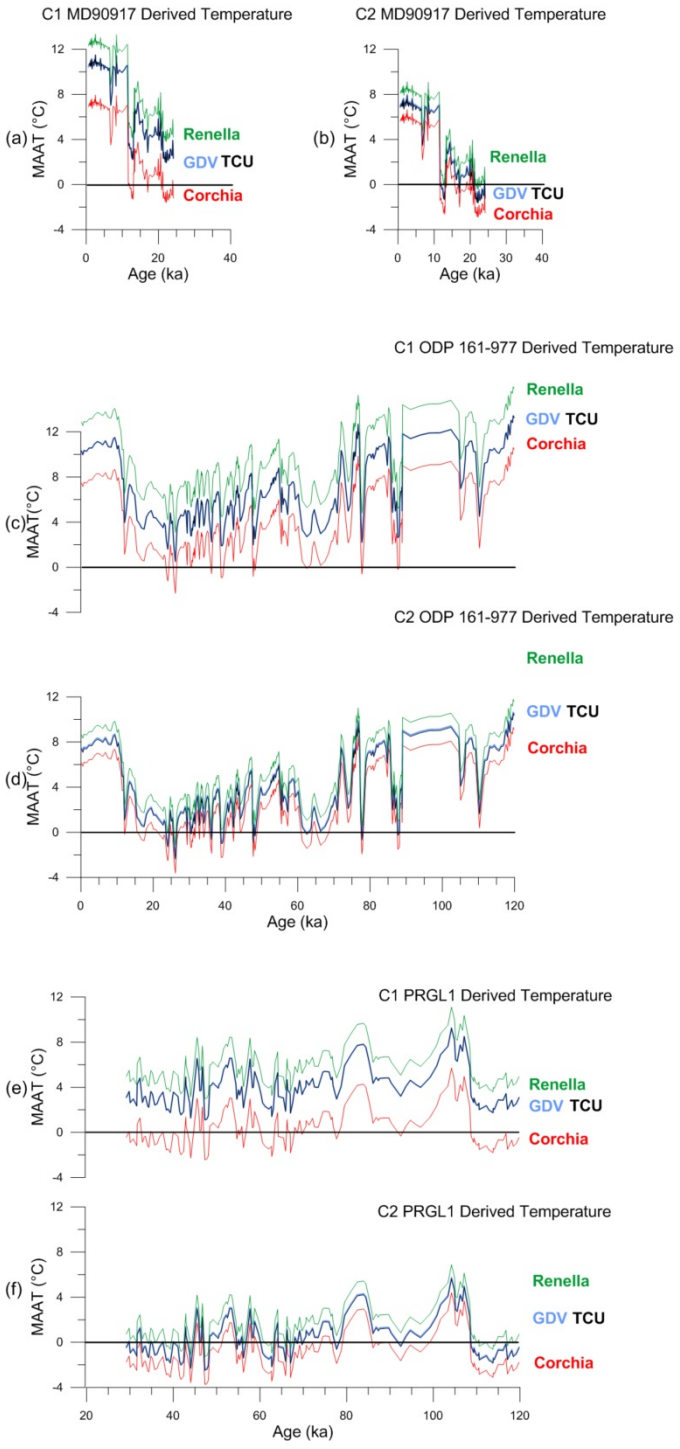

Fig. 4. MAAT curves derived for all the caves from MD90917: (a) C1 (see the text for explanation), (b) C2; from ODP 161-977, (c) C1 and (d) C2 ; and from PRGL1, (e) C1 and (f) C2. Black horizontal lines indicate the 0°C MAAT.

449

450 According to the timing of speleothem growth and MAAT estimations, it can be seen that above CC
451 both the C1 and C2 MAAT reconstructions experienced a number of long-lasting sub-zero periods.
452 Indeed, the Equilibrium Line Altitude (ELA) of 1200-1300 m a.s.l. in the Apuan Alps during the
453 MIS 2 (Merciai, 1912; Braschi et al., 1987; Jaurand, 1998) supports the hypothesis that in the CC
454 catchments (both C1 1240 m a.s.l. and C2 1460m a.s.l.) glaciers were existing. These unfavorable
455 conditions for speleothem deposition (MAAT subzero or near 0 °C) persisted, discontinuously,
456 above CC not only during the MIS 2, but also during MIS 4 (Fig. 4). This is consistent with
457 evidence of a phase of glaciation during MIS 4 from the Alps and other peri-Mediterranean
458 mountain ranges (Hughes et al. 2013; 2018; Sarikya et al., 2014; Pope et al., 2017) (blue bars in
459 Fig. 5~~b~~a). There are evidences of very small growth phases during MIS4-MIS2 (Fig. 2, 3, 5~~e~~d) that
460 may have occurred during warming reversals, most likely associated with the millennia-scale
461 interstadials observed in the Greenland ice-core records (i.e. Dansgaard-Oeschger events,
462 Dansgaard et al., 1993; Fig. 5~~f~~e), but also indicated by SST changes in the western Mediterranean
463 (Cacho et al., 1999).

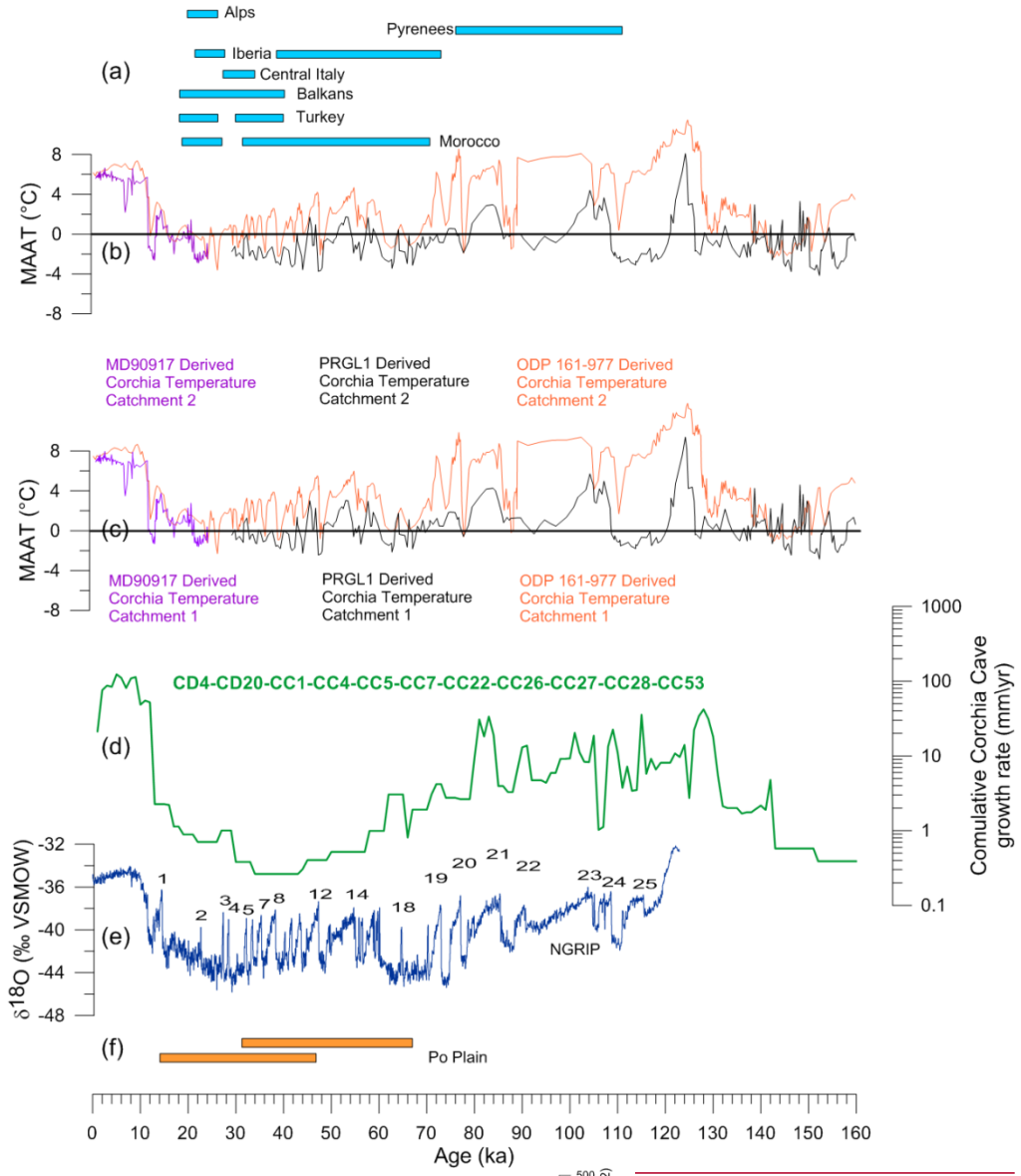
Alps
Pyrenees
Iberia
Central Italy
Balkans
Turkey
Morocco
(a)
(b)
(c)
(d)
(e)
(f)
MAAT (°C)
MD90917 Derived Corchia Temperature Catchment 2
PRGL1 Derived Corchia Temperature Catchment 2
ODP 161-977 Derived Corchia Temperature Catchment 2
MD90917 Derived Corchia Temperature Catchment 1
PRGL1 Derived Corchia Temperature Catchment 1
ODP 161-977 Derived Corchia Temperature Catchment 1
CD4-CD20-CC1-CC4-CC5-CC7-CC22-CC26-CC27-CC28-CC53
Comulative Corchia Cave growth rate (mm\yr)
δ18O (‰ VSMOW)
NGRIP
Po Plain
Age (ka)

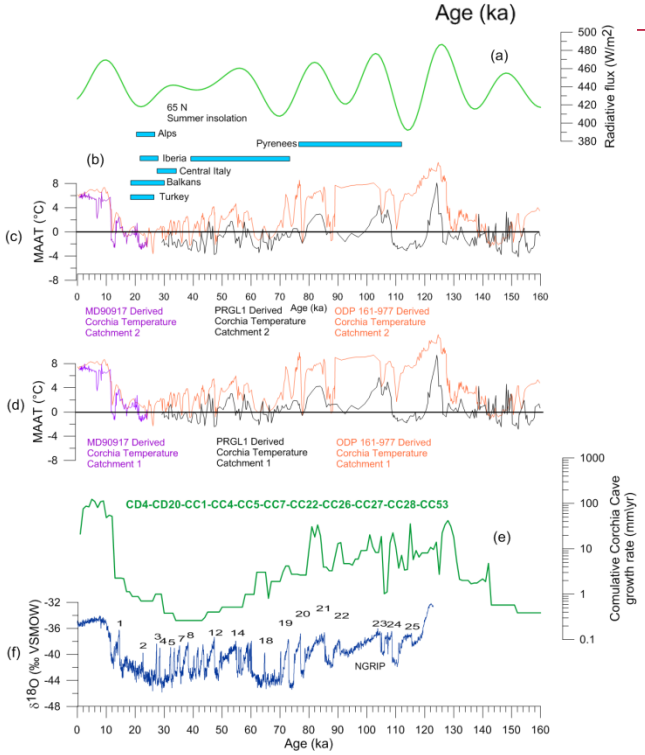
(a)
65 N Summer insolation
Radiative flux (W/m2)
(b)
(c)
(d)
(e)
(f)
Age (ka)

Fig. 5. Northern Hemisphere proxies for the Pleniglaciation~~: a) summer insolation curve at 65°N (Berger and Loutre, 1991); b~~a) the approximate timing of maximum extent of glaciers in the Mediterranean mountains (after Hughes et al., 2013; 2018; Sarikya et al., 2014; Pope et al., 2017); ~~c~~b) the derived MAAT curves in the C2 case above the Galleria delle Stalattiti: red curve is derived from ODP 161-977, purple curve from MD90917 data, black curve is derived from PRGL1 data. Horizontal black line indicates the 0°C MAAT; ~~d~~c) the derived MAAT curves in the C1 case above the Galleria delle Stalattiti: red curve is derived from ODP 161-977, purple curve from MD90917 data, black curve is derived from PRGL1 data and horizontal black line indicates the 0°C MAAT; ~~e~~d) Cumulative growth curve calculated for interval of 1000 yr for Corchia cave speleothems (green line); ~~f~~e) NGRIP $\delta^{18}O$ values from North Greenland Ice Core (North Greenland Ice Core Project members, 2004). Numbers over the graph mark the position of the Dansgaard-Oeschger interstadials (Dansgaard et al., 1993); f) approximate interval of extensive loess accumulation in Po Plain (after Cremaschi et al., 2015b; Zerboni et al., 2015).

In general, pollen data from the western Mediterranean show that cold SSTs characteristic of Greenland stadials were contemporaneous with the expansion of semi-desert or steppic vegetation. On the contrary, Greenland interstadials were synchronous with the expansion of open forests (Sánchez-Goñi et al., 2008). Presumably, phases of forest expansion prompted the development of deeper soils. However, the very limited speleothem growth and the available ages prevent a precise correlation with the warmer intervals. On the other hand, according to Atkinson (1983) and Sp□tl et al. (2007), speleothems may form, although with a lower rate of growth, in caves overlain by temperate glaciers with available glacial meltwater infiltrating the karst system. The very low partial pressure of CO_2 in such water due to the absence of soil can be balanced by pyrite oxidation during the flow paths through fractures, providing the dissolved carbonate necessary for speleothem deposition. This process is demonstrably present at Corchia (Piccini et al., 2008; Bajo et al., 2017) and can be responsible of the very thin deposition layers included between two hiatus.

Summing up, growth histories and temperature estimation support the hypothesis that interruptions or strong reductions in speleothem growth at Corchia could have been due to a combination of glaciation and/or ice-free but cold temperatures with low or absent soil activity.

Glacial phases occurring in this period in the mountain regions around the Mediterranean are confirmed by multi-proxy analyses carried out on the glacial lacustrine sequences, as evidenced by a maximum of glacier expansion of Pyrenean glaciers before 30 ka (Garcia-Riuz at al., 2003) and in Picos de Europa dated at about 40 ka (Moreno et al. 2010; Serrano et al., 2012). Consistently in the central Apennines, tephra layers in lacustrine sediments bracket the maximum glacier extent between 33-27 ka, not a period of maximum cold conditions but one that was humid (Giraudi, 2012). Regarding the Alps there is a controversial discussion about glaciers extent before MIS 2 when the maximum expansion was reached (Ivy-Ochs et al. 2008; Preusser et al. 2011; Hughes et al. 2013). The uncertainties mainly derive from the fact that the majority of terrestrial records (i.e. glacial deposit, pro-glacial outwash, river terrace, lake deposit) were eroded, or at least remoulded or reworked, when MIS 2 glaciers invaded the valleys and in many cases spread out in piedmont lowlands. Indeed, while in the Eastern Alps no evidence for the presence of pre-MIS 2 glaciers are clearly found (Ivy-Ochs et al., 2008), an important glaciation reaching the lowlands of the Western Alps during MIS 4 is documented by OSL dating of pro-glacial outwash (Preusser et al. 2007) and lake sediments (Link and Preusser 2006).

~~This~~ The above described asynchronicity is not contradictory a priori, because it may be explained by the short reaction times of small glaciers (like those of most of the Mediterranean mountains) to changes in precipitation and/or temperature. Further sampling may reveal sporadic or very slow episodes of growth during this time interval, allowing better and more precise interpretations of MIS 3 climatic oscillations.

7. Conclusions

Speleothems in the Apuan Alps grew near-continuously during most of MIS5 (from ca. 130 ka to about 75 ka), then experienced a long period of absent to very low deposition covering the MIS4 to MIS2 interval, until ~12.5 ka. This growth history can be explained as the result of development of glaciers at high elevations, not necessarily continuously existent for the whole considered period, and/or low soil development and near-zero temperatures. The speleothem growth curves may suggest that glacial expansion in the Apuan Alps was not only limited to the LGM (MIS2) but also to MIS3 and MIS4, analogous to other peri-Mediterranean mountains.

During spring and summer ice-melting periods, high water discharges occurred and caves located at lower altitudes were flooded, resulting in phreatic conditions, inhibiting speleothem deposition and infilling caves with thick fluvial deposits.

There is no evidence of significant growth during interstadials within MIS3, which supports the fact that no particularly warm conditions occurred in the Apuan Alps during those climatic events.

Sustained speleothem growth resumed close to the beginning of the Holocene both at lower and high-altitude caves. This can be interpreted as the result of a definitive melting of ice cover and the consequent progressive soil development at high altitude, and the stabilisation of loose glacial debris and reduced flooding for lower altitude caves.

These data indicate the potential for cumulative speleothems growth curve to chronologically constrain large-scale geomorphological processes, like the timing of glaciers presence. However, other processes can locally bias the speleothem growth (i.e. cold-non glacial conditions, absence/limited soils), suggesting that this approach is restricted to a first-order approximation which should be followed by a direct dating of glacial features. Moreover, the adoption of speleothem growth curves needs to be verified in other mountain ranges, where U/Th dating can be used for constraining glacial events.

Acknowledgments

We would like to thank two anonymous reviewers for their comments on this paper and helpful suggestions for improvements. We thank the Federazione Speleologica Toscana and Parco Regionale delle Alpi Apuane for supporting our work on Apuan speleothems. This work is part of Australian Research Council *Discovery Projects* grant DP110102185 (leader RD), and the ARCA project "Arctic: present climatic change and past extreme events" founded by the Italian Ministry of Education, Universities and Research (MIUR). These analyses contribute to the project "Clima ed eventi alluvionali estremi in Versilia: integrazione di nuove tecniche geoarcheologiche, geomorfologiche, geochimiche e simulazioni numeriche" (leader M. Bini), funded by "Fondazione Cassa di Risparmio di Lucca Call 2016" and Project PRA (2017/18) "Palaeoclimatic palaeoenvironmental evolution of the Apuan area since the Last Glacial Maximum". (leader C. Baroni), funded by Pisa University.

References

Akçar, N., Yavuz, V., Yeşilyurt, S., Ivy-Ochs, S., Reber, R., Bayrakdar, C., ... & Schlüchter, C. (2017). Synchronous last glacial maximum across the Anatolian Peninsula. From Hughes, P.D. & Woodward J.C. (eds) 2017 Quaternary glaciation in Mediterranean Mountains, Geological Society, London, Special Publications, 433, 137-159

Atkinson, T. C. (1983). Growth mechanisms of speleothems in castleguard cave, Columbia Icefields, Alberta, Canada. Arctic and Alpine Research, 15(4), 523-536.

Atkinson, T. C., Lawson, T. J., Smart, P. L., Harmon, R. S., & Hess, J. W. (1986). New data on speleothem deposition and palaeoclimate in Britain over the last forty thousand years. Journal of Quaternary Science, 1(1), 67-72.

568 Ayalon, A., Bar-Matthews, M., Frumkin, A., & Matthews, A., 2013. Last Glacial warm events on
569 Mount Hermon: the southern extension of the Alpine karst range of the east Mediterranean.
570 Quaternary Science Reviews, 59, 43-56.
571 Bajo, P., Borsato, A., Drysdale, R., Hua, Q., Frisia, S., Zanchetta, G., ... & Woodhead, J. (2017).
572 Stalagmite carbon isotopes and dead carbon proportion (DCP) in a near-closed-system
573 situation: An interplay between sulphuric and carbonic acid dissolution. *Geochimica et*
574 *Cosmochimica Acta*, *210*, 208-227.
575 Baldini, J. U., McDermott, F., & Fairchild, I. J., 2002. Structure of the 8200-year cold event
576 revealed by a speleothem trace element record. Science, 296, 5576, 2203-2206.
577 Bar-Matthews, M., Ayalon, A., Matthews, A., Sass, E., Halicz, L., 1996. Carbon and oxygen
578 isotope study of the active water-carbonate system in a karstic Mediterranean cave:
579 implications for paleoclimate research in semiarid regions. Geochim. Cosmoch. Acta, 60, 337-
580 347.
581 Baroni, C., Bini, M., Coltorti, M., Fantozzi, P., Guidobaldi, G., Nannini, D., Pieruccini, P., Ribolini,
582 A., Salvatore, M.C., 2013. Geomorphological maps as a key approach for enhancing the natural
583 and cultural heritage of the Apuan Alps Regional Park area and surroundings (Tuscany, Italy)
584 Rendiconti Online Societa Geologica Italiana, 28, 10-14.
585 Baroni, C., Pieruccini, P., Bini, M., Coltorti, M., Fantozzi, P. L., Guidobaldi, G., ... & Salvatore, M.
586 C. 2015. Geomorphological and neotectonic map of the Apuan Alps (Tuscany,
587 Italy). Geografia Fisica e Dinamica Quaternaria, 38(2), 201-227.
588 Beneo, E., 1945. Nuova località fossilifera e nuovo ghiacciaio nelle Alpi Apuane.Boll. Soc. Geol.
589 It., 64, 40-41.
590 Baroni, C., Guidobaldi, G., Salvatore, M. C., Christl, M., Ivy-Ochs, S. 2018. Last glacial maximum
591 glaciers in the Northern Apennines reflect primarily the influence of southerly storm-tracks in
592 the western Mediterranean. Quaternary Science Reviews, 197, 352-367.

593 Berger, A., Loutre, M.F., 1991. Insolation values for the climate of the last 10 million years.
594 Quaternary Science Reviews 10, 297–317.
595 Berstad, I.M., Lundberg,J., Lauritzen, SE., Linge, H.C. 2002. Comparison of the Climate during
596 Marine Isotope Stage 9 and 11 Inferred from a Speleothem Isotope Record from Northern
597 Norway. Quaternary Research 58, 361–371.
598 Bini, M., 2005. Glacial landforms in the Apuan Alps (Tuscany), features in danger of extinction. Il
599 Quaternario, Italian Journal of Quaternary Sciences, 18, 1, Volume Speciale, 173-176.
600 Braschi, S., Del Freo, P., Trevisan, L., 1987. Ricostruzione degli antichi ghiacciai sulle Alpi
601 Apuane . Atti Soc. Tosc. Sc. Nat., Mem., Serie A. 93, 203-219, fig. 10, tav.f.t. 1, 1987.
602 Burns, S.J., Fleitmann D., Matter, A., Neff U., Mangini A., 2001. Speleothem evidence from Oman
603 for continental pluvial events during interglacial periods. Geology, Geology; July 2001; v. 29
604 (7); pp. 623–626;
605 Carmignani L. & Kligfield R, 1990. Crustal extension in the Northern Apennines: the transition
606 from compression to extension in the Alpi Apuane Core Complex. Tectonics, 9, 6, 1275-1303.
607 Cacho, I., Grimalt, J. O., Pelejero, C., Canals, M., Sierro, F. J., Flores, J. A., & Shackleton, N.
608 (1999). Dansgaard-Oeschger and Heinrich event imprints in Alboran Sea
609 paleotemperatures. Paleoceanography, 14(6), 698-705.
610 Cheng, H., Lawrence Edwards, R., Shen, C.-C., Polyak, V. J., Asmerom, Y., Woodhead, J. D.,
611 Hellstrom, J., Wang, Y., Kong, X., Spötl, C., Wang, X., & Calvin Alexander, E. (2013),
612 Improvements in 230Th dating, 230Th and 234U half-life values, and U–Th isotopic
613 measurements by multi-collector inductively coupled plasma mass spectrometry, Earth Planet.
614 Sci. Lett., 371-372, 82–91
615 Çiner, A., & Sarıkaya, M. A. (2017). Cosmogenic 36Cl geochronology of late Quaternary glaciers
616 in the Bolkar Mountains, south central Turkey. Geological Society, London, Special
617 Publications, 433(1), 271-287. From Hughes, P.D. & Woodward J.C. (eds) 2017 Quaternary

618 glaciation in Mediterranean Mountains, Geological Society, London, Special Publications, 433,
619 137-159
620 Clark, P.U., Dyke, A.S., Shakun, J.D., Carlson, A.E., Clark, J., Wohlfarth, B., Mitrovica, J.X.,
621 Hostetler, S.W., McCabe, A.M., 2009. The Last Glacial Maximum. *Science* 325, 710-714.
622 Cocchi I., 1872. Del terreno glaciale delle Alpi Apuane. Boll. Del R. Com. Geol. 3, 7-8.
623 Cortina, A., Sierro, F. J., Flores, J. A., Martrat, B., & Grimalt, J. O. (2015). The response of SST to
624 insolation and ice sheet variability from MIS 3 to MIS 11 in the northwestern Mediterranean
625 Sea (Gulf of Lions). *Geophysical Research Letters*, *42*(23).
626 Cremaschi, M., Zerboni, A., Charpentier, V., Crassard, R., Isola, I., Regattieri, E., & Zanchetta, G.
627 (2015a). Early–Middle Holocene environmental changes and pre-Neolithic human occupations
628 as recorded in the cavities of Jebel Qara (Dhofar, southern Sultanate of Oman). Quaternary
629 International, 382, 264-276
630 Cremaschi, M., Zerboni, A., Nicosia, C., Negrino, F., Rodnight, H., & Spötl, C., 2015b. Age, soil-
631 forming processes, and archaeology of the loess deposits at the Apennine margin of the Po
632 plain (northern Italy): New insights from the Ghiardo area. Quaternary International, 376, 173-
633 188.
634 Dansgaard, W., Johnsen, S. J., Clausen, H. B., Dahl-Jensen, D., Gundestrup, N. S., Hammer, C. U.,
635 ... & Bond, G. (1993). Evidence for general instability of past climate from a 250-kyr ice-core
636 record. *Nature*, *364*(6434), 218.
637 De Stefani C., 1874. Gli antichi ghiacciai dell'Alpe di Corfino, ed altri dell'Appennino settentrionale
638 e delle Alpi Apuane. Boll. R. Com. Geol. d'It, 5, 86-95.
639 De Stefani C., 1875. Dei depositi alluvionali e della mancanza di terreni glaciali nell'Appennino
640 della valle del Serchio e nelle Alpi Apuane. Boll. R. Com. Geol. d'It., 1, 2, 3-18.
641 De Stefani C., 1890. Gli antichi ghiacciai delle Alpi Apuane. Boll. del C.A.I. 24, 57, 175-202.
642 Douville, E., Sallé, E., Frank, N., Eisele, M., Pons-Branchu, E., & Ayrault, S. (2010), Rapid and
643 precise ^{230}Th/U dating of ancient carbonates using Inductively Coupled Plasma - Quadrupole

644 Mass Spectrometry. Chem. Geol., 272, 1-11.
645 Dykoski, C. A., Edwards, R. L., Cheng, H., Yuan, D., Cai, Y., Zhang, M., Lin, Y., Qing, J,
646 Zhisheng A., Revenaugh, J., 2005. A high-resolution, absolute-dated Holocene and deglacial
647 Asian monsoon record from Dongge Cave, China. Earth and Planetary Science Letters, 233, 1,
648 71-86.
649 Drysdale, R.N., Zanchetta, G., Hellstrom, J.C., Fallick, A.E., Zhao, J.X., Isola, I., Bruschi, G., 2004.
650 Palaeoclimatic implications of the growth history and stable isotope (δ18O and δ13601 C)
651 geochemistry of a Middle to Late Pleistocene stalagmite from central-western Italy. Earth and
652 Planetary Science Letters 227, 215-229.
653 Drysdale, R.N., Zanchetta, G., Hellstrom, J 604 .C., Fallick, A.E., Zhao, J.X., 2005. Stalagmite
654 evidence for the onset of the Last Interglacial in southern Europe at 129+/−1 ka. Geophysical
655 Research Letters 32, 1-4.
656 Drysdale, R.N., Zanchetta, G., Hellstrom, J.C., Maas, R., Fallick, A.E., Pickett, M., Cartwright, I.,
657 Piccini, L., 2006. Late Holocene drought responsible for the collapse of old World civilizations
658 is recorded in an Italian cave flowstone. Geology 34, 101-104.
659 Drysdale, R.N., Zanchetta, G., Hellstrom, J.C., Fallick, A.E., McDonald, J., Cartwright, I., 2007.
660 Stalagmite evidence for the precise timing of North Atlantic cold events during the early last
661 glacial. Geology 35, 77–80.
662 Drysdale, R.N., Zanchetta, G., Hellstrom, J.C., Fallick, A.E., Sanchez-Goni, M.F., Couchoud, I.,
663 McDonald, J., Maas, R., Lohmann, G., Isola, I., 2009. Evidence for obliquity forcing of glacial
664 termination II. Science 325, 1527-1531.
665 Edwards, R. L., Chen, J. H., & Wasserburg, G. J., 1987. 238 U 234 U 230 Th 232 Th systematics
666 and the precise measurement of time over the past 500,000 years. Earth and Planetary Science
667 Letters, 81, 2, 175-192.
668 Federici, P.R., 1981. The Quaternary Glaciation on the sea ward side of the Apuan Alps . Riv.
669 Geogr. It., 88, 183-199.

670 Federici, P.R., 2005. Aspetti e problemi della glaciazione pleistocenica nelle Alpi Apuane. Istituto
671 Italiano di Speleologia Mem. XVIII, s II, 19-32.
672 Federici, P.R., Granger, D.E., Pappalardo, M., Ribolini, A., Spagnolo, M., Cyr, A.J. 2008. Exposure
673 age dating and Equilibrium Line Altitude reconstruction of an Egesen moraine in the Maritime
674 Alps, Italy. Boreas, 37, 2,245-253.
675 Federici, P.R., Granger, D.E., Ribolini, A., Spagnolo, M., Pappalardo, M., Cyr, A.J., 2012. Last
676 Glacial Maximum and the Gschnitz stadial in the Maritime Alps according to 10Be cosmogenic
677 dating. Boreas, 41, 2, 277-291.
678 Federici, P.R., Ribolini, A., Spagnolo M., 2017. Glacial history of the Martime Alps from the last
679 Glacial maximum to Little Ice Age. From Hughes, P.D. & Woodward J.C. (eds) 2017
680 Quaternary glaciation in Mediterranean Mountains, Geological Society, London, Special
681 Publications, 433, 137-159
682 Fellin, M. G., Reiners, P. W., Brandon, M. T., Wüthrich, E., Balestrieri, M. L., & Molli, G. (2007).
683 Thermochronologic evidence for the exhumational history of the Alpi Apuane metamorphic
684 core complex, northern Apennines, Italy. *Tectonics*, *26*(6).
685 Finsinger, W., Ribolini, A., 2001. Late Glacial to Holocene deglaciation of the Colle del Vei del
686 Bouc-Colle del Sabbione area (Argentera Massif, Maritime Alps, Italy-France) [Deglaciazione
687 Tardiglaciale-Olocenica dell'area Colle del Sabbione-Colle del Vei del Bouc (Massiccio
688 dell'Argentera, Alpi Marittime, Italia-Francia)] Geografia Fisica e Dinamica Quaternaria, 24, 2)
689 141-156.
690 Fleitmann , D., Burns, S.J., Pekala, M., Mangini, A., Al-Subbary, A., Al-Aowah, M., Kramers, J.,
691 Matter, A. 2011. Holocene and Pleistocene pluvial periods in Yemen, southern Arabia.
692 Quaternary Science Reviews 30 (2011) 783e787
693 García-Ruiz, J. M., Valero-Garcés, B. L., Martí-Bono, C., González-Sampériz, P. 2003.
694 Asynchroneity of maximum glacier advances in the central Spanish Pyrenees. Journal of
695 Quaternary Science 18, 61-72.

696 Gascoyne, M., & Nelson, D. E. (1983). Growth mechanisms of recent speleothems from
697 Castleguard Cave, Columbia Icefields, Alberta, Canada, inferred from a comparison of
698 uranium-series and carbon-14 age data. *Arctic and Alpine Research*, *15*(4), 537-542.
699 Gascoyne, M., 1992. Palaeoclimate determination from cave calcite deposits. Quaternary
700 Science Reviews 11 (6), 609–632. doi:10.1016/0277-3791(92)90074-I.
701 Genty, D., Baker, A., & Vokal, B. (2001). Intra-and inter-annual growth rate of modern
702 stalagmites. Chemical Geology, 176(1-4), 191-212.
703 Genty, D., Blamart, D., Ouahdi, R., Gilmour, M., Baker, A., Jouzel, J., & Van-Exter, S., 2003.
704 Precise dating of Dansgaard–Oeschger climate oscillations in western Europe from stalagmite
705 data. Nature, 421(6925), 833-837.
706 Genty, D., Combourieu Nebout N., Hatté C., Blamart D., Ghaleb B. & Isabello L., 2005. Rapid
707 climatic changes of the last 90 kyr recorded on the european continent. Comptes Rendus de
708 l'Académie des Sciences de Paris, 337, pp. 970-982.
709 Giraudi, C. 2012. The Campo Felice Late Pleistocene Glaciation (Apennines, Central Italy). Journal
710 of Quaternary Science, 27, 4 pp. 432-440
711 Giraudi, C, Bodrato G, Ricci Lucchi M, Cipriani M., Villa I.M., Giaccio, B. & Zuppi, G.M., 2011.
712 Middle and Late Pleistocene Glaciations in the Campo Felice basin (Central Apennines-Italy).
713 Quaternary Research 75, pp. 219–230.
714 Giraudi C., Giaccio, B. The middle Pleistocene glaciations on the Apennines (Italy): new
715 chronological data and considerations about the preservation of the glacial deposits.
716 Form Hughes, P.D. & Woodward J.C. (eds) 2017 Quaternary glaciation in Mediterranean
717 Mountains, Geological Society, London, Special Publications, 433, 161-178
718 Gordon, D., Smart, P. L., Ford, D. C., Andrews, J. N., Atkinson, T. C., Rowe, P. J., & Christopher,
719 N. S. J. (1989). Dating of late Pleistocene interglacial and interstadial periods in the United
720 Kingdom from speleothem growth frequency. Quaternary research, 31(1), 14-26.

721 Gromig, R., Mechernich, S., Ribolini, A., Wagner, B., Zanchetta, G., Isola, I., Bini, M., Dunai, T.J.
722 Evidence for a Younger Dryas deglaciation in the Galicica Mountains (FYROM) from
723 cosmogenic 36Cl (2017) Quaternary International
724 Hannah, G.H., Hughes, P.D., Gibbard, P.L. 2017. Plistocene plateau ice fields in the High Atlas,
725 Morocco. Form Hughes, P.D. & Woodward J.C. (eds) 2017 Quaternary glaciation in
726 Mediterranean Mountains, Geological Society, London, Special Publications, 433, 25-54
727 Hellstrom, J. 2003 Rapid and accurate U/Th dating using parallel ion-counting multi-collector ICP-
728 MS, J. Anal. At. Spectrom.18, pp. 135– 1346.
729 Hellstrom, J. 2006. U–Th dating of speleothems with high initial 230 Th using stratigraphical
730 constraint. Quaternary Geochronology, 1,4, 289-29.
731 Hodge, E. J., Richards, D. A., Smart, P. L., Ginés, A., & Mattey, D. P. (2008). Sub-millennial
732 climate shifts in the western Mediterranean during the last glacial period recorded in a
733 speleothem from Mallorca, Spain. Journal of Quaternary Science, 23(8), 713-718.
734 Hughes, P. D.; Gibbard, P. L.; Woodward, J. C., 2004. Quaternary glaciation in the Atlas
735 Mountains of North Africa. Developments in Quaternary Sciences, 2, 255-260.
736 Hughes, P.D. & Gibbard, P.L. 2015. A stratigraphical basis for the Last Glacial Maximum (LGM).
737 Quaternary International. DOI: 10.1016/j.quaint.2014.06.006
738 Hughes, P. D., Woodward, J. C., Van Calsteren, P. C., & Thomas, L. E., 2011. The glacial history
739 of the Dinaric Alps, Montenegro. Quaternary Science Reviews, 30 23, 3393-3412.
740 Hughes, P.D., Fenton, C.R., Fink, D., Schnabel, C., and Rother, H., 2011. Extent, timing and
741 palaeoclimatic signifi cance of glaciation in the High Atlas, Morocco. Quaternary International,
742 v. 279–280, 210.
743 Hughes, P.D., Gibbard, P.L., and Ehlers, J., 2013. Timing of glaciation during the last glacial cycle:
744 evaluating the meaning and significance of the ‘Last Glacial Maximum’ (LGM). Earth Science
745 Reviews, v. 125, 171-198.

746 Hughes, P.D. & Woodward J.C. 2017. Quaternary glaciation in the Mediterranean mountains: a
747 new synthesis. Form Hughes, P.D. & Woodward J.C. (eds) 2017 Quaternary glaciation in
748 Mediterranean Mountains, Geological Society, London, Special Publications, 433, 1-23
749 Hughes, P.D., Fink, D., Rodés, Á., Fenton, C.R., 2018. ^{10}Be and ^{36}Cl exposure ages and
750 palaeoclimatic significance of glaciations in the High Atlas, Morocco. Quaternary Science
751 Reviews 180, 193-213.
752 Isola, I., Zanchetta, G., Drysdale, R. N., Regattieri, E., Bini, M., Bajo, P., Hellstrom, J., Baneschi,
753 I., Lionello, P., Woodhead, J., Greig, A. 2018. The 4.2 ka BP event in the Central Mediterranean:
754 New data from Corchia speleothems (Apuan Alps, central Italy). Accepted Climate of the Past,
755 doi.org/10.5194/cp-2018-127

756 Ivy-Ochs, S., Kerschner, H., Reuther, A., Preusser, F., Heine, K., Maisch, M., Kubik, P.W. &
757 Schluchter, C. 2008. Chronology of the last glacial cycle in the European Alps. Journal of
758 Quaternary Sciences, 23, 559-573.

759 Jaffey, A.H., Flynn, K.F., Glendenin, L.E., Bentley, W.C., & Essling, A.M. (1971), Precision
760 measurements of half-lives and specific activities of ^{235}U and ^{238}U. Phys. Rev. C, 4(5), 1889–1906.

761 Jaurand, E., 1998. Les glaciers disparus de l'Apennin. In Geomorphologie et paleoenvironments
762 glaciaires de l'Italie peninsulaire. Vol 10. Publications de la Sorbonne.
763 Kotarba, A., Herman, H. and Dramis, F., 2001. On the age of Campo Imperatore glaciations, Gran
764 Sasso Massif, Central Italy. Geografia Fisica e Dinamica Quaternaria 24, 65–69.
765 Kuhlemann, J., Rohling, E. J., Krumrei, I., Kubik, P., Ivy-Ochs, S., Kucera, M., 2008. Regional
766 synthesis of Mediterranean atmospheric circulation during the Last Glacial
767 Maximum. Science, 321, 5894, 1338-1340.
768 Lambeck, K:, and Bard E.. 2000. "Sea-level change along the French Mediterranean coast for the
769 past 30 000 years." Earth and Planetary Science Letters 175.3, 203-222.

770 Lambeck, K., Rouby, H., Purcell, A., Sun, Y., & Sambridge, M. (2014). Sea level and global ice
771 volumes from the Last Glacial Maximum to the Holocene. *Proceedings of the National*
772 *Academy of Sciences*, *111*(43), 15296-15303.
773 Link, A, Preusser, F. 2006. Hinweise auf eine Vergletscherung des Kemptener Beckens während
774 des Mittelwürms. Eiszeitalter und Gegenwart, 55, 65–88.
775
776 Locarnini, R. A., A. V. Mishonov, J. I. Antonov, T. P. Boyer, H. E. Garcia, O. K. Baranova, M. M.
777 Zweng, and Johnson, D. R., 2010. World Ocean Atlas 2009, Volume 1: Temperature.S.
778 Levitus, Ed. NOAA Atlas NESDIS 68, U.S. Government Printing Office, Washington, D.C.,
779 184.
780 López-Moreno, J. I., Vicente-Serrano, S. M., Morán-Tejeda, E., Lorenzo-Lacruz, J., Kenawy, A., &
781 Beniston, M. (2011). Effects of the North Atlantic Oscillation (NAO) on combined temperature
782 and precipitation winter modes in the Mediterranean mountains: observed relationships and
783 projections for the 21st century. Global and Planetary Change, 77(1-2), 62-76.
784 Ludwig, K.R., & Titterington, D.M. (1994), Calculation of ^{230}Th/U isochrons, ages, and errors,
785 Geochimica et Cosmochimica Acta, 58(22), 5031–5042.
786 Martrat, B., Grimalt, J.O., Lopez-Martinez, C., Chaco, I., Sierro, F.J., Flores, J.A., Zahn, R., Canals,
787 M., Jason, H.C., Hodell, D.A., 2004. Abrupt temperature changes in the Western
788 Mediterranean over the past 250,000 years. Science 306, 1762–1765
789 Martrat, B.; Jimenez-Amat, P.; Zahn, R.; Grimalt, J. O, 2014. Sea surface temperatures, alkenones
790 and sedimentation rates at the Alboran basin from ODP Site 161-977. PANGAEA,
791 https://doi.org/10.1594/PANGAEA.787969,
792 McDermott, F., 2004. Palaeo-climate reconstruction from stable isotope variations in speleothems:
793 a review. Quaternary Science Reviews, 23 pp. 901-918.
794 Masini, R., 1970. I massi erratici della Valle dell' Edron e il glacialismo nelle Alpi Apuane. Bool.
795 Soc. Geol. It. 89, (2), 45-5.

796 Meyer, M.C., Spötl, C., Mangini, A., Tessadri, R., 2012. Speleothem deposition at the glaciation
797 threshold—An attempt to constrain the age and paleoenvironmental significance of a detrital-
798 rich flowstone sequence from Entrische Kirche Cave (Austria): Palaeogeography,
799 Palaeoclimatology, Palaeoecology, v. 319–320, pp. 93–106
800 Merciai, G., 1912. Fenomeni glaciali delle Alpi Apuane . Att. Soc. Tosc. Sc. Nat., Pisa, XXVIII,
801 70-89.
802 Molli G. & Vaselli L., 2006. Structures, interference patterns, and strain regimes during midcrustal
803 deformation in the Alpi Apuane (Northern Apennines Italy). Geological Society of America,
804 Spec. Pub. 414: 79-93.
805 Moreno, A., Stoll, H., Jiménez-Sánchez, M., Cacho, I., Valero-Garcés, B., Ito, E., Edwards, R. L.,
806 2010. A speleothem record of glacial (25–11.6 kyr BP) rapid climatic changes from northern
807 Iberian Peninsula. Global and Planetary Change, 71(3), 218-231.
808 Müller, P.J., Kirst, G., Ruhland, G., von Storch, I., Rosell-Melé, A., 1998. Calibration of the
809 alkenone paleotemperature index U^{K}_{37} based on core-tops from the eastern South Atlantic and
810 the global ocean (60°N-60°S). Geochim. Cosmochim. Acta 62, pp. 1757-1772.
811 North Greenland Ice Core Project members. 2004. High-resolution record of Northern Hemisphere
812 climate extending into the last interglacial period. Nature, 431, 7005,147-151
813 Paci M., 1935. Revisione dei terreni morenici quaternari delle Alpi Apuane. Atti Soc. Tosc. Sc.
814 Nat. Proc Verb. 44, 13-30
815 Oliva M., Žebre M., Guglielmin M., Hughes P.D., Çiner A., Vieira G, Bodin X., Andrés N.,
816 Colucci R.R., García-Hernández C., Mora C., Nofre J., Palacios D., Pérez-Alberti A., Ribolini
817 A., Ruiz-Fernández J.,. Sarıkaya M.A, Serrano E., Urdea P., Valcárcel M., Woodward J.C.,
818 Yıldırım C., 2018. Permafrost conditions in the Mediterranean region since the Last Glaciation.
819 Earth-Science Reviews, 10.1016/j.earscirev.2018.06.018

820 Pérez-Alberti, A., Valcárcel, M., Blanco, R., 2004. Pleistocene glaciation in Spain. In: Ehlers, J.,
821 Gibbard, P.L. (Eds.), Quaternary Glaciations- Extent and Chronology. Elsevier, London, pp.
822 389–394.
823 Piccini L., 1998. Evolution of karst in the Alpi Apuane (Italy): Relationships with the
824 morphotectonic history. Suppl. Geografia Fisica e Dinamica Quaternaria, 3, 4, 21-31.
825 Piccini L., 2011. Speleogenesis in highly geodynamic contexts: The quaternary evolution of Monte
826 Corchia multi-level karst system (Alpi Apuane, Italy). Geomorphology, 134, 1–2, 49-61
827 Piccini, L., Borsato, A., Frisia, S., Paladini, M., Salzani, R., Sauro, U., & Tuccimei, P., 2003.
828 Concrezionamento olocenico e aspetti geomorfologici della Grotta del Vento (Alpi Apuane–
829 Lucca): analisi paleoclimatica e implicazioni morfogenetiche. Studi Trent. Sci. Nat., Acta
830 Geol., 80, pp. 127-138
831 Piccini, L., Zanchetta, G., Drysdale, R. N., Hellstrom, J., Isola, I., Fallick, A. E., Leone G., Doveri
832 M., Mussi M. 8, Mantelli F. 9, Molli G. 2, Lotti L. 10, Roncioni A. 11, Regattieri E., Meccheri
833 M., Vaselli, L., 2008. The environmental features of the Monte Corchia cave system (Apuan
834 Alps, central Italy) and their effects on speleothem growth. International Journal of
835 Speleology, 37(3), pp. 153-172.
836 Pons-Branchu, E., Hillaire-Marcel, C., Ghaleb, B., Deschamps, P., & Sinclair, D. (2005), Early
837 diagenesis impact on precise U-series dating of Deep-Sea corals. Example of a 100-200 years
838 old *Lophelia pertusa* sample from NE Atlantic. Geochimica et Cosmochimica Acta, 69 (20),
839 4865-4879.
840 Pons-Branchu, E., Hamelin, B., Losson, B., Jaillet, S., & Brulhet, J. (2010). Speleothem evidence of
841 warm episodes in northeast France during Marine Oxygen Isotope Stage 3 and implications for
842 permafrost distribution in northern Europe. Quaternary Research, 74(2), 246-251.
843 Pons-Branchu, E., Douville, E., Roy-Barman, M., Dumont, E., Branchu, P., Thil, F., Frank, N.,
844 Bordier, L., & Borst, W. (2014), A geochemical perspective on Parisian urban history based on
845 U-Th dating, laminae counting and yttrium and REE concentrations of recent carbonates in

underground aqueducts. Quat. Geochronol., 24, 44-53.

Pope, R.J., Hughes, P.D., Skourtsos, E., 2017. Glacial history of Mt Chelmos, Peloponnesus, Greece. In: Hughes, P.D., Woodward, J.C. (Eds.) Quaternary glaciation in the Mediterranean Mountains. Geological Society of London Special Publications 433, 211-236. https://doi.org/10.1144/SP433.11

Potzolu, P.P., 1995. Osservazioni geomorfologiche nell'alta avelle del Serchio di Gramolazzo (Alpi Apuane). Memorie dell'Accademia Lunigiane di Scienze "Giovanni Cappellini" 64-65, 213-250.

Preusser, F., Blei A, Graf H.R & Schlüchter. C. 2007. Luminescence dating of Würmian (Weichselian) proglacial sediments from Switzerland: methodological aspects and stratigraphical conclusions. Boreas. 36,130–142.

Preusser, F., Graf, H.R., Keller, O., Krayss, E. & Schlüchter, C., 2011. Quaternary glaciation history of northern Switzerland. Eizeitalter und Gegenwart, 60, 282–305.

Pujol, C., & Grazzini, C. V. (1995). Distribution patterns of live planktic foraminifers as related to regional hydrography and productive systems of the Mediterranean Sea. *Marine Micropaleontology*, *25*(2-3), 187-217

Rapetti F. & Vittorini S., 1994. Carta climatica della Toscana centro-settentrionale. Pacini Editore, Pisa.

Rapetti, F., & Vittorini, S. (2012). Note illustrative della carta climatica della Toscana. *Atti della Società Toscana di Scienze Naturali, Memorie, Serie A*, 117-119.

Reale, M., & Lionello, P. (2013). Synoptic climatology of winter intense precipitation events along the Mediterranean coasts. Natural Hazards and Earth System Sciences, 13(7), 1707-1722.

Regattieri, E., Isola, I., Zanchetta, G, Drysdale, R.N., Hellstrom, J.C., Baneschi, I., 2012. Stratigraphy, petrography and chronology of speleothem deposition at Tana che Urla (Lucca, Italy): paleoclimatic implications. Geografia Fisica e Dinamica del Quaternario 35, 141-152.

871 Regattieri E., Zanchetta G., Drysdale R.N., Isola I., Hellstrom J., Roncioni A., 2014a. A continuous
872 stable isotopic record from Penultimaye glacial maximum on to the Last Interglacial (159-121
873 ka) from Tana Che Urla Cave (Apuan Alps, central Italy). Quaternary Research, 82, 450-461.
874 Regattieri E., Zanchetta G., Drysdale R., Isola I., Hellstrom J., Dallai, L. 2014b. Lateglacial to
875 Holocene trace element record (Ba, Mg, Sr) from Corchia Cave (Apuan Alps, central Italy):
876 paleoenvironmental implications. Journal of Quaternary Science, 29(4), 381-392
877 Regattieri E., Zanchetta **G.**, Drysdale R.N., Isola I., Woodhead J.D., Helstromm J.C., Giaccio,
878 Greig A., Baneschi I., Dotsika E., 2016. Environmental variability between the penultimate
879 deglaciation and the mid Eemian: Insights from Tana che Urla (central Italy) speleothem trace
880 element record. *Quaternary Science Reviews*, 152, 80-92.
881 Ribolini, A., Isola, I., Bini, M., Zanchetta, G., Sulpizio, R. 2011. Glacial features on the Galicica
882 Mountains, Macedonia: preliminary report. Geogr. Fis. Dinam. Quat. 34, pp. 247-255.
883 Ribolini, A., Bini, M., Isola, I., Zanchetta, G., Pellitero, R., Mechernich, S., Gromig, R., Dunai, T.,
884 Wagner, B., Milevski, I. An oldest dryas glacier expansion on mount pelister (former
885 Yugoslavian Republic of Macedonia) according to10Be cosmogenic dating (2018) Journal of
886 the Geological Society, 175 (1), pp. 100-110.
887 Rigual-Hernández, A. S., Bárcena, M. A., Jordan, R. W., Sierro, F. J., Flores, J. A., Meier, K. S., ...
888 & Heussner, S. (2013). Diatom fluxes in the NW Mediterranean: evidence from a 12-year
889 sediment trap record and surficial sediments. *Journal of plankton research*, *35*(5), 1109-1125.
890 Sanchez -Goñi, M. S., Eynaud, F., Turon, J. L., & Shackleton, N. J. (1999). High resolution
891 palynological record off the Iberian margin: direct land-sea correlation for the Last Interglacial
892 complex. Earth and Planetary Science Letters, 171(1), 123-137.
893 Sanchez -Goñi, M. F. S., Landais, A., Fletcher, W. J., Naughton, F., Desprat, S., & Duprat, J.
894 (2008). Contrasting impacts of Dansgaard–Oeschger events over a western European latitudinal
895 transect modulated by orbital parameters. *Quaternary Science Reviews*, 27(11), 1136-1151.

896 Sarıkaya, M. A., Çiner, A., Haybat, H., & Zreda, M. (2014). An early advance of glaciers on Mount
897 Akdağ, SW Turkey, before the global Last Glacial Maximum; insights from cosmogenic
898 nuclides and glacier modeling. *Quaternary Science Reviews*, 88, 96-109.
899 Sarıkaya, M. A., & Çiner, A. (2017). Late Quaternary glaciations in the eastern
900 Mediterranean. Geological Society, London, Special Publications, 433(1), 289-305. From Hughes,
901 P.D. & Woodward J.C. (eds) 2017 Quaternary glaciation in Mediterranean Mountains,
902 Geological Society, London, Special Publications, 433, 137-159
903 Scholz, D., Hoffmann, D. L., Hellstrom, J., & Ramsey, C. B. (2012). A comparison of different
904 methods for speleothem age modelling. *Quaternary Geochronology*, *14*, 94-104.
905 Serrano, E., González-Trueba, J. J., González-García, M., 2012. Mountain glaciation and
906 paleoclimate reconstruction in the Picos de Europa (Iberian Peninsula, SW Europe). Quaternary
907 Research, 78, 2, 303-314.
908 Siani, G., Magny, M., Paterne, M., Debret, M., & Fontugne, M., 2013. Paleohydrology
909 reconstruction and Holocene climate variability in the South Adriatic Sea. Climate of the
910 Past,9(1), 499-515.
911 Smith, J. R., Giegengack, R., & Schwarcz, H. P. (2004). Constraints on Pleistocene pluvial climates
912 through stable-isotope analysis of fossil-spring tufas and associated gastropods, Kharga Oasis,
913 Egypt. Palaeogeography, Palaeoclimatology, Palaeoecology, 206(1-2), 157-175.
914 Spötl C., Mangini A. 2006. U/Th age constraints on the absence of ice in the central Inn Valley
915 (eastern Alps, Austria) during Marine Isotope Stages 5c to 5a. Quaternary Research 66, 167–
916 175.
917 Spotl, C., Mangini A., 2007. Speleothems and glaciers. Earth and Planetary Science Letters, 254,
918 323-331
919 Stoll, H. M., Moreno, A., Mendez-Vicente, A., Gonzalez-Lemos, S., Jimenez-Sanchez, M.,
920 Dominguez-Cuesta, M. J., ... & Wang, X. (2013). Paleoclimate and growth rates of

speleothems in the northwestern Iberian Peninsula over the last two glacial cycles. Quaternary Research, 80(2), 284-290.

Stoppani A., 1872. Sull'esitsenza di un antico ghiaciaio nelle Alpi Apuane. Rend. R. Ist. Lomb. di Sc. e Lett., 5, 733.

Tongiorgi E. Trevisan L., 1940. Aspetti glaciali e forestali delle Alpi Apuane durante l' ultima glaciazione. Atti Soc. Tosc. SC. Nat. Proc. Verb. 49, 3, 55-62.

Trigo, I.F., Bigg, G.R., Davies, T.D., 2002. Climatology of cyclogenesis mechanisms in the Mediterranean. Am. Meteorol. Soc. 130, 549–569.

Vaks, A., Bar-Matthews, M., Ayalon, A., Matthews, A., Frumkin, A., Dayan, U., ... & Schilman, B. (2006). Paleoclimate and location of the border between Mediterranean climate region and the Saharo–Arabian Desert as revealed by speleothems from the northern Negev Desert, Israel. Earth and Planetary Science Letters, 249(3-4), 384-399.

Vaks, A., Bar-Matthews, M., Ayalon, A., Matthews, A., Halicz, L., & Frumkin, A. (2007). Desert speleothems reveal climatic window for African exodus of early modern humans. Geology, 35(9), 831-834.

Vaks, A., Bar-Matthews, M., Matthews, A., Ayalon, A., & Frumkin, A. (2010). Middle-Late Quaternary paleoclimate of northern margins of the Saharan-Arabian Desert: reconstruction from speleothems of Negev Desert, Israel. Quaternary Science Reviews, 29(19-20), 2647-2662.

Vaks, A., Gutareva, O. S., Breitenbach, S. F., Avirmed, E., Mason, A. J., Thomas, A. L., ... & Henderson, G. M. (2013). Speleothems reveal 500,000-year history of Siberian permafrost. Science, 340(6129), 183-186.

Wang, Y., Cheng, H., Edwards, R. L., Kong, X., Shao, X., Chen, S., Wu, J., Jiang, X., Wang, X., An, Z., 2008. Millennial-and orbital-scale changes in the East Asian monsoon over the past 224,000 years. Nature, 451(7182), 1090-1093.

945 Wilson, G. P., Reed, J. M., Frogley, M. R., Hughes, P. D., & Tzedakis, P. C. (2015). Reconciling
946 diverse lacustrine and terrestrial system response to penultimate deglacial warming in southern
947 Europe. Geology, 43(9), 819-822.
948 Zaccagna, D., 1937. Sulla estensione dei ghiacciai delle Alpi Apuane. Att. Soc. Tosc. Sc. Nat. Proc
949 Verb., 46, 65-66
950 Zanchetta, G., Drysdale, R.N., Hellstrom, J.C., Fallick, A.E., Isola, I., Gagan, M., Pareschi, M.T.,
951 2007. Enhanced rainfall in the western Mediterranean during deposition of sapropel S1:
952 stalagmite evidence from Corchia Cave (Central Italy). Quaternary Science Reviews 26, 279-
953 286.
954 Zerboni, A., Trombino, L., Frigerio, C., Livio, F., Berlusconi, A., Michetti, A. M., Rodnight, H.,
955 Spötl, C., 2015. The loess-paleosol sequence at Monte Netto: a record of climate change in the
956 Upper Pleistocene of the central Po Plain, northern Italy. Journal of Soils and Sediments, 15(6),
957 1329-1350.
958 Zhornyak, L.V., Zanchetta, G., Drysdale, R.N., Hellstrom, J.C., Isola, I., Regattieri, E., Piccini, L.,
959 Baneschi, I., Couchoud, I., 2011. Stratigraphic evidence for a “pluvial phase” between ca 8200
960 and 7100 ka from Renella cave (Central Italy). Quaternary Science Reviews 30, 409-417.
961

962 **List of tables (supplementary materials)**

963 Tab. 1 U/Th data used for the age distribution

964 Tab. 2 Elevation used to to estimate the MAAT in the speleothem catchment areas (C1, C2)

965

Highlights

speleothem growth curves used to better constrain the timing of glacial features

293 U\Th ages from 19 speleothems collected in five caves at different elevations

glacial expansion in the Apuan Alps was not only limited to the MIS2

Speleothem U/Th age constraints for the Last Glacial conditions in the Apuan Alps, northwestern Italy.

Isola I.[1], Ribolini A.[2], Zanchetta G.[1,2], Bini M.[1,2], Regattieri E.[2,3], Drysdale R.N.[4,5], Hellstrom J.C.[6] , Bajo P.[6], Montagna P.[7], Edwige Pons-Branchu[8]

[1]Istituto Nazionale di Geofisica e Vulcanologia, Pisa Italy

[2]Dipartimento di Scienze della Terra, University of Pisa

[3]Istituto di Geoscienze e Georisorse-CNR, Pisa

[4]School of Geography, University of Melbourne, Victoria 3010, Australia

[5]Environnements, Dynamiques et Territoires de la Montagne, UMR CNRS, Universite´ de Savoie-Mont Blanc, France

[6]School of Earth Sciences, University of Melbourne, Victoria 3010, Australia

[7]Istituto di Scienze Marine (ISMAR-CNR), Bologna, Italy

[8]Laboratoire des Sciences du Climat et de l'Environnemen, LSCE/IPSL, CEA-CNRS-UVSQ, Université Paris-Saclay, Gif-sur-Yvette, France

Corresponding author: Ilaria Isola Ilaria.isola@ingv.it

Istituto Nazionale di Geofisica e Vulcanologia,via delle Faggiola 32, 56126 Pisa Italy

Abstract

During the Quaternary several glaciations occurred in the mountain regions around the Mediterranean and, in recent years, new ages have better constrained their timing. However, this is not the case for the Apuan Alps, a high-rainfall mountain chain adjacent to the Mediterranean Sea. Here, in spite of the widespread evidence for glaciers, the complete lack of geochronological

information hinders our understanding of glaciation history. In this paper, we utilize speleothem ages to better constrain the timing of these glacial features. We re-examine 293 uranium-thorium ages from 19 speleothems collected in five caves at different elevations. After a period of very low growth between 160 and 132 ka, the analysed speleothems grew almost continuously to ~75 ka, this period was followed by intermittent growth with lower deposition rate and presence of hiatuses until ~12.5 /12 ka. This is consistent with an ice coverage persisting over the Apuan Alps, inhibiting or interrupting the growth of speleothems via the limited availability of groundwater and the scarcity/absence of soils. This interval is much greater than the time interval that has previously been attributed to the existence of glaciers on the Apuan Alps, which has been assumed to be restricted to Marine Isotope Stage (MIS) 2. Instead, ice cover probably also appeared in the Apuan Alps during MIS 4. The phase of restarting of growth, which may implies the definitive or substantial glacier melts seem to predate the Holocene.

Keywords: Glacier; Pleniglacial; MIS2; MIS3; MIS4; Italy

1. Introduction

Speleothems (i.e. cave carbonate deposits) are multi-proxy paleoclimate archives, which can be accurately dated back to several hundred thousand years before present thanks to U-Th isotope systematic (Edwards et al. 1987; Hellstrom, 2006). Most of the paleoclimate research conducted using speleothems focused on the interpretation of stable isotope and trace element proxy records (e.g. Dykoski et al., 2005; Bar-Matthews et al., 1996; Wang et al., 2008; Regattieri et al., 2016). However, speleothems need certain conditions to grow continuously, such as the presence of liquid water, CO_2 and high Ca concentrations in drip waters (e.g. Atkinson et al., 1986; Gascoyne 1992; Genty et al., 2001). This generally implies relatively wet climate conditions, surface temperature above 0 °C and a well-developed soil above the cave (Gordon et al., 1989; Genty et al., 2001,2005). For instance, in desert environments, phases of speleothem growth are important indicators of past

53 humid periods (Burns et al., 2001; Fleitmann et al., 2011; Vaks et al., 2006, 2007, 2010), as well as
54 tufa, which occurrence significantly correlates with wetter phases (Smith et al., 2004; Cremaschi et
55 al., 2015a). Similarly, the growth of speleothems in permafrost or glacier-dominated environments,
56 often marks interruptions of cold conditions (i.e. Berstad et al., 2002; Spötl and Mangini, 2006;
57 Pons-Branchu et al., 2010; Vaks et al., 2013). This is potentially consistent with degradation of
58 permafrost and the formation of large ice-free surfaces, favoring water infiltration and soil
59 formation (Varks et al., 2013). Growth hiatuses within a single or multiple speleothems have been
60 interpreted as evidences of particularly dry and/or cold conditions (e.g. Hodges et al., 2008; Genty
61 et al., 2003, Baldini, 2002; Moreno et al., 2010; Mayer et al. 2012, Stoll et al., 2013), even if the
62 nature and duration of hiatuses in speleothems cannot be unambiguously correlated to climatic
63 conditions. However, stacking multiple speleothem records can give more robust information about
64 the relationship between growth cessations and climate (e.g. Stoll et al., 2013).
65 During glacial periods, depressed external air temperatures at high latitudes and/or high altitudes
66 sites may cause extensive freezing at the surface above a cave, strongly limiting water infiltration
67 (Berstad et al., 2002; Genty et al., 2003,2005; Ayalon et al., 2013) and totally inhibiting soil activity
68 (McDermott, 2004). This implies a strong reduction in the CO_2 transfer to the epikarst, a
69 prerequisite for bedrock dissolution and speleothem growth. Therefore, development of glacial
70 conditions (i.e. the presence of glaciers) in the water-infiltering area over a cave (catchment area
71 from here onwards) would be a factor for reduced or ceased speleothem growth. In such conditions,
72 the only possibility for the deposition of calcite can be related to sulphide oxidation if liquid water
73 is present (Atkinson 1983; Gascoyne and Nelson, 1983; Spötl and Mangini, 2007).
74 In the Mediterranean region there are numerous mountains where geomorphological and
75 geological evidence for the presence of glaciers has been dated (Baroni et al., 2018; Finsinger and
76 Ribolini 2001; Perez-Alberti et al., 2004; Federici et al., 2008; 2012; 2017; Kuhlemann et al., 2008;
77 Hughes et al., 2004, 2011, 2013; Giraudi et al., 2011 Giraudi and Giaccio, 2017; Ribolini al., 2011,
78 2018; Serrano et al. 2012; Hughes and Woodward, 2017 and references therein, Gromig et al.,

79 2018; Hannah et al., 2017; Akçar et al., 2017; Çiner et al., 2017; Sarikaya and Çiner, 2017).
80 However, for some regions, it is still challenging to identify the glacial cycles to which this
81 evidence belongs. This is particularly true for the Apuan Alps, a mid-latitude (44°N) mountain
82 chain in northwestern Italy where, despite the recognition of numerous glacial features, no precise
83 chronological data exist so far.
84 In this paper, we use periods of speleothem deposition as an indicator of ice-free conditions in
85 cave catchment areas, and periods of very low or absent stalagmite growth as proxy for constraining
86 the chronology of glacier presence in the Apuan Alps. To achieve this, we use previously published
87 and new U/Th ages of speleothems from five different caves located at different altitudes (Fig. 1).
88
89 **2. Site description**
90
91 The Apuan Alps is a NW-SE-oriented mountain range rising abruptly to about 2000 m a.s.l. from
92 the narrow coastal plain bordered by the Ligurian Sea (Fig. 1). The atmospheric circulation is
93 dominated by the important cyclogenesis centre of the Gulf of Genoa (Trigo et al., 2002) and by the
94 humid westerly air masses of North Atlantic provenance (e.g. Reale and Lionello, 2013; Fig. 1).
95 These sources of moisture impact on the Apuan Alps mountain chain, which acts as a natural barrier
96 by forcing an adiabatic rise of air masses, resulting in high precipitation (> 2,500 mm/yr Rapetti and
97 Vittorini, 1994; Piccini et al., 2008). As with most of the Apennine chain, winter rainfall amount,
98 which is the main period of recharge of Apuan caves (Piccini et al., 2008), is strongly regulated by
99 the North Atlantic Oscillation (NAO), with a negative correlations observed between NAO index
100 and winter precipitation (López-Moreno et al., 2011).
101 Two main tectono-metamorphic regional events have determined the structural setting of the
102 Apuan Alps (e.g. Carmignani and Kligfield, 1990; Molli and Vaselli, 2006), where extensive areas
103 of carbonate lithologies outcrop (Mesozoic marbles and metadolostones). The actions of glacial,

104 fluvial and karst processes led to an Alpine-like landscape, where exokarst landforms and
105 Quaternary cave systems are particularly developed (Piccini, 1998, 2003, 2011).

106 The Apuan Alps is one of the first places amongst the larger Apennine chain where glacial
107 landforms have been described (Cocchi, 1872; Stopani, 1872). Following these pioneering studies,
108 in the second half of nineteenth and throughout the twentieth century, further qualitative evidence
109 of glacial landforms were reported (De Stefani, 1874,1875,1890; Merciai, 1912; Paci, 1935;
110 Zaccagna, 1937; Tongiorgi and Trevisan, 1940; Beneo, 1945; Masini, 1970; Federici, 1981; 2005;
111 Braschi al., 1987; Putzolu, 1995, Baroni et al. 2013; 2015). Most of these glacial features are now
112 under risk of destruction due to marble quarrying (Bini, 2005). Despite only traces of small glaciers
113 have been reported on the seaward side of the mountain chain (i.e. erosional landforms and a few
114 scattered glacial deposits, Federici, 1981), features associated with at least nine glaciers have been
115 identified on the northern side. These include lateral and terminal moraines, cirques and polished
116 surfaces. Different phases of expansion have been described and, in some cases, the glacier termini
117 reached exceptionally low elevations (~600 a.s.l.) considering the latitude (Braschi et al., 1987;
118 Jaurand, 1998). The best-preserved glacial features, with relatively unweathered, incoherent detrital
119 materials, are traditionally attributed to the Last Glacial Maximum (LGM) by all previous authors
120 on the basis of their fresh appearance and by analogy with the Apennines and Alpine landforms,
121 The temporal definition of LGM itself is not univocal, depending on the considered references, e.g.
122 Clark at al. (2009) defined the LGM as the duration of sea-level lowstand during the interval 26.5-
123 20/19 ka, while Hughes and Gibbard (2015) as the event between the top (end) of Greenland
124 Interstadial 3 and the base (onset) of Greenland Interstadial 2, spanning the interval 27.540-23.340
125 ka (Greenland Stadial 3). In both cases within MIS2.
126 Inner terminal moraines have been interpreted as the Late-Glacial readvance/stillstand phases
127 (Braschi et al., 1987; Federici, 2005). Cemented glacial deposits, rarely outcropping, have been
128 attributed to a pre-LGM glacial event according to their appearance, altitude and stratigraphic
129 position (Braschi et al. 1987). The presence of these older, cemented deposits, attributed to “Riss

130 glaciation" (i.e. penultimate glaciation), has long been debated but no conclusive results have been
131 forthcoming due to the absence of chronological constraints (Federici, 2005), moreover, Kotarba et
132 al. (2001) have dated in the Apennines, similar types of older cemented moraines to the Riss, using
133 U-series.
134
135 **3. Cave descriptions**
136
137 In the Apuan Alps karst massif, about 2000 cave entrances are now mapped with a composite
138 length of cave development of ~500 km (http://www.speleotoscana.it). About 80 caves are carved
139 below the areas potentially covered by glaciers during the Last Glacial expansion, as reconstructed
140 by Braschi et al. (1987). Despite most of the Apuan caves are mainly vertical with active drainage
141 systems, many kilometres of passages are relict and nowadays host carbonate (usually calcite)
142 concretions. Here we focus on speleothems from five caves located at different elevations (Fig. 1).
143 The largest and highest cave is Antro del Corchia (CC), a large complex cave system (~60 km
144 long ~1200 m deep) mainly developed in the Upper Triassic-Liassic marble, dolomitic marble and
145 metadolostone of the Mt Corchia syncline confined by the non-karstifiable, low-permeable rocks of
146 the Paleozoic basement (Piccini et al., 2008).
147 Tana che Urla (TCU) is a small resurgence cave with a permanent stream (~600 m of total length
148 of which almost half is submerged; +45 m of total difference in height), developed at the contact
149 between Paleozoic schist basement and Triassic metadolostone (Regattieri et al., 2012). The
150 entrance is located at ~620 m a.s.l. on the south-eastern side of Panie Massif and functions as an
151 overflow spring during intense rainfall and snowmelt.
152 Grotta Del Vento (GDV) is an almost fossil phreatic cave (~4.5 km total length and over 450 m
153 of elevation change) developed at the contact between the Paleozoic schist basement and Triassic
154 metadolostone. The entrance is located at ~630 m a.s.l. on the south-eastern side of the Panie Massif
155 (Piccini et al., 2003).

Buca della Renella (RL) is a small, shallow cave at the confluence of Canale Regolo and the Frigido River (Drysdale et al. 2006; Zhornyak et al., 2011). The entrance is located at ~275 m a.s.l., only a few metres above the stream confluence. The cave, predominantly horizontal (~200 m length), is carved in Triassic metadolostone close to the contact with the Paleozoic phyllite.

Buca Cava dell'Onice (BCO) is a fossil small cave (85 m long and 65 m deep), carved in Lower Jurassic cherty metalimestone. The entrance is located in the northwest side of Mt. Castagnolo at ~700 m a.s.l.

4. Methods

We consider 19 speleothems (ages in supplementary material, Table 1), collected from the five caves described above. Nine stalagmites and two cores drilled from flowstones have been collected from the "Galleria delle Stalattiti" of the Corchia Cave. This part of the cave is a near-horizontal chamber carved at ~840 m a.s.l., vertically overlain by ~400 m of rock. The chamber lies hundreds of metres above the present groundwater table and is characterised by a mean annual air temperature of 7.8 °C (Piccini et al., 2008). Five speleothems have already been described in previous papers (CC1, CC5, CC7, CC26, CC27 and CC28, Drysdale et al., 2004, 2005, 2007, 2009; Zanchetta et al., 2007; Bajo et al., 2017; Isola et al., 2018). We present new ages for stalagmites CC4, CC7, CC22, CC27, CC53, and two flowstone cores CD4 and CD20.

At TCU two cores have been drilled from the same flowstone in the main gallery, about 100 m from the entrance. The mean air temperature is 10.2 °C (Regattieri et al., 2014a). Speleothem stratigraphy, chronology and geochemistry have been discussed by Regattieri et al. (2012, 2014a, 2016).

Two cores have been drilled from different flowstones located in the middle level of GDV (Piccini et al., 2003).

181 At RL, three samples have been collected in different stratigraphic levels from a fan-like
182 flowstone deposited at the margin of an epiphreatic passage in the inner part of the cave (average air
183 temperature ca. 12 °C) and their stratigraphy and chronology have been discussed by Drysdale et al.
184 (2006) and Zhornyak et al. (2011).
185 Only one stalagmite (BCO1) has been collected in BCO, in a fossil gently dipping gallery, about
186 30 m from the entrance.
187 All ages from Corchia, Tana Che Urla and Renella have been obtained following the same
188 procedure at the University of Melbourne (Victoria, Australia). Briefly, uranium and thorium
189 isotopes were analysed using a Nu Instruments Multicollector Inductively Coupled Plasma–Mass
190 Spectrometer (MC-ICP-MS), according to the analytical method and corrections (where necessary)
191 described by Hellstrom (2003, 2006).
192 Age-depth models and speleothems growth rates were obtained from a Monte Carlo-derived
193 method (described in Drysdale et al. 2005 and Scholz et al. 2012). Dating methods for Grotta del
194 Vento are discussed by Piccini et al. (2003).
195 BCO1 $^{230}Th/^{234}U$ ages were determined at LSCE from 9 subsamples collected along the growth
196 axis of the stalagmite. Subsamples were crushed in an agate pestle and aliquots of typically ~400
197 mg were rinsed twice with MilliQ, dissolved in diluted HCl (~10%) and equilibrated with a mixed
198 ^{236}U-^{233}U-^{229}Th spike that was calibrated against a Harwell Uraninite solution (HU-1) assumed to
199 be at secular equilibrium. Uranium and thorium were purified and separated using Eichrom
200 UTEVA® and pre-filter resins in nitric media following a procedure modified from Pons-Branchu
201 et al. (2005) and Douville et al. (2010). The isotopes of uranium and thorium were analysed by
202 solution multi-collector ICPMS using a ThermoScientific Neptune^{Plus} hosted at the Laboratoire des
203 Sciences du Climat et de l'Environnement (LSCE, Gif-sur-Yvette, France) following the procedure
204 described by Pons-Branchu et al. (2014). Based on the measured atomic ratios, the $^{230}Th/^{234}U$ ages
205 were calculated through iterative age estimation (Ludwig and Titterington, 1994) using the ^{230}Th,
206 ^{234}U and ^{238}U decay constants of Cheng et al. (2013) and Jaffey et al. (1971). An initial $^{230}Th/^{232}Th$

activity ratio of 0.9±50% was used for correction of the non-radiogenic, detrital ^{230}Th fraction.

In order to highlight the higher and lower periods of speleothems deposition rate, we calculate the growth rate for all the considered speleothems from Corchia Cave and for speleothems from lower altitude caves, cumulated at 1000-yr intervals. Uncertainties in the growth rates were obtained using the standard errors propagation.

It is worth estimating potential changes in air temperature at the altitude of the different infiltration areas of the four caves (we ignore BCO because the sole sampled stalagmite covers only MIS 5), in order to understand causes of any leads and lags in speleothem growth phases in the context of likely glacier development. The following calculations represent a first-order estimate that can be used to underpin the interpretations proposed below.

Speleothem growth patterns described above were compared with sea-surface temperature (SST) series from three Mediterranean cores: ODP 161-977 (Martrat et al., 2014) spanning all over the considered period; PRGL1 (Cortina et al., 2015), the nearest core to the Apuan Alps; and MD 90917 (Siani et al 2013), a high-resolution dataset covering the last ~25 kyr (cores locations are shown in Fig. 1). As these cores (ODP 161-977, PRGL1) provide SST data based on Alkenone unsaturation indices (Müller at al., 1998; Conte et al., 2006) and planktonic foraminifera assemblages (Siani et al 2013), they do not reflect exactly the same temperature signal. SST records in the Alboran Sea (ODP191-977) are more related to spring-summer conditions (Martrat et al., 2004, 2014), while the SST records from the Gulf of Lyon reflects a winter-spring temperature signal showing a colder imprint than other more southern SST records (Rigual-Hernández et al., 2013, Cortina et al., 2015). Finally, planktonic foraminifera assemblages coincide with the most productive period during the spring and the synchronous bloom of *G. bulloides* in the Mediterranean Sea (Pujol and Vergnaud-Grazzini, 1995; Siani et al., 2013). In performing the ocean-cave comparisons, we make several assumptions. First, we assume that the difference in mean annual SST (MASST) between the selected marine cores and the MASST offshore of the

232 Apuan Alps (Locarnini et al., 2010) was constant through time; second, that the difference between
233 the MASST and the Mean Annual Air Temperature (MAAT) measured along the coast facing the
234 Apuan Alps (http://www.autorita.bacinoserchio.it/) was constant through time; third, we adopt an
235 air temperature lapse rate of 0.6 °C/100 m (as calculated for the area by Rapetti and Vittorini, 2012)
236 to estimate the MAAT in the speleothem catchment areas of four of the studied caves. For the
237 elevations of the water recharge area feeding the caves, two values are considered: the elevation of
238 the surface above the cave on the vertical of the sampling sites (C1, supplementary material Table
239 2) and the average between this point and the highest point of the drainage basin (C2,
240 supplementary material 2). The first is the most conservative value representing the minimum
241 elevation of recharge area while the second is probably more realistic because takes into account the
242 whole hydrographic basin upvalley the cave. A more refined estimate of MAAT could incorporate
243 also the effects of sea-level lowering during glaciations and tectonic uplift (estimates to be 0.6
244 mm/yr; Fellin et al. 2007; Piccini 2011) of the Apuan Alps. However, both effects introduce
245 negligible temperature variations. Indeed, the maximum increase in relative elevation of the
246 infiltration area above the contemporary sea level is during the LGM (e.g. ca. 100-120 m for the
247 LGM, Lambeck and Bard 2000; Lambeck et al., 2014), corresponding to a total temperature
248 variation (ΔT) of about -0.6°C, while the lowest, during MIS6, corresponds to ΔT of about +0.1°C.
249

250 **5. Results**

251 For the 19 speleothems considered, the dataset comprises 293 U/Th ages (supplementary
252 material Table 1). In Figure 2, the ages are plotted vs the elevation of the sampling sites.
253 Despite some differences, there are many common features. All caves show a major episodes of
254 calcite deposition during the Holocene and the latest Late Glacial. Available samples from RL and
255 GDV do not show phases of growth older than this period and the studied concretions cover, or are
256 stratigraphically located over, thick fluvial deposits. TCU shows continuous deposition between ca.

160 and 121 ka (Regattieri et al., 2014a), followed by a discontinuous deposition to ca. 75 ka, after which there is a long hiatus from ca. 75 to 12.5 ka. The most relevant record is represented by Corchia Cave, showing almost continuous calcite deposition from ca. 145 to 79 ka. A long lag of growth, with only very reduced phases of calcite deposition is evident during the Pleniglacial. The stalagmite from BCO has an intermittent growth phase throughout MIS 5, confirming a speleothems deposition phase during this period in the Apuan Alps. No information about other periods including the Holocene are available for this site until now, but we cannot exclude further growing phases, in fact, a single speleothem cannot be considered representative of the whole speleothems growth history of this cave.

More interesting than the simple ages distribution is the cumulative growth curve which takes into account the propagation of age errors for Corchia cave speleothems and for the other studied caves located at lower altitudes (Fig. 3). It is evident that speleothem growth at Corchia, after a period of low values, becomes significant between ca.132 and 80 ka (curve b in figure 3), after which it decreases abruptly until ca. 60 ka, and then almost stops for ca. 44 kyr. Continuous growth resumes at ca. 15 ka and increases later at ca. 12 ka.

The growth of speleothems belonging to the lower-altitude caves evidently decreases after 130 ka, reaching a local minimum at ca. 100 ka. An increase of composite growth rate is then observed around 80 ka, followed by an interruption in calcite deposition up to 13 ka.

Figure 4 shows the estimation of MAAT as described above. Due to the very similar geographic location (fig. 1), GDV and TCU temperature estimates are almost indistinguishable in all the reconstructions (blue and black lines in Fig. 4). The MAAT curves obtained for each cave using MD90917 data (~ 0.6 - 24 ka interval), including the two different infiltrating elevations (C1 and C2), are shown respectively in Figure 4a and b. The MAAT curves obtained using ODP 161-977 data (~ 0.06 - 120 ka interval) are shown respectively in figure 4c and d. The MAAT curves obtained using PRGL1 data (~ 29 - 120 ka interval) are shown respectively in Figure 4e and f. In the C1 cases (Fig. 4a, c, e) only the CC series displays excursions where MAAT is <0°C. In the C2

283 scenario (Fig. 4b, d, f), GDV and TCU areas also show periods when MAAT is <0°C. As expected,
284 the temperature above RL is the mildest.
285
286 **6. Discussion**
287
288 According to the presented data, there is a long interval during the Pleniglacial where calcite
289 deposition at CC and TCU caves slows down or is absent (fig. 3). This interval roughly corresponds
290 to an extensive loess deposition in the Po Plain (Fig. 1 and 5; Cremaschi et al., 2015b; Zarboni et
291 al., 2015). This marks a wide phase of aridity in northern Italy that might have involved also the
292 Apuan Alps, but probably with different effects. Nowadays the mean annual precipitation in Po
293 Plain does not exceed 1000 mm (www.arpalombardia.it), while the Apuan Alps are characterized
294 by higher precipitations exceeding 2500mm/yr (Rapetti and Vittorini, 1994; Piccini et al., 2008).
295 The different geographic position underpinning the actual rainfall regime, certainly played a role in
296 the past too, mitigating the drought effect in the Apuan Alps. Moreover, it is very difficult to
297 explain in a dry regime, the strong fluvial activity suggested, in the low elevation caves, by the
298 presence of thick fluvial deposits, stratigraphically older than the phase of speleothems regrowth
299 (about 12.5 ka). The resumption of calcite deposition is almost coeval in all caves, with evidence of
300 sustained growth slightly preceding the beginning of the Holocene, instead,the period of deposition
301 decrease, at the end of MIS5, is not coeval between TCU and CC. However, the CC dataset is more
302 extensive because the number of analyzed speleothems.
303 Moreover, this cave is very close to areas of the catchment occupied by glaciers in the Last
304 Glacial (Fig.1). Specifically, the recharge basin of the "Galleria delle Stalattiti", mainly consisting
305 of the higher slopes of the northern side of Monte Corchia, was covered by a glacier according to
306 Braschi et al. (1987). The most obvious process responsible for the strong reduction of speleothem
307 growth at the "Galleria delle Stalattiti" would thus be a persistent ice cover. This long interval of
308 extremely reduced or absent calcite deposition covers most of MIS4-MIS2, a time span more

309 extensive than the classical attribution of Apuan glacial activity to the only Last Glacial Maximum
310 (Federici, 2005; Jaurand 1998). This hypothesis is supported by evidence of moraines formed
311 during MIS3 and MIS4 glacier expansions in the Central Apennines (Giraudi et al. 2011; Giraudi
312 and Giaccio, 2015, 2017). In this regard, the Corchia speleothems cumulative growth curve delimits
313 for the first time the temporal interval of possible glacier existence over the Apuan Alps or
314 temperature lower enough to inhibit speleothem growth at higher altitudes. Although the
315 chronological constraints are indirect because they do not refer to moraine ages, there is
316 considerable robustness in the speleothem-age dataset. However, cessation of speleothem growth
317 can be related to combined effect of low air temperature, soil-CO_2 deficiency and reduction of
318 dripping. These conditions might have been present without invoking continuous ice covering of the
319 slopes, i.e. where permafrost inhibits water infiltration and following dryer cave conditions. In the
320 nearby Apennine chain, landforms diagnostic of permanently frozen ground are rare and essentially
321 limited to the southern latitudes, where higher elevations are reached (Kotarba et al., 2001; Giraudi
322 et al., 2011; Oliva et al., 2018).

323 The absence of speleothem growth in the other caves during the glacial period cannot be directly
324 related to the reconstructed ice cover (Braschi et al. 1987) because of their lower altitudes. A recent
325 geomorphology synthesis of the Apuan Alps (Baroni et al., 2015) does not report glacial deposits
326 indicative of a glacial cover of the lower caves.

327 At RL and GDV, the presence of thick fluvial deposits stratigraphically older than the phase of
328 speleothem growth (about 12.5 ka) suggests strong fluvial activity during the glacial period, which
329 would inhibit speleothem growth (Zhornyak et al., 2011). This strong activity might be related to
330 seasonal snow/ice melting and abundant availability of loose material coming from physical
331 weathering. A similar explanation is also valid for the long deposition hiatus at TCU (about 12.6-75
332 ka). A continuous glacier cover nearby is unlikely throughout this period.

333 It is noteworthy that both CC and TCU show speleothem deposition during part of MIS6,
334 suggesting that temperatures over the Apuan Alps during this period were not as low as those for

MIS2-4. The transition between the penultimate glacial and the last interglacial, is marked by the abrupt increase of speleothems growth about 132 ka, as already described for CC by Drysdale et al., (2009) and for TCU by Regattieri et al. (2014a) and in agreement with other proxies like the more umid-temperate vegetation in Southern Europe (Sanchez –Goñi et al., 1999), or the high level in Ioannina Lake (Wilson et al., 2015). Then, speleothem growth, which was possible for most of MIS5, decreases or ceases during the interval MIS2-4 (Fig. 3).

The almost coeval resumption of calcite deposition in all the investigated caves requires further discussion. At CC, some U/Th ages indicate that a small growth phase also occurs at the beginning of the Late Glacial, but significant growth did not occur before ca. 12 ka. However, given the southern latitude and the relatively low altitude of the Apuan Alps, it is hard to argue that glaciers still existed during the middle part of the Lateglacial (Hughes and Gibbard, 2015). Based on deglacial trends in CC speleothem carbon isotope composition, Drysdale et al. (2004) and Zanchetta et al. (2007) have suggested that soil development at CC is delayed after glacial periods due to intense erosive processes active at high altitudes during the first phases of climatic amelioration, under conditions of increasing rainfall. After the definitive ice melting at the end of MIS2, cold but ice-free conditions and delayed soil development would have retarded significant speleothem growth, which did not accelerate until ca. 12 ka. The fundamental elements of this hypothesis are supported by Bajo et al. (2017), who also invoked near-closed-system conditions and sulphuric-acid dissolution as additional processes to carbonate-acid dissolution (from soil-sourced CO_2) to explain the unusually high carbon isotope composition of CC26 stalagmite during late Late Glacial and the beginning of Holocene. However, an implication of this study is that growth was unsuitable before ca. 12 ka, in spite of the possibility of sulphuric-acid dissolution substituting for carbonic-acid dissolution, thus suggesting that speleothem growth was inhibited by cold climate conditions. From the same stalagmite, Regattieri et al. (2014b) concluded, based on the presence of an aragonite layer at the base of the CC26 succession and on trace element/Ca ratios (Ba, Sr, Mg) changes, that the

start of growth of CC26 was related to a re-opening of a dripping point due to the replenishing of the cave plumbing system previously interrupted by reduced recharge.

Whilst we cannot detail the point at which resumption of speleothem growth occurred in CC during the Late Glacial, conditions generally favoring speleothem growth seem to have occurred when the plumbing system was newly recharged significantly even if ice cover should have already disappeared. It is probably not obvious that these conditions did not concomitantly occur in upper and lower altitude caves. Studying the transition between MIS6 and MIS5 at TCU Regattieri et al. (2014a) suggested that the delay in soil development as inferred for CC is not supported for TCU, due to its lower altitude. This may suggest that an earlier resumption of speleothem growth would be anticipated at lower altitude compared to CC. Data collected until now agree with this hypothesis (Fig. 3). We suggest that significant resumption of calcite deposition at CC can occur only when soil development and drip recharge are restored to a certain level.

According to the timing of speleothem growth and MAAT estimations, it can be seen that above CC both the C1 and C2 MAAT reconstructions experienced a number of long-lasting sub-zero periods. Indeed, the Equilibrium Line Altitude (ELA) of 1200-1300 m a.s.l. in the Apuan Alps during the MIS 2 (Merciai, 1912; Braschi et al., 1987; Jaurand, 1998) supports the hypothesis that in the CC catchments (both C1 1240 m a.s.l. and C2 1460m a.s.l.) glaciers were existing. These unfavorable conditions for speleothem deposition (MAAT subzero or near 0 °C) persisted, discontinuously, above CC not only during the MIS 2, but also during MIS 4 (Fig. 4). This is consistent with evidence of a phase of glaciation during MIS 4 from the Alps and other peri-Mediterranean mountain ranges (Hughes et al. 2013; 2018; Sarikya et al., 2014; Pope et al., 2017) (blue bars in Fig. 5a). There are evidences of very small growth phases during MIS4-MIS2 (Fig. 2, 3, 5d) that may have occurred during warming reversals, most likely associated with the millennia-scale interstadials observed in the Greenland ice-core records (i.e. Dansgaard-Oeschger events,

386 Dansgaard et al., 1993; Fig. 5e), but also indicated by SST changes in the western Mediterranean
387 (Cacho et al., 1999).

388 In general, pollen data from the western Mediterranean show that cold SSTs characteristic of
389 Greenland stadials were contemporaneous with the expansion of semi-desert or steppic vegetation.
390 On the contrary, Greenland interstadials were synchronous with the expansion of open forests
391 (Sánchez-Goñi et al., 2008). Presumably, phases of forest expansion prompted the development of
392 deeper soils. However, the very limited speleothem growth and the available ages prevent a precise
393 correlation with the warmer intervals. On the other hand, according to Atkinson (1983) and Sp□tl et
394 al. (2007), speleothems may form, although with a lower rate of growth, in caves overlain by
395 temperate glaciers with available glacial meltwater infiltrating the karst system. The very low
396 partial pressure of CO_2 in such water due to the absence of soil can be balanced by pyrite oxidation
397 during the flow paths through fractures, providing the dissolved carbonate necessary for speleothem
398 deposition. This process is demonstrably present at Corchia (Piccini et al., 2008; Bajo et al., 2017)
399 and can be responsible of the very thin deposition layers included between two hiatus.

400 Summing up, growth histories and temperature estimation support the hypothesis that
401 interruptions or strong reductions in speleothem growth at Corchia could have been due to a
402 combination of glaciation and/or ice-free but cold temperatures with low or absent soil activity.

403 Glacial phases occurring in this period in the mountain regions around the Mediterranean are
404 confirmed by multi-proxy analyses carried out on the glacial lacustrine sequences, as evidenced by
405 a maximum of glacier expansion of Pyrenean glaciers before 30 ka (Garcia-Riuz at al., 2003) and in
406 Picos de Europa dated at about 40 ka (Moreno et al. 2010; Serrano et al., 2012). Consistently in the
407 central Apennines, tephra layers in lacustrine sediments bracket the maximum glacier extent
408 between 33-27 ka, not a period of maximum cold conditions but one that was humid (Giraudi,
409 2012). Regarding the Alps there is a controversial discussion about glaciers extent before MIS 2
410 when the maximum expansion was reached (Ivy-Ochs et al. 2008; Preusser et al. 2011; Hughes et
411 al. 2013). The uncertainties mainly derive from the fact that the majority of terrestrial records (i.e.

glacial deposit, pro-glacial outwash, river terrace, lake deposit) were eroded, or at least remoulded or reworked, when MIS 2 glaciers invaded the valleys and in many cases spread out in piedmont lowlands. Indeed, while in the Eastern Alps no evidence for the presence of pre-MIS 2 glaciers are clearly found (Ivy-Ochs et al., 2008), an important glaciation reaching the lowlands of the Western Alps during MIS 4 is documented by OSL dating of pro-glacial outwash (Preusser et al. 2007) and lake sediments (Link and Preusser 2006).

The above described asynchronicity is not contradictory a priori, because it may be explained by the short reaction times of small glaciers (like those of most of the Mediterranean mountains) to changes in precipitation and/or temperature. Further sampling may reveal sporadic or very slow episodes of growth during this time interval, allowing better and more precise interpretations of MIS 3 climatic oscillations.

7. Conclusions

Speleothems in the Apuan Alps grew near-continuously during most of MIS5 (from ca. 130 ka to about 75 ka), then experienced a long period of absent to very low deposition covering the MIS4 to MIS2 interval, until ~12.5 ka. This growth history can be explained as the result of development of glaciers at high elevations, not necessarily continuously existent for the whole considered period, and/or low soil development and near-zero temperatures. The speleothem growth curves may suggest that glacial expansion in the Apuan Alps was not only limited to the LGM (MIS2) but also to MIS3 and MIS4, analogous to other peri-Mediterranean mountains.

During spring and summer ice-melting periods, high water discharges occurred and caves located at lower altitudes were flooded, resulting in phreatic conditions, inhibiting speleothem deposition and infilling caves with thick fluvial deposits.

There is no evidence of significant growth during interstadials within MIS3, which supports the fact that no particularly warm conditions occurred in the Apuan Alps during those climatic events.

Sustained speleothem growth resumed close to the beginning of the Holocene both at lower and high-altitude caves. This can be interpreted as the result of a definitive melting of ice cover and the consequent progressive soil development at high altitude, and the stabilisation of loose glacial debris and reduced flooding for lower altitude caves.

These data indicate the potential for cumulative speleothems growth curve to chronologically constrain large-scale geomorphological processes, like the timing of glaciers presence. However, other processes can locally bias the speleothem growth (i.e. cold-non glacial conditions, absence/limited soils), suggesting that this approach is restricted to a first-order approximation which should be followed by a direct dating of glacial features. Moreover, the adoption of speleothem growth curves needs to be verified in other mountain ranges, where U/Th dating can be used for constraining glacial events.

Acknowledgments

We would like to thank two anonymous reviewers for their comments on this paper and helpful suggestions for improvements. We thank the Federazione Speleologica Toscana and Parco Regionale delle Alpi Apuane for supporting our work on Apuan speleothems. This work is part of Australian Research Council *Discovery Projects* grant DP110102185 (leader RD), and the ARCA project “Arctic: present climatic change and past extreme events” founded by the Italian Ministry of Education, Universities and Research (MIUR). These analyses contribute to the project "Clima ed eventi alluvionali estremi in Versilia: integrazione di nuove tecniche geoarcheologiche, geomorfologiche, geochimiche e simulazioni numeriche” (leader M. Bini), funded by "Fondazione Cassa di Risparmio di Lucca Call 2016" and Project PRA (2017/18) “Palaeoclimatic

462 palaeoenvironmental evolution of the Apuan area since the Last Glacial Maximum". (leader C.
463 Baroni), funded by Pisa University.
464
465 **References**
466

467 Akçar, N., Yavuz, V., Yeşilyurt, S., Ivy-Ochs, S., Reber, R., Bayrakdar, C., Kubik, P.W., Conradin,
468 Z., Schlüchter, C. 2017. Synchronous last glacial maximum across the Anatolian Peninsula.
469 From Hughes, P.D., Woodward J.C. (eds) Quaternary glaciation in Mediterranean Mountains,
470 Geological Society, London, Special Publications, 433, 137-159
471 Atkinson, T. C. 1983. Growth mechanisms of speleothems in castleguard cave, Columbia Icefields,
472 Alberta, Canada. Arctic and Alpine Research, 15,4, 523-536.
473 Atkinson, T. C., Lawson, T. J., Smart, P. L., Harmon, R. S., Hess, J. W. 1986. New data on
474 speleothem deposition and palaeoclimate in Britain over the last forty thousand years. Journal
475 of Quaternary Science, 1,1, 67-72.
476 Ayalon, A., Bar-Matthews, M., Frumkin, A., Matthews, A., 2013. Last Glacial warm events on
477 Mount Hermon: the southern extension of the Alpine karst range of the east Mediterranean.
478 Quaternary Science Reviews, 59, 43-56.
479 Bajo, P., Borsato, A., Drysdale, R., Hua, Q., Frisia, S., Zanchetta, G., Hellstrom, J., Woodhead, J.
480 2017. Stalagmite carbon isotopes and dead carbon proportion (DCP) in a near-closed-system
481 situation: An interplay between sulphuric and carbonic acid dissolution. *Geochimica et*
482 *Cosmochimica Acta*, *210*, 208-227.
483 Baldini, J. U., McDermott, F., Fairchild, I. J., 2002. Structure of the 8200-year cold event revealed
484 by a speleothem trace element record. Science, 296, 5576, 2203-2206.
485 Bar-Matthews, M., Ayalon, A., Matthews, A., Sass, E., Halicz, L., 1996. Carbon and oxygen
486 isotope study of the active water-carbonate system in a karstic Mediterranean cave:

implications for paleoclimate research in semiarid regions. Geochim. Cosmoch. Acta, 60, 337-347.

Baroni, C., Bini, M., Coltorti, M., Fantozzi, P., Guidobaldi, G., Nannini, D., Pieruccini, P., Ribolini, A., Salvatore, M.C., 2013. Geomorphological maps as a key approach for enhancing the natural and cultural heritage of the Apuan Alps Regional Park area and surroundings (Tuscany, Italy) Rendiconti Online Societa Geologica Italiana, 28, 10-14.

Baroni, C., Pieruccini, P., Bini, M., Coltorti, M., Fantozzi, P. L., Guidobaldi, G., Nannini, D., Ribolini, A., Salvatore, M. C. 2015. Geomorphological and neotectonic map of the Apuan Alps (Tuscany, Italy). Geografia Fisica e Dinamica Quaternaria, 38,2, 201-227.

Beneo, E., 1945. Nuova località fossilifera e nuovo ghiacciaio nelle Alpi Apuane.Boll. Soc. Geol. It., 64, 40-41.

Baroni, C., Guidobaldi, G., Salvatore, M. C., Christl, M., Ivy-Ochs, S. 2018. Last glacial maximum glaciers in the Northern Apennines reflect primarily the influence of southerly storm-tracks in the western Mediterranean. Quaternary Science Reviews, 197, 352-367.Berger, A., Loutre, M.F., 1991. Insolation values for the climate of the last 10 million years. Quaternary Science Reviews 10, 297–317.

Berstad, I.M., Lundberg,J., Lauritzen, SE., Linge, H.C. 2002. Comparison of the Climate during Marine Isotope Stage 9 and 11 Inferred from a Speleothem Isotope Record from Northern Norway. Quaternary Research 58, 361–371.

Bini, M., 2005. Glacial landforms in the Apuan Alps (Tuscany), features in danger of extinction. Il Quaternario, Italian Journal of Quaternary Sciences, 18, 1, Volume Speciale, 173-176.

Braschi, S., Del Freo, P., Trevisan, L., 1987. Ricostruzione degli antichi ghiacciai sulle Alpi Apuane . Atti Soc. Tosc. Sc. Nat., Mem., Serie A. 93, 203-219, fig. 10, tav.f.t. 1, 1987.

511 Burns, S.J., Fleitmann D., Matter, A., Neff U., Mangini A., 2001. Speleothem evidence from Oman
512 for continental pluvial events during interglacial periods. Geology, Geology; July 2001; v. 29
513 (7); pp. 623–626;
514 Carmignani L., Kligfield R, 1990. Crustal extension in the Northern Apennines: the transition from
515 compression to extension in the Alpi Apuane Core Complex. Tectonics, 9, 6, 1275-1303.
516 Cacho, I., Grimalt, J. O., Pelejero, C., Canals, M., Sierro, F. J., Flores, J. A., Shackleton, N., 1999.
517 Dansgaard-Oeschger and Heinrich event imprints in Alboran Sea
518 paleotemperatures. Paleoceanography, 14,6, 698-705.
519 Cheng, H., Lawrence Edwards, R., Shen, C.-C., Polyak, V. J., Asmerom, Y., Woodhead, J. D.,
520 Hellstrom, J., Wang, Y., Kong, X., Spötl, C., Wang, X., Calvin Alexander, E., 2013.
521 Improvements in 230Th dating, 230Th and 234U half-life values, and U–Th isotopic
522 measurements by multi-collector inductively coupled plasma mass spectrometry, Earth Planet.
523 Sci. Lett., 371-372, 82–91

524 Çiner, A., Sarıkaya, M. A., 2017. Cosmogenic 36Cl geochronology of late Quaternary glaciers in
525 the Bolkar Mountains, south central Turkey. Geological Society, London, Special
526 Publications, 433,1, 271-287. From Hughes, P.D., Woodward J.C. (eds) Quaternary glaciation
527 in Mediterranean Mountains, Geological Society, London, Special Publications, 433, 137-159
528 Clark, P.U., Dyke, A.S., Shakun, J.D., Carlson, A.E., Clark, J., Wohlfarth, B., Mitrovica, J.X.,
529 Hostetler, S.W., McCabe, A.M., 2009. The Last Glacial Maximum. *Science* 325, 710-714.
530 Cocchi I., 1872. Del terreno glaciale delle Alpi Apuane. Boll. Del R. Com. Geol. 3, 7-8.
531 Cortina, A., Sierro, F. J., Flores, J. A., Martrat, B., Grimalt, J. O., 2015. The response of SST to
532 insolation and ice sheet variability from MIS 3 to MIS 11 in the northwestern Mediterranean
533 Sea (Gulf of Lions). *Geophysical Research Letters*, *42,* 23.
534 Cremaschi, M., Zerboni, A., Charpentier, V., Crassard, R., Isola, I., Regattieri, E., Zanchetta, G.
535 2015a. Early–Middle Holocene environmental changes and pre-Neolithic human occupations

536 as recorded in the cavities of Jebel Qara (Dhofar, southern Sultanate of Oman). Quaternary
537 International, 382, 264-276
538 Cremaschi, M., Zerboni, A., Nicosia, C., Negrino, F., Rodnight, H., Spötl, C., 2015b. Age, soil-
539 forming processes, and archaeology of the loess deposits at the Apennine margin of the Po
540 plain (northern Italy): New insights from the Ghiardo area. Quaternary International, 376, 173-
541 188.
542 Dansgaard, W., Johnsen, S. J., Clausen, H. B., Dahl-Jensen, D., Gundestrup, N. S., Hammer, C. U.,
543 Hvidberg, J.P., Steffensen, A.E., Sveinbj□rnsdottir, A.E., Jouzel, J., Bond, G., 1993. Evidence
544 for general instability of past climate from a 250-kyr ice-core record. *Nature*, *364*, 6434, 218.
545 De Stefani C., 1874. Gli antichi ghiacciai dell'Alpe di Corfino, ed altri dell'Appennino settentrionale
546 e delle Alpi Apuane. Boll. R. Com. Geol. d'It, 5, 86-95.
547 De Stefani C., 1875. Dei depositi alluvionali e della mancanza di terreni glaciali nell'Appennino
548 della valle del Serchio e nelle Alpi Apuane. Boll. R. Com. Geol. d'It., 1, 2, 3-18.
549 De Stefani C., 1890. Gli antichi ghiacciai delle Alpi Apuane. Boll. del C.A.I. 24, 57, 175-202.
550 Douville, E., Sallé, E., Frank, N., Eisele, M., Pons-Branchu, E., Ayrault, S., 2010. Rapid and
551 precise ^{230}Th/U dating of ancient carbonates using Inductively Coupled Plasma - Quadrupole
552 Mass Spectrometry. Chem. Geol., 272, 1-11.
553 Dykoski, C. A., Edwards, R. L., Cheng, H., Yuan, D., Cai, Y., Zhang, M., Lin, Y., Qing, J,
554 Zhisheng A., Revenaugh, J., 2005. A high-resolution, absolute-dated Holocene and deglacial
555 Asian monsoon record from Dongge Cave, China. Earth and Planetary Science Letters, 233, 1,
556 71-86.
557 Drysdale, R.N., Zanchetta, G., Hellstrom, J.C., Fallick, A.E., Zhao, J.X., Isola, I., Bruschi, G., 2004.
558 Palaeoclimatic implications of the growth history and stable isotope (δ^{18}O and δ^{13}C)
559 geochemistry of a Middle to Late Pleistocene stalagmite from central-western Italy. Earth and
560 Planetary Science Letters 227, 215-229.

561 Drysdale, R.N., Zanchetta, G., Hellstrom, J 604 .C., Fallick, A.E., Zhao, J.X., 2005. Stalagmite
562 evidence for the onset of the Last Interglacial in southern Europe at 129+/−1 ka. Geophysical
563 Research Letters 32, 1-4.
564 Drysdale, R.N., Zanchetta, G., Hellstrom, J.C., Maas, R., Fallick, A.E., Pickett, M., Cartwright, I.,
565 Piccini, L., 2006. Late Holocene drought responsible for the collapse of old World civilizations
566 is recorded in an Italian cave flowstone. Geology 34, 101-104.
567 Drysdale, R.N., Zanchetta, G., Hellstrom, J.C., Fallick, A.E., McDonald, J., Cartwright, I., 2007.
568 Stalagmite evidence for the precise timing of North Atlantic cold events during the early last
569 glacial. Geology 35, 77–80.
570 Drysdale, R.N., Zanchetta, G., Hellstrom, J.C., Fallick, A.E., Sanchez-Goni, M.F., Couchoud, I.,
571 McDonald, J., Maas, R., Lohmann, G., Isola, I., 2009. Evidence for obliquity forcing of glacial
572 termination II. Science 325, 1527-1531.
573 Edwards, R. L., Chen, J. H., Wasserburg, G. J., 1987. 238 U 234 U 230 Th 232 Th systematics and
574 the precise measurement of time over the past 500,000 years. Earth and Planetary Science
575 Letters, 81, 2, 175-192.
576 Federici, P.R., 1981. The Quaternary Glaciation on the sea ward side of the Apuan Alps . Riv.
577 Geogr. It., 88, 183-199.
578 Federici, P.R., 2005. Aspetti e problemi della glaciazione pleistocenica nelle Alpi Apuane. Istituto
579 Italiano di Speleologia Mem. XVIII, s II, 19-32.
580 Federici, P.R., Granger, D.E., Pappalardo, M., Ribolini, A., Spagnolo, M., Cyr, A.J. 2008. Exposure
581 age dating and Equilibrium Line Altitude reconstruction of an Egesen moraine in the Maritime
582 Alps, Italy. Boreas, 37, 2,245-253.
583 Federici, P.R., Granger, D.E., Ribolini, A., Spagnolo, M., Pappalardo, M., Cyr, A.J., 2012. Last
584 Glacial Maximum and the Gschnitz stadial in the Maritime Alps according to 10Be cosmogenic
585 dating. Boreas, 41, 2, 277-291.

586 Federici, P.R., Ribolini, A., Spagnolo M., 2017. Glacial history of the Martime Alps from the last
587 Glacial maximum to Little Ice Age. From Hughes, P.D., Woodward J.C. (eds) 2017 Quaternary
588 glaciation in Mediterranean Mountains, Geological Society, London, Special Publications, 433,
589 137-159
590 Fellin, M. G., Reiners, P. W., Brandon, M. T., Wüthrich, E., Balestrieri, M. L., Molli, G., 2007.
591 Thermochronologic evidence for the exhumational history of the Alpi Apuane metamorphic
592 core complex, northern Apennines, Italy. *Tectonics*, *26*,6.
593 Finsinger, W., Ribolini, A., 2001. Late Glacial to Holocene deglaciation of the Colle del Vei del
594 Bouc-Colle del Sabbione area (Argentera Massif, Maritime Alps, Italy-France) [Deglaciazione
595 Tardiglaciale-Olocenica dell'area Colle del Sabbione-Colle del Vei del Bouc (Massiccio
596 dell'Argentera, Alpi Marittime, Italia-Francia)] Geografia Fisica e Dinamica Quaternaria, 24, 2)
597 141-156.
598 Fleitmann , D., Burns, S.J., Pekala, M., Mangini, A., Al-Subbary, A., Al-Aowah, M., Kramers, J.,
599 Matter, A. 2011. Holocene and Pleistocene pluvial periods in Yemen, southern Arabia.
600 Quaternary Science Reviews 30, 783-787
601 García-Ruiz, J. M., Valero-Garcés, B. L., Martí-Bono, C., González-Sampériz, P. 2003.
602 Asynchroneity of maximum glacier advances in the central Spanish Pyrenees. Journal of
603 Quaternary Science 18, 61-72.
604 Gascoyne, M., Nelson, D. E., 1983. Growth mechanisms of recent speleothems from Castleguard
605 Cave, Columbia Icefields, Alberta, Canada, inferred from a comparison of uranium-series and
606 carbon-14 age data. *Arctic and Alpine Research*, *15,*4, 537-542.
607 Gascoyne, M., 1992. Palaeoclimate determination from cave calcite deposits. Quaternary
608 Science Reviews 11 (6), 609–632. doi:10.1016/0277-3791, 92, 90074-I.
609 Genty, D., Baker, A., Vokal, B., 2001. Intra-and inter-annual growth rate of modern
610 stalagmites. Chemical Geology, 176, 1-4, 191-212.

611 Genty, D., Blamart, D., Ouahdi, R., Gilmour, M., Baker, A., Jouzel, J., Van-Exter, S., 2003. Precise
612 dating of Dansgaard–Oeschger climate oscillations in western Europe from stalagmite
613 data. Nature, 421, 6925, 833-837.
614 Genty, D., Combourieu Nebout N., Hatté C., Blamart D., Ghaleb B., Isabello L., 2005. Rapid
615 climatic changes of the last 90 kyr recorded on the european continent. Comptes Rendus de
616 l'Académie des Sciences de Paris, 337, 970-982.
617 Giraudi, C. 2012. The Campo Felice Late Pleistocene Glaciation (Apennines, Central Italy). Journal
618 of Quaternary Science, 27, 4, 432-440
619 Giraudi, C, Bodrato G, Ricci Lucchi M, Cipriani M., Villa I.M., Giaccio, B. Zuppi, G.M., 2011.
620 Middle and Late Pleistocene Glaciations in the Campo Felice basin (Central Apennines-Italy).
621 Quaternary Research 75, 219–230.
622 Giraudi C., Giaccio, B. 2017. The middle Pleistocene glaciations on the Apennines (Italy): new
623 chronological data and considerations about the preservation of the glacial deposits.
624 Form Hughes, P.D., Woodward J.C. (eds) Quaternary glaciation in Mediterranean Mountains,
625 Geological Society, London, Special Publications, 433, 161-178
626 Gordon, D., Smart, P. L., Ford, D. C., Andrews, J. N., Atkinson, T. C., Rowe, P. J., Christopher, N.
627 S. J., 1989. Dating of late Pleistocene interglacial and interstadial periods in the United
628 Kingdom from speleothem growth frequency. Quaternary research, 31, 1, 14-26.
629 Gromig, R., Mechernich, S., Ribolini, A., Wagner, B., Zanchetta, G., Isola, I., Bini, M., Dunai, T.J.,
630 2017. Evidence for a Younger Dryas deglaciation in the Galicica Mountains (FYROM) from
631 cosmogenic 36Cl. Quaternary International
632 Hannah, G.H., Hughes, P.D., Gibbard, P.L., 2017. Plistocene plateau ice fields in the High Atlas,
633 Morocco. Form Hughes, P.D., Woodward J.C. (eds) Quaternary glaciation in Mediterranean
634 Mountains, Geological Society, London, Special Publications, 433, 25-54
635 Hellstrom, J. 2003 Rapid and accurate U/Th dating using parallel ion-counting multi-collector ICP-
636 MS, J. Anal. At. Spectrom.18, 135– 1346.

637 Hellstrom, J. 2006. U–Th dating of speleothems with high initial 230 Th using stratigraphical
638 constraint. Quaternary Geochronology, 1,4, 289-29.
639 Hodge, E. J., Richards, D. A., Smart, P. L., Ginés, A., Mattey, D. P., 2008. Sub-millennial climate
640 shifts in the western Mediterranean during the last glacial period recorded in a speleothem from
641 Mallorca, Spain. Journal of Quaternary Science, 23, 8, 713-718.
642 Hughes, P. D.; Gibbard, P. L.; Woodward, J. C., 2004. Quaternary glaciation in the Atlas
643 Mountains of North Africa. Developments in Quaternary Sciences, 2, 255-260.
644 Hughes, P.D., Gibbard, P.L., 2015. A stratigraphical basis for the Last Glacial Maximum (LGM).
645 Quaternary International. DOI: 10.1016/j.quaint.2014.06.006
646 Hughes, P. D., Woodward, J. C., Van Calsteren, P. C., Thomas, L. E., 2011. The glacial history of
647 the Dinaric Alps, Montenegro. Quaternary Science Reviews, 30 23, 3393-3412.
648 Hughes, P.D., Fenton, C.R., Fink, D., Schnabel, C., and Rother, H., 2011. Extent, timing and
649 palaeoclimatic signifi cance of glaciation in the High Atlas, Morocco. Quaternary International,
650 v. 279–280, 210.
651 Hughes, P.D., Gibbard, P.L., and Ehlers, J., 2013. Timing of glaciation during the last glacial cycle:
652 evaluating the meaning and significance of the 'Last Glacial Maximum' (LGM). Earth Science
653 Reviews, v. 125, 171-198.
654 Hughes, P.D., Woodward J.C. 2017. Quaternary glaciation in the Mediterranean mountains: a new
655 synthesis. Form Hughes, P.D., Woodward J.C. (eds) Quaternary glaciation in Mediterranean
656 Mountains, Geological Society, London, Special Publications, 433, 1-23
657 Hughes, P.D., Fink, D., Rodés, Á., Fenton, C.R., 2018. ^{10}Be and ^{36}Cl exposure ages and
658 palaeoclimatic significance of glaciations in the High Atlas, Morocco. Quaternary Science
659 Reviews 180, 193-213.
660 Isola, I., Zanchetta, G., Drysdale, R. N., Regattieri, E., Bini, M., Bajo, P., Hellstrom, J., Baneschi,
661 I., Lionello, P., Woodhead, J., Greig, A. 2018. The 4.2 ka BP event in the Central Mediterranean:
662 New data from Corchia speleothems (Apuan Alps, central Italy). Accepted Climate of the Past,

663 doi.org/10.5194/cp-2018-127

664 Ivy-Ochs, S., Kerschner, H., Reuther, A., Preusser, F., Heine, K., Maisch, M., Kubik, P.W.
665 Schluchter, C. 2008. Chronology of the last glacial cycle in the European Alps. Journal of
666 Quaternary Sciences, 23, 559-573.

667 Jaffey, A.H., Flynn, K.F., Glendenin, L.E., Bentley, W.C., Essling, A.M., 1971. Precision
668 measurements of half-lives and specific activities of ^{235}U and ^{238}U. Phys. Rev. C, 4(5), 1889–1906.

669 Jaurand, E., 1998. Les glaciers disparus de l'Apennin. In Geomorphologie et paleoenvironments
670 glaciaires de l'Italie peninsulaire. Vol 10. Publications de la Sorbonne.

671 Kotarba, A., Herman, H. and Dramis, F., 2001. On the age of Campo Imperatore glaciations, Gran
672 Sasso Massif, Central Italy. Geografia Fisica e Dinamica Quaternaria 24, 65–69.

673 Kuhlemann, J., Rohling, E. J., Krumrei, I., Kubik, P., Ivy-Ochs, S., Kucera, M., 2008. Regional
674 synthesis of Mediterranean atmospheric circulation during the Last Glacial
675 Maximum. Science, 321, 5894, 1338-1340.

676 Lambeck, K:, and Bard E.. 2000. "Sea-level change along the French Mediterranean coast for the
677 past 30 000 years." Earth and Planetary Science Letters 175.3, 203-222.

678 Lambeck, K., Rouby, H., Purcell, A., Sun, Y., Sambridge, M., 2014. Sea level and global ice
679 volumes from the Last Glacial Maximum to the Holocene. *Proceedings of the National*
680 *Academy of Sciences*, *111*, 43, 15296-15303.

681 Link, A, Preusser, F. 2006. Hinweise auf eine Vergletscherung des Kemptener Beckens während
682 des Mittelwürms. Eiszeitalter und Gegenwart, 55, 65–88.

683

684 Locarnini, R. A., A. V. Mishonov, J. I. Antonov, T. P. Boyer, H. E. Garcia, O. K. Baranova, M. M.
685 Zweng, and Johnson, D. R., 2010. World Ocean Atlas 2009, Volume 1: Temperature.S.
686 Levitus, Ed. NOAA Atlas NESDIS 68, U.S. Government Printing Office, Washington, D.C.,
687 184.

López-Moreno, J. I., Vicente-Serrano, S. M., Morán-Tejeda, E., Lorenzo-Lacruz, J., Kenawy, A., Beniston, M., 2011. Effects of the North Atlantic Oscillation (NAO) on combined temperature and precipitation winter modes in the Mediterranean mountains: observed relationships and projections for the 21st century. Global and Planetary Change, 77, 1-2, 62-76.

Ludwig, K.R., Titterington, D.M., 1994. Calculation of ^{230}Th/U isochrons, ages, and errors, Geochimica et Cosmochimica Acta, 58(22), 5031–5042.

Martrat, B., Grimalt, J.O., Lopez-Martinez, C., Chaco, I., Sierro, F.J., Flores, J.A., Zahn, R., Canals, M., Jason, H.C., Hodell, D.A., 2004. Abrupt temperature changes in the Western Mediterranean over the past 250,000 years. Science 306, 1762–1765

Martrat, B.; Jimenez-Amat, P.; Zahn, R.; Grimalt, J. O, 2014. Sea surface temperatures, alkenones and sedimentation rates at the Alboran basin from ODP Site 161-977. PANGAEA, https://doi.org/10.1594/PANGAEA.787969,

McDermott, F., 2004. Palaeo-climate reconstruction from stable isotope variations in speleothems: a review. Quaternary Science Reviews, 23 901-918.

Masini, R., 1970. I massi erratici della Valle dell' Edron e il glacialismo nelle Alpi Apuane. Bool. Soc. Geol. It. 89, 2, 45-5.

Meyer, M.C., Spötl, C., Mangini, A., Tessadri, R., 2012. Speleothem deposition at the glaciation threshold—An attempt to constrain the age and paleoenvironmental significance of a detrital-rich flowstone sequence from Entrische Kirche Cave (Austria): Palaeogeography, Palaeoclimatology, Palaeoecology, v. 319–320, 93–106

Merciai, G., 1912. Fenomeni glaciali delle Alpi Apuane . Att. Soc. Tosc. Sc. Nat., Pisa, XXVIII, 70-89.

Molli G., Vaselli L., 2006. Structures, interference patterns, and strain regimes during midcrustal deformation in the Alpi Apuane (Northern Apennines Italy). Geological Society of America, Spec. Pub. 414: 79-93.

713 Moreno, A., Stoll, H., Jiménez-Sánchez, M., Cacho, I., Valero-Garcés, B., Ito, E., Edwards, R. L.,
714 2010. A speleothem record of glacial (25–11.6 kyr BP) rapid climatic changes from northern
715 Iberian Peninsula. Global and Planetary Change, 71, 3, 218-231.
716 Müller, P.J., Kirst, G., Ruhland, G., von Storch, I., Rosell-Melé, A., 1998. Calibration of the
717 alkenone paleotemperature index U^{K}_{37} based on core-tops from the eastern South Atlantic and
718 the global ocean (60°N-60°S). Geochim. Cosmochim. Acta 62, 1757-1772.
719 North Greenland Ice Core Project members, 2004. High-resolution record of Northern Hemisphere
720 climate extending into the last interglacial period. Nature, 431, 7005,147-151
721 Paci M., 1935. Revisione dei terreni morenici quaternari delle Alpi Apuane. Atti Soc. Tosc. Sc.
722 Nat. Proc Verb. 44, 13-30
723 Oliva M., Žebre M., Guglielmin M., Hughes P.D., Çiner A., Vieira G, Bodin X., Andrés N.,
724 Colucci R.R., García-Hernández C., Mora C., Nofre J., Palacios D., Pérez-Alberti A., Ribolini
725 A., Ruiz-Fernández J.,. Sarıkaya M.A, Serrano E., Urdea P., Valcárcel M., Woodward J.C.,
726 Yıldırım C., 2018. Permafrost conditions in the Mediterranean region since the Last Glaciation.
727 Earth-Science Reviews, 10.1016/j.earscirev.2018.06.018
728 Pérez-Alberti, A., Valcárcel, M., Blanco, R., 2004. Pleistocene glaciation in Spain. In: Ehlers, J.,
729 Gibbard, P.L. (Eds.), Quaternary Glaciations- Extent and Chronology. Elsevier, London, 389–
730 394.
731 Piccini L., 1998. Evolution of karst in the Alpi Apuane (Italy): Relationships with the
732 morphotectonic history. Suppl. Geografia Fisica e Dinamica Quaternaria, 3, 4, 21-31.
733 Piccini L., 2011. Speleogenesis in highly geodynamic contexts: The quaternary evolution of Monte
734 Corchia multi-level karst system (Alpi Apuane, Italy). Geomorphology, 134, 1–2, 49-61
735 Piccini, L., Borsato, A., Frisia, S., Paladini, M., Salzani, R., Sauro, U., Tuccimei, P., 2003.
736 Concrezionamento olocenico e aspetti geomorfologici della Grotta del Vento (Alpi Apuane–
737 Lucca): analisi paleoclimatica e implicazioni morfogenetiche. Studi Trent. Sci. Nat., Acta
738 Geol., 80, 127-138

739 Piccini, L., Zanchetta, G., Drysdale, R. N., Hellstrom, J., Isola, I., Fallick, A. E., Leone G., Doveri
740 M., Mussi M., Mantelli F., Molli G., Lotti L., Roncioni A., Regattieri E., Meccheri M., Vaselli,
741 L., 2008. The environmental features of the Monte Corchia cave system (Apuan Alps, central
742 Italy) and their effects on speleothem growth. International Journal of Speleology, 37, 3, 153-
743 172.

744 Pons-Branchu, E., Hillaire-Marcel, C., Ghaleb, B., Deschamps, P., Sinclair, D., 2005. Early
745 diagenesis impact on precise U-series dating of Deep-Sea corals. Example of a 100-200 years
746 old *Lophelia pertusa* sample from NE Atlantic. Geochimica et Cosmochimica Acta, 69, 20,
747 4865-4879.

748 Pons-Branchu, E., Hamelin, B., Losson, B., Jaillet, S., Brulhet, J., 2010. Speleothem evidence of
749 warm episodes in northeast France during Marine Oxygen Isotope Stage 3 and implications for
750 permafrost distribution in northern Europe. Quaternary Research, 74, 2, 246-251.

751 Pons-Branchu, E., Douville, E., Roy-Barman, M., Dumont, E., Branchu, P., Thil, F., Frank, N.,
752 Bordier, L., Borst, W., 2014. A geochemical perspective on Parisian urban history based on U-
753 Th dating, laminae counting and yttrium and REE concentrations of recent carbonates in
754 underground aqueducts. Quat. Geochronol., 24, 44-53.

755 Pope, R.J., Hughes, P.D., Skourtsos, E., 2017. Glacial history of Mt Chelmos, Peloponnesus,
756 Greece. In: Hughes, P.D., Woodward, J.C. (Eds.) Quaternary glaciation in the Mediterranean
757 Mountains. Geological Society of London Special Publications 433, 211-236.
758 https://doi.org/10.1144/SP433.11

759 Potzolu, P.P., 1995. Osservazioni geomorfologiche nell'alta avelle del Serchio di Gramolazzo (Alpi
760 Apuane). Memorie dell'Accademia Lunigiane di Scienze "Giovanni Cappellini" 64-65, 213-
761 250.

762 Preusser, F., Blei A, Graf H.R, Schlüchter. C., 2007. Luminescence dating of Würmian
763 (Weichselian) proglacial sediments from Switzerland: methodological aspects and
764 stratigraphical conclusions. Boreas. 36,130–142.
765 Preusser, F., Graf, H.R., Keller, O., Krayss, E., Schlüchter, C., 2011. Quaternary glaciation history
766 of northern Switzerland. Eizeitalter und Gegenwart, 60, 282–305.
767 Pujol, C., Grazzini, C. V., 1995. Distribution patterns of live planktic foraminifers as related to
768 regional hydrography and productive systems of the Mediterranean Sea. *Marine*
769 *Micropaleontology*, *25*, 2-3, 187-217
770 Rapetti F., Vittorini S., 1994. Carta climatica della Toscana centro-settentrionale. Pacini Editore,
771 Pisa.
772 Rapetti, F., Vittorini, S., 2012. Note illustrative della carta climatica della Toscana. *Atti della*
773 *Società Toscana di Scienze Naturali, Memorie, Serie A*, 117-119.
774 Reale, M., Lionello, P., 2013. Synoptic climatology of winter intense precipitation events along the
775 Mediterranean coasts. Natural Hazards and Earth System Sciences, 13,7, 1707-1722.
776 Regattieri, E., Isola, I., Zanchetta, G, Drysdale, R.N., Hellstrom, J.C., Baneschi, I., 2012.
777 Stratigraphy, petrography and chronology of speleothem deposition at Tana che Urla (Lucca,
778 Italy): paleoclimatic implications. Geografia Fisica e Dinamica del Quaternario 35, 141-152.
779 Regattieri E., Zanchetta G., Drysdale R.N., Isola I., Hellstrom J., Roncioni A., 2014a. A continuous
780 stable isotopic record from Penultimaye glacial maximum on to the Last Interglacial (159-121
781 ka) from Tana Che Urla Cave (Apuan Alps, central Italy). Quaternary Research, 82, 450-461.
782 Regattieri E., Zanchetta G., Drysdale R., Isola I., Hellstrom J., Dallai, L. 2014b. Lateglacial to
783 Holocene trace element record (Ba, Mg, Sr) from Corchia Cave (Apuan Alps, central Italy):
784 paleoenvironmental implications. Journal of Quaternary Science, 29, 4, 381-392
785 Regattieri E., Zanchetta **G.**, Drysdale R.N., Isola I., Woodhead J.D., Helstromm J.C., Giaccio,
786 Greig A., Baneschi I., Dotsika E., 2016. Environmental variability between the penultimate

787 deglaciation and the mid Eemian: Insights from Tana che Urla (central Italy) speleothem trace
788 element record. *Quaternary Science Reviews*, 152, 80-92.
789 Ribolini, A., Isola, I., Bini, M., Zanchetta, G., Sulpizio, R. 2011. Glacial features on the Galicica
790 Mountains, Macedonia: preliminary report. Geogr. Fis. Dinam. Quat. 34, 247-255.
791 Ribolini, A., Bini, M., Isola, I., Zanchetta, G., Pellitero, R., Mechernich, S., Gromig, R., Dunai, T.,
792 Wagner, B., Milevski, I., 2018. An oldest dryas glacier expansion on mount pelister (former
793 Yugoslavian Republic of Macedonia) according to10Be cosmogenic dating. Journal of the
794 Geological Society, 175, 1, 100-110.
795 Rigual-Hernández, A. S., Bárcena, M. A., Jordan, R. W., Sierro, F. J., Flores, J. A., Meier, K. S.,
796 Beaufort, L., Heussner, S., 2013. Diatom fluxes in the NW Mediterranean: evidence from a 12-
797 year sediment trap record and surficial sediments. *Journal of plankton research*, *35*, 5, 1109-
798 1125.
799 Sanchez -Goñi, M. S., Eynaud, F., Turon, J. L., Shackleton, N. J., 1999. High resolution
800 palynological record off the Iberian margin: direct land-sea correlation for the Last Interglacial
801 complex. Earth and Planetary Science Letters, 171, 1, 123-137.
802 Sanchez -Goñi, M. F. S., Landais, A., Fletcher, W. J., Naughton, F., Desprat, S., Duprat, J., 2008.
803 Contrasting impacts of Dansgaard–Oeschger events over a western European latitudinal
804 transect modulated by orbital parameters. *Quaternary Science Reviews*, 27, 11, 1136-1151.
805 Sarıkaya, M. A., Çiner, A., Haybat, H., Zreda, M., 2014. An early advance of glaciers on Mount
806 Akdağ, SW Turkey, before the global Last Glacial Maximum; insights from cosmogenic
807 nuclides and glacier modeling. *Quaternary Science Reviews*, 88, 96-109.Sarıkaya, M. A.,
808 Çiner, A., 2017. Late Quaternary glaciations in the eastern
809 Mediterranean. Geological Society, London, Special Publications, 433, 1, 289-305. From Hughes,
810 P.D., Woodward J.C. (eds) Quaternary glaciation in Mediterranean Mountains, Geological
811 Society, London, Special Publications, 433, 137-159

812 Scholz, D., Hoffmann, D. L., Hellstrom, J., Ramsey, C. B., 2012. A comparison of different
813 methods for speleothem age modelling. *Quaternary Geochronology*, *14*, 94-104.
814 Serrano, E., González-Trueba, J. J., González-García, M., 2012. Mountain glaciation and
815 paleoclimate reconstruction in the Picos de Europa (Iberian Peninsula, SW Europe). Quaternary
816 Research, 78, 2, 303-314.
817 Siani, G., Magny, M., Paterne, M., Debret, M., Fontugne, M., 2013. Paleohydrology reconstruction
818 and Holocene climate variability in the South Adriatic Sea. Climate of the Past, 9, 1, 499-515.
819 Smith, J. R., Giegengack, R., Schwarcz, H. P., 2004. Constraints on Pleistocene pluvial climates
820 through stable-isotope analysis of fossil-spring tufas and associated gastropods, Kharga Oasis,
821 Egypt. Palaeogeography, Palaeoclimatology, Palaeoecology, 206, 1-2, 157-175.
822 Spötl C., Mangini A., 2006. U/Th age constraints on the absence of ice in the central Inn Valley
823 (eastern Alps, Austria) during Marine Isotope Stages 5c to 5a. Quaternary Research 66, 167–
824 175.
825 Spotl, C., Mangini A., 2007. Speleothems and glaciers. Earth and Planetary Science Letters, 254,
826 323-331
827 Stoll, H. M., Moreno, A., Mendez-Vicente, A., Gonzalez-Lemos, S., Jimenez-Sanchez, M.,
828 Dominguez-Cuesta, M. J., Laurence, E.R., Cheng, H., Wang, X., 2013. Paleoclimate and
829 growth rates of speleothems in the northwestern Iberian Peninsula over the last two glacial
830 cycles. Quaternary Research, 80, 2, 284-290.
831 Stoppani A., 1872. Sull'esitsenza di un antico ghiaciaio nelle Alpi Apuane. Rend. R. Ist. Lomb. di
832 Sc. e Lett., 5, 733.
833 Tongiorgi E. Trevisan L., 1940. Aspetti glaciali e forestali delle Alpi Apuane durante l' ultima
834 glaciazione. Atti Soc. Tosc. SC. Nat. Proc. Verb. 49, 3, 55-62.
835 Trigo, I.F., Bigg, G.R., Davies, T.D., 2002. Climatology of cyclogenesis mechanisms in the
836 Mediterranean. Am. Meteorol. Soc. 130, 549–569.

837 Vaks, A., Bar-Matthews, M., Ayalon, A., Matthews, A., Frumkin, A., Dayan, U., Halicz, L.,
838 Almogi-Labin, A., Schilman, B., 2006. Paleoclimate and location of the border between
839 Mediterranean climate region and the Saharo–Arabian Desert as revealed by speleothems from
840 the northern Negev Desert, Israel. Earth and Planetary Science Letters, 249, 3-4, 384-399.
841 Vaks, A., Bar-Matthews, M., Ayalon, A., Matthews, A., Halicz, L., Frumkin, A., 2007. Desert
842 speleothems reveal climatic window for African exodus of early modern humans. Geology, 35,
843 9, 831-834.
844 Vaks, A., Bar-Matthews, M., Matthews, A., Ayalon, A., Frumkin, A., 2010. Middle-Late
845 Quaternary paleoclimate of northern margins of the Saharan-Arabian Desert: reconstruction
846 from speleothems of Negev Desert, Israel. Quaternary Science Reviews, 29, 19-20, 2647-2662.
847 Vaks, A., Gutareva, O. S., Breitenbach, S. F., Avirmed, E., Mason, A. J., Thomas, A. L., Osinzev,
848 A.V., Konov, A.M., Henderson, G. M., 2013. Speleothems reveal 500,000-year history of
849 Siberian permafrost. Science, 340(6129), 183-186.
850 Wang, Y., Cheng, H., Edwards, R. L., Kong, X., Shao, X., Chen, S., Wu, J., Jiang, X., Wang, X.,
851 An, Z., 2008. Millennial-and orbital-scale changes in the East Asian monsoon over the past
852 224,000 years. Nature, 451(7182), 1090-1093.
853 Wilson, G. P., Reed, J. M., Frogley, M. R., Hughes, P. D., Tzedakis, P. C., 2015. Reconciling
854 diverse lacustrine and terrestrial system response to penultimate deglacial warming in southern
855 Europe. Geology, 43, 9, 819-822.
856 Zaccagna, D., 1937. Sulla estensione dei ghiacciai delle Alpi Apuane. Att. Soc. Tosc. Sc. Nat. Proc
857 Verb., 46, 65-66
858 Zanchetta, G., Drysdale, R.N., Hellstrom, J.C., Fallick, A.E., Isola, I., Gagan, M., Pareschi, M.T.,
859 2007. Enhanced rainfall in the western Mediterranean during deposition of sapropel S1:
860 stalagmite evidence from Corchia Cave (Central Italy). Quaternary Science Reviews 26, 279-
861 286.

862 Zerboni, A., Trombino, L., Frigerio, C., Livio, F., Berlusconi, A., Michetti, A. M., Rodnight, H.,
863 Spötl, C., 2015. The loess-paleosol sequence at Monte Netto: a record of climate change in the
864 Upper Pleistocene of the central Po Plain, northern Italy. Journal of Soils and Sediments, 15, 6,
865 1329-1350.
866 Zhornyak, L.V., Zanchetta, G., Drysdale, R.N., Hellstrom, J.C., Isola, I., Regattieri, E., Piccini, L.,
867 Baneschi, I., Couchoud, I., 2011. Stratigraphic evidence for a "pluvial phase" between ca 8200
868 and 7100 ka from Renella cave (Central Italy). Quaternary Science Reviews 30, 409-417.
869

870 **Captions**

871 Figure 1. Glacier extent (light blue) during the LGM according to the reconstruction of Braschi et
872 al. (2001). Sampled sites are shown in yellow.

873 Figure 2. 293 U/Th ages from 19 Apuan speleothems over the past 160 ka (2σ error bars) vs the
874 elevation of sampling sites. Details on dating can be found in the original papers (Drysdale et al.,
875 2004; 2009; Regattieri et al., 2012, 2014a, 2014b; Piccini et al, 2003; Drysdale et al., 2006;
876 Zhornyak et al 2011, Isola et al., 2018).
877

878 Figure 3. Cumulative growth curves (i.e. the total speleothem growth calculated for all the
879 considered speleothems and binned into 1000-yr intervals) for Corchia Cave speleothems (red lines
880 a and b) and for the caves located at lower altitude (blue lines, c and d), the associated errors in
881 shaded strips. Note the linear (b and d) and the logarithmic (a and c) scales in the vertical axes.
882 Shown in black (e) is the LR04 stack (Lisiecki and Raymo 2005) from benthic foraminifera $\delta^{18}O$
883 data. Numbers indicate Marine Isotope Substages.
884

885 Figure 4. MAAT curves derived for all the caves from MD90917: (a) C1 (see the text for
886 explanation), (b) C2; from ODP 161-977, (c) C1 and (d) C2 ; and from PRGL1, (e) C1 and (f) C2.
887 Black horizontal lines indicate the 0°C MAAT.
888
889 Figure 5. Northern Hemisphere proxies for the Pleniglaciation: a) the approximate timing of
890 maximum extent of glaciers in the Mediterranean mountains (after Hughes et al., 2013; 2018;
891 Sarikya et al., 2014; Pope et al., 2017); b) the derived MAAT curves in the C2 case above the
892 Galleria delle Stalattiti: red curve is derived from ODP 161-977, purple curve from MD90917 data,
893 black curve is derived from PRGL1 data. Horizontal black line indicates the 0°C MAAT; c) the
894 derived MAAT curves in the C1 case above the Galleria delle Stalattiti: red curve is derived from
895 ODP 161-977, purple curve from MD90917 data, black curve is derived from PRGL1 data and
896 horizontal black line indicates the 0°C MAAT; d) Cumulative growth curve calculated for interval
897 of 1000 yr for Corchia cave speleothems (green line); e) NGRIP $\delta^{18}O$ values from North Greenland
898 Ice Core (North Greenland Ice Core Project members, 2004). Numbers over the graph mark the
899 position of the Dansgaard-Oeschger interstadials (Dansgaard et al., 1993); f) approximate interval
900 of extensive loess accumulation in Po Plain (after Cremaschi et al., 2015b; Zerboni et al., 2015).
901
902
903 **List of tables (supplementary materials)**
904 Tab. 1 U/Th data used for the age distribution
905 Tab. 2 Elevation used to to estimate the MAAT in the speleothem catchment areas (C1, C2)
906

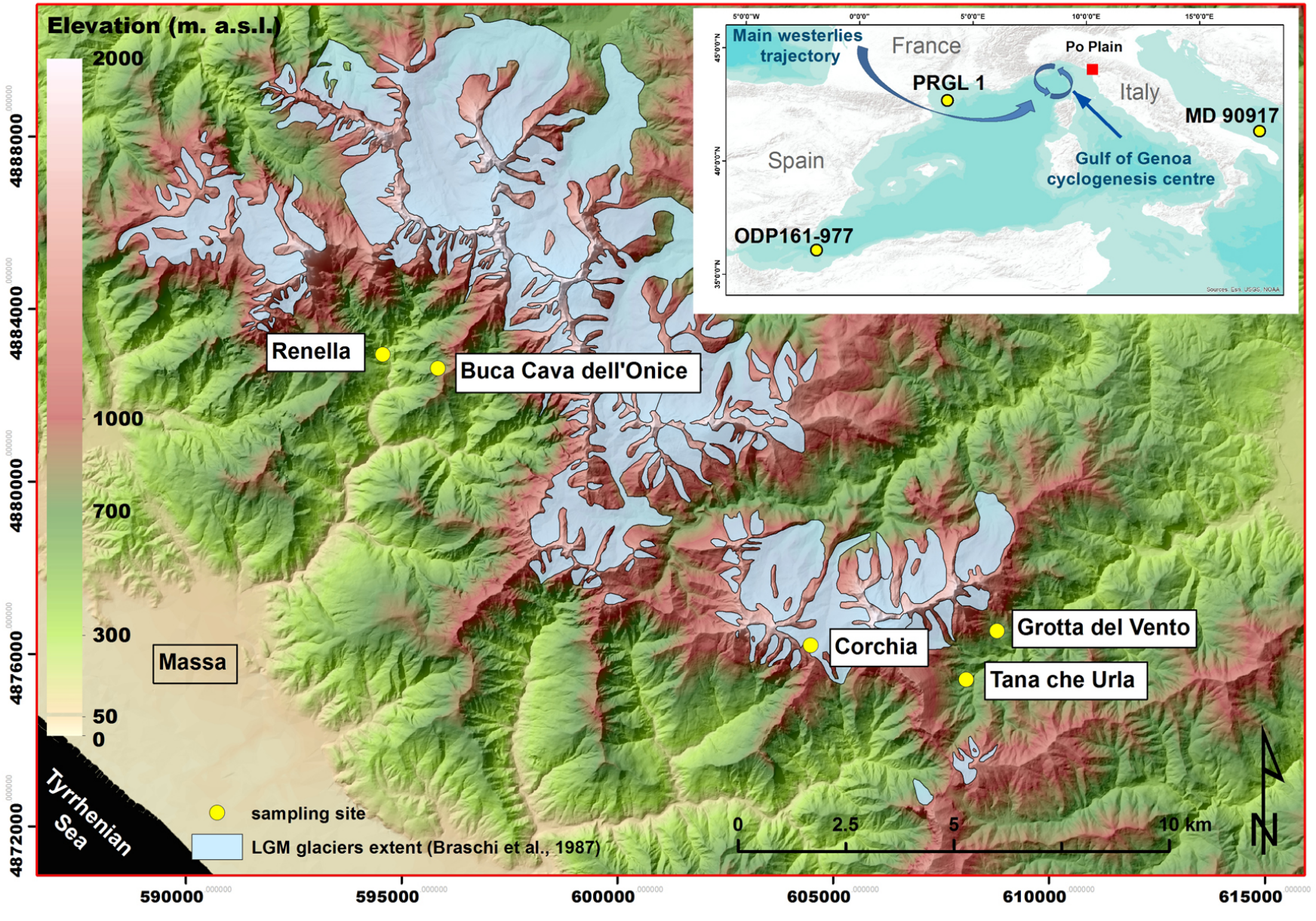
Elevation (m. a.s.l.)
2000
1000
700
300
50
0
Renella
Buca Cava dell'Onice
Massa
Corchia
Grotta del Vento
Tana che Urla
Tyrrhenian Sea
sampling site
LGM glaciers extent (Braschi et al., 1987)
0
2.5
5
10 km
N
Main westerlies trajectory
France
Po Plain
PRGL 1
Italy
MD 90917
Spain
Gulf of Genoa cyclogenesis centre
ODP161-977
4888000
4884000
4880000
4876000
4872000
590000
595000
600000
605000
610000
615000

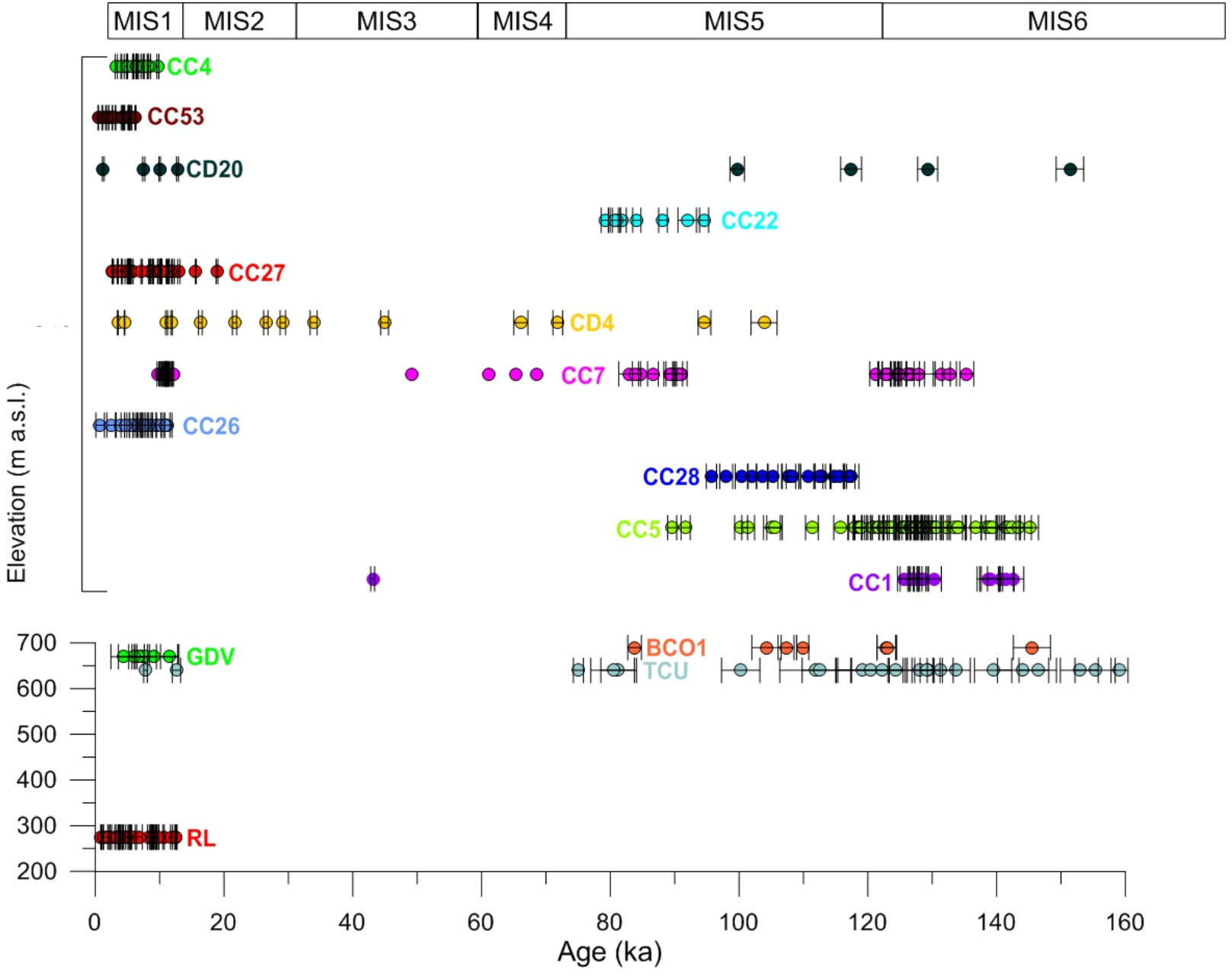
MIS1
MIS2
MIS3
MIS4
MIS5
MIS6
CC4
CC53
CD20
CC22
CC27
CD4
CC7
CC26
CC28
CC5
CC1
GDV
BCO1
TCU
RL
Elevation (m a.s.l.)
700
600
500
400
300
200
0
20
40
60
80
100
120
140
160
Age (ka)

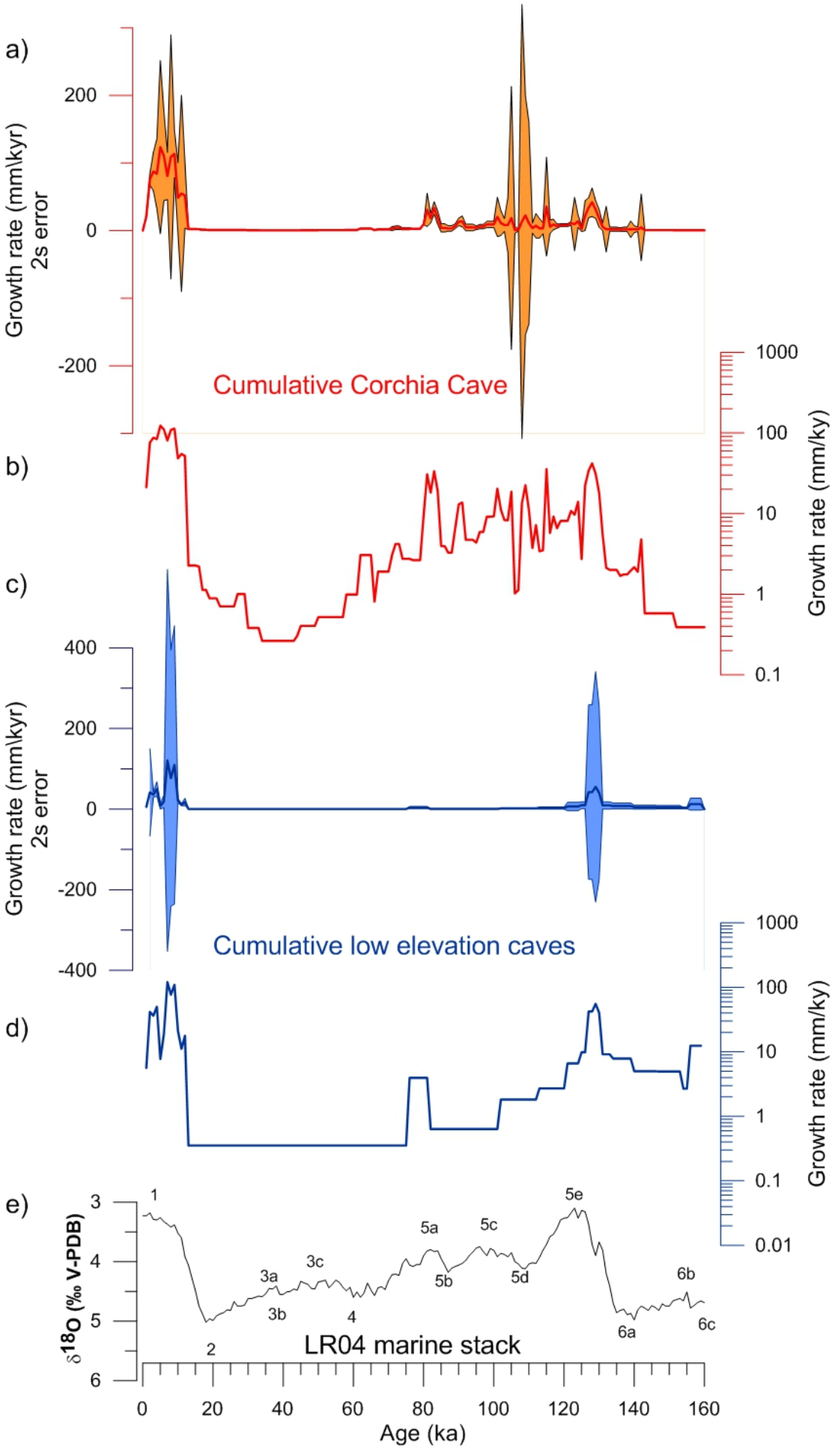
a)
200
0
-200
Growth rate (mm\kyr)
2s error
Cumulative Corchia Cave
b)
1000
100
10
1
0.1
Growth rate (mm/ky)
c)
400
200
0
-200
-400
Growth rate (mm\kyr)
2s error
Cumulative low elevation caves
d)
1000
100
10
1
0.1
0.01
Growth rate (mm/ky)
e)
3
4
5
6
δ18O (‰ V-PDB)
1
2
3a
3b
3c
4
5a
5b
5c
5d
5e
6a
6b
6c
LR04 marine stack
0
20
40
60
80
100
120
140
160
Age (ka)

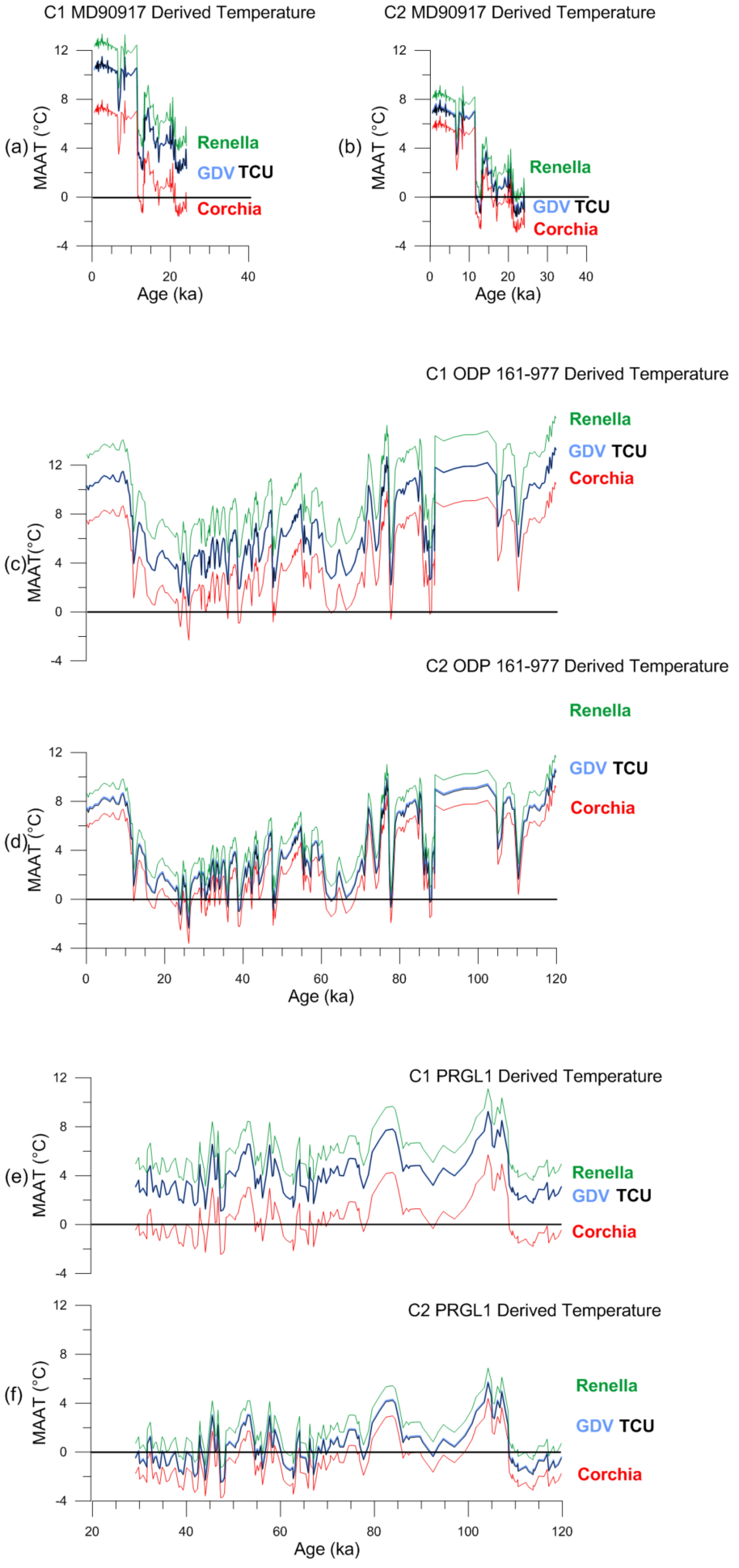
C1 MD90917 Derived Temperature
C2 MD90917 Derived Temperature
(a)
(b)
MAAT (°C)
Age (ka)
Renella
GDV TCU
Corchia
C1 ODP 161-977 Derived Temperature
C2 ODP 161-977 Derived Temperature
(c)
(d)
C1 PRGL1 Derived Temperature
C2 PRGL1 Derived Temperature
(e)
(f)

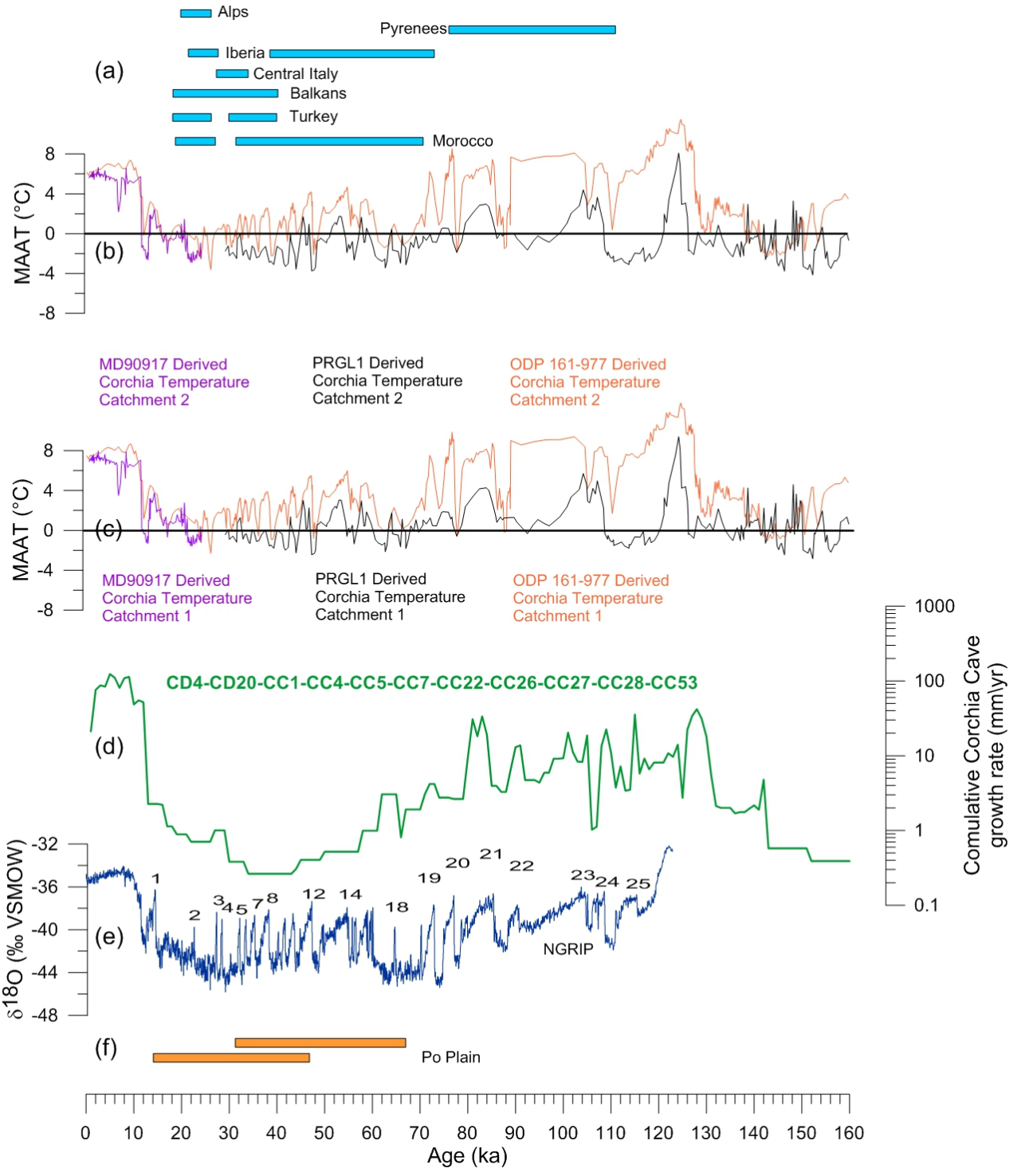
Alps
Pyrenees
Iberia
Central Italy
Balkans
Turkey
Morocco
(a)
(b)
MAAT (°C)
8
4
0
-4
-8
MD90917 Derived
Corchia Temperature
Catchment 2
PRGL1 Derived
Corchia Temperature
Catchment 2
ODP 161-977 Derived
Corchia Temperature
Catchment 2
(c)
MD90917 Derived
Corchia Temperature
Catchment 1
PRGL1 Derived
Corchia Temperature
Catchment 1
ODP 161-977 Derived
Corchia Temperature
Catchment 1
CD4-CD20-CC1-CC4-CC5-CC7-CC22-CC26-CC27-CC28-CC53
(d)
Comulative Corchia Cave
growth rate (mm\yr)
1000
100
10
1
0.1
δ18O (‰ VSMOW)
-32
-36
-40
-44
-48
(e)
1
2
3
4
5
7
8
12
14
18
19
20
21
22
23
24
25
NGRIP
(f)
Po Plain
0
10
20
30
40
50
60
70
80
90
100
110
120
130
140
150
160
Age (ka)

Table 1 U/Th data used for the age distribution

Cave	Sample	Age (ka)	2σ	Sample site elevation (m a.s.l.)	Sampling depth (mm from top)	References
Corchia	CC110	139	1.4	840	40	drysdale et al., 2004
Corchia	Cor4	126.4	1.4	840	13	drysdale et al., 2004
Corchia	CC117	130.2	1.2	840	35	drysdale et al., 2004
Corchia	CC116	141.5	1.1	840	43	drysdale et al., 2004
Corchia	CC119	125.6	1	840	11	drysdale et al., 2004
Corchia	CC118	127.2	0.8	840	23	drysdale et al., 2004
Corchia	Cor12	126.9	0.7	840	19	drysdale et al., 2004
Corchia	Cor11	127.8	0.6	840	23	drysdale et al., 2004
Corchia	Cor3	43.1	0.3	840	8	drysdale et al., 2004
Corchia	CC5-133	139.4	1.8	850	247	drysdale et al., 2005
Corchia	CC5-5	122.4	1.7	850	129	drysdale et al., 2005
Corchia	CC5-4	120.7	1.6	850	118	drysdale et al., 2005
Corchia	CC5-13	129.9	1.5	850	239	drysdale et al., 2005
Corchia	CC5-127	145.1	1.4	850	253	drysdale et al., 2005
Corchia	CC5-4R	120.7	1.4	850	118	drysdale et al., 2005
Corchia	CC5-136	138.9	1.3	850	244	drysdale et al., 2005
Corchia	CC5-2	105.1	1.3	850	60	drysdale et al., 2005
Corchia	CC5-328	126.6	1.3	850	144	drysdale et al., 2005
Corchia	CC5-6	128.7	1.3	850	169	drysdale et al., 2005
Corchia	CC5-3	105.5	1.2	850	63	drysdale et al., 2005
Corchia	CC5-7	134	1.2	850	242	drysdale et al., 2005
Corchia	CC5-271	115.8	1.1	850	84	drysdale et al., 2005
Corchia	CC5-32	129.5	1.1	850	231	drysdale et al., 2005
Corchia	CC5-227	100.3	1	850	36	drysdale et al., 2005
Corchia	CC5-239	101.4	1	850	50	drysdale et al., 2005
Corchia	CC5-253	111.3	1	850	67	drysdale et al., 2005
Corchia	CC5-288	118.8	1	850	103	drysdale et al., 2005
Corchia	CC5-30	128.5	1	850	234	drysdale et al., 2005
Corchia	CC5-31	128.6	0.9	850	228	drysdale et al., 2005
Corchia	CC5-333	127.6	0.9	850	148	drysdale et al., 2005
Corchia	CC5-12	89.6	0.7	850	16	drysdale et al., 2005
Corchia	CC5-217	91.7	0.7	850	24	drysdale et al., 2005
Corchia	CC28-829	114.7	1.7	860	76	drysdale et al., 2007
Corchia	CC28-597	108	1.3	860	53	drysdale et al., 2007
Corchia	CC28-1020	117.4	1.2	860	107	drysdale et al., 2007
Corchia	CC28-801-803	112.9	1.2	860	73	drysdale et al., 2007
Corchia	CC28-883	115.5	1.2	860	81	drysdale et al., 2007
Corchia	CC28-473	107.7	1.1	860	40	drysdale et al., 2007
Corchia	CC28-667	110.7	1.1	860	60	drysdale et al., 2007
Corchia	CC28-135	100.4	1	860	13	drysdale et al., 2007
Corchia	CC28-635	108.3	1	860	56	drysdale et al., 2007
Corchia	CC28-81	98	1	860	8	drysdale et al., 2007
Corchia	CC28-1144	117.1	0.9	860	94	drysdale et al., 2007
Corchia	CC28-334	103.6	0.9	860	33	drysdale et al., 2007
Corchia	CC28-732-734	112.5	0.9	860	66	drysdale et al., 2007
Corchia	CC28-2	95.7	0.8	860	1	drysdale et al., 2007
Corchia	CC28-439-440	105.2	0.8	860	37	drysdale et al., 2007
Corchia	CC28-281	102	0.7	860	28	drysdale et al., 2007

Corchia	CC1-632	147.6	3.5	840	39	drysdale et al., 2009
Corchia	CC5696+697	138.4	2.4	850	241	drysdale et al., 2009
Corchia	CC5-734	132.3	2.4	850	237	drysdale et al., 2009
Corchia	CC1-587	136.3	2.2	840	35	drysdale et al., 2009
Corchia	CC1-609	139.7	2.2	840	37	drysdale et al., 2009
Corchia	CC1615-616	140.6	2.1	840	38	drysdale et al., 2009
Corchia	CC5-653	143.3	2.1	850	245	drysdale et al., 2009
Corchia	CC5-766	130.5	2.1	850	234	drysdale et al., 2009
Corchia	CC7-325	126.8	2	900	140	drysdale et al., 2009
Corchia	CC1-570	130.3	1.9	840	33	drysdale et al., 2009
Corchia	CC5638-636	142.4	1.9	870	247	drysdale et al., 2009
Corchia	CC1-578	132.1	1.8	840	34	drysdale et al., 2009
Corchia	CC5-685	141.7	1.8	850	242	drysdale et al., 2009
Corchia	CC1-549	128.5	1.7	840	31	drysdale et al., 2009
Corchia	CC1593-594	138.6	1.7	840	35	drysdale et al., 2009
Corchia	CC5-722	133.4	1.7	850	239	drysdale et al., 2009
Corchia	CC5-749	130.6	1.7	850	236	drysdale et al., 2009
Corchia	CC7331-332	126.3	1.7	900	139	drysdale et al., 2009
Corchia	CC1-503	128.5	1.6	840	22	drysdale et al., 2009
Corchia	CC1623-624	142.6	1.6	840	38	drysdale et al., 2009
Corchia	CC1-508	129	1.5	840	26	drysdale et al., 2009
Corchia	CC1605-606	139	1.5	840	37	drysdale et al., 2009
Corchia	CC5673-671	141.5	1.5	850	244	drysdale et al., 2009
Corchia	CC5-707	136.8	1.5	850	240	drysdale et al., 2009
Corchia	*CC1-528	127.6	1.4	840	29	drysdale et al., 2009
Corchia	CC5-136	138.9	1.3	850	242	drysdale et al., 2009
Corchia	CC5-328	126.6	1.3	850	144	drysdale et al., 2009
Corchia	CC5-4R	120.7	1.3	850	120	drysdale et al., 2009
Corchia	CC5-6	128.5	1.3	850	169	drysdale et al., 2009
Corchia	CC5784-783	130.4	1.3	850	232	drysdale et al., 2009
Corchia	CC5-877	127.5	1.3	850	223	drysdale et al., 2009
Corchia	CC5a467-469	121.7	1.3	850	128	drysdale et al., 2009
Corchia	*CC5834-836	130	1.2	850	227	drysdale et al., 2009
Corchia	CC5-32	129.4	1.2	850	232	drysdale et al., 2009
Corchia	CC5-7R	134	1.2	850	239	drysdale et al., 2009
Corchia	CC5c210-212	123.6	1.2	850	131	drysdale et al., 2009
Corchia	CC5f17-19	127.2	1.2	850	134	drysdale et al., 2009
Corchia	CC7-11	124.7	1.2	900	138	drysdale et al., 2009
Corchia	CC7728-732	122.9	1.2	900	125	drysdale et al., 2009
Corchia	CC7804-806	124.8	1.2	900	138	drysdale et al., 2009
Corchia	CC1773	128.3	1.1	840	19	drysdale et al., 2009
Corchia	CC5-30	128.3	1.1	850	233	drysdale et al., 2009
Corchia	CC5a504-506	125.5	1.1	850	144	drysdale et al., 2009
Corchia	CC5c203+205	122.9	1.1	850	132	drysdale et al., 2009
Corchia	CC5f4+6	126	1.1	850	133	drysdale et al., 2009
Corchia	*CC7688-692	123.4	1	850	121	drysdale et al., 2009
Corchia	CC5-288	118.8	1	850	101	drysdale et al., 2009
Corchia	CC5-31	128.4	1	850	230	drysdale et al., 2009
Corchia	CC5c4+6	119	1	850	102	drysdale et al., 2009
Corchia	CC5d73	118	1	850	93	drysdale et al., 2009
Corchia	CC7635-639	121.5	1	850	115	drysdale et al., 2009
Corchia	CC5a327-331	126.8	0.9	850	147	drysdale et al., 2009
Corchia	CC5a572-575	125.6	0.9	850	137	drysdale et al., 2009
Corchia	CC5d61-65	118	0.9	850	94	drysdale et al., 2009
Corchia	CC5d76-80	118.6	0.9	850	92	drysdale et al., 2009

Corchia	CC5f9-11	125.2	0.9	850	133	drysdale et al., 2009
Corchia	CC1511-513	128.5	0.8	840	27	drysdale et al., 2009
Corchia	CC5-333	127.6	0.8	850	148	drysdale et al., 2009
Corchia	CC5a437-439	122.5	0.8	850	125	drysdale et al., 2009
Corchia	CC26-10	7.16	0.67	890	96	Zanchetta et al., 2007
Corchia	CC26-15	9.54	0.67	890	133	Zanchetta et al., 2007
Corchia	CC26-9	6.52	0.67	890	86	Zanchetta et al., 2007
Corchia	CC26-14	8.8	0.67	890	123	Zanchetta et al., 2007
Corchia	CC26-12	7.98	0.67	890	108	Zanchetta et al., 2007
Corchia	CC26-13	8.2	0.67	890	112	Zanchetta et al., 2007
Corchia	CC26-2	6	0.67	890	77	Zanchetta et al., 2007
Corchia	CC26-8	6.54	0.67	890	85	Zanchetta et al., 2007
Corchia	CC26-16	10.14	0.67	890	142	Zanchetta et al., 2007
Corchia	CC26-11	7.62	0.66	890	102	Zanchetta et al., 2007
Corchia	CC26-17	11.26	0.66	890	152	Zanchetta et al., 2007
Corchia	CC26-7	5.57	0.66	890	68	Zanchetta et al., 2007
Corchia	CC26-4	0.75	0.66	890	4	Zanchetta et al., 2007
Corchia	CC26-1	10.93	0.66	890	151	Zanchetta et al., 2007
Corchia	CC26-5	2.48	0.66	890	27	Zanchetta et al., 2007
Corchia	CC26-3	3.9	0.66	890	45	Zanchetta et al., 2007
Corchia	CC26-6	4.65	0.66	890	54	Zanchetta et al., 2007
Corchia	CC7-1	9.736	0.15	900	2	this work
Corchia	CC74.5	10.15	0.07	900	5	this work
Corchia	H	10.460	0.118	900	5	this work
Corchia	G	10.735	0.093	900	15	this work
Corchia	F	10.931	0.059	900	22	this work
Corchia	CC727.5	10.674	0.117	900	28	this work
Corchia	E	11.142	0.095	900	30	this work
Corchia	D	11.109	0.078	900	37	this work
Corchia	CC739.5	10.992	0.053	900	40	this work
Corchia	C	11.436	0.098	900	48	this work
Corchia	CC754.1	11.212	0.098	900	54	this work
Corchia	B	11.615	0.124	900	59	this work
Corchia	A	11.862	0.097	900	68	this work
Corchia	CC776.1	12.080	0.110	900	76	this work
Corchia	CD4A-2	3.504	0.069	910	0.4	this work
Corchia	CD4A-212	11.079	0.149	910	42.2	this work
Corchia	CD4A-244	11.853	0.095	910	48.0	this work
Corchia	CD4A-286	16.322	0.273	910	56.0	this work
Corchia	CD4A-335	33.929	0.544	910		this work
Corchia	CD4A-340	44.938	0.595	910	65.6	this work
Corchia	CD4A-360	66.097	1.091	910	66.6	this work
Corchia	CD4A-43.44	4.556	0.036	910	70.6	this work
Corchia	CD4T-15	29.129	0.425	910	8.6-8.8	this work
Corchia	CD4T-26	26.482	0.345	910	64.6	this work
Corchia	CD4T-40	21.619	0.328	910	62.4	this work
Corchia	CD4-3	71.839	0.763	910	59.8	this work
Corchia	CD4-4	94.611	0.988	910	75.0	this work
Corchia	CD4-5	103.872	2.011	910	131.0	this work
Corchia	CC27 1005	15.61	0.06	920	165.0	this work
Corchia	CC27 1008,1009,1010	12.977	0.174	920	202	this work
Corchia	CC27 1018,1019	12.152	0.135	920	204	this work
Corchia	CC27 1035,1036	11.682	0.165	920	21	this work
Corchia	CC27 1041,1042	11.155	0.153	920	208	this work
Corchia	CC27 1071,1072,1073	10.239	0.099	920	214	this work

Corchia	CC27 1080	10.08	0.05	920	189	this work
Corchia	CC27 1160	9.72	0.06	920	173	this work
Corchia	CC27 1164	8.99	0.05	920	172	this work
Corchia	CC27 1183	8.44	0.07	920	168	this work
Corchia	CC27 140	3.53	0.03	920	28	this work
Corchia	CC27 275	4.09	0.02	920	55	this work
Corchia	CC27 31,32,33	2.761	0.071	920	6	Isola et al., 2018
Corchia	CC27 410	4.99	0.03	920	82	this work
Corchia	CC27 437	5.189	0.072	920	87	Isola et al., 2018
Corchia	CC27 497	5.267	0.072	920	99	Isola et al., 2018
Corchia	CC27 555	5.46	0.02	920	111	this work
Corchia	CC27 844,845	8.426	0.149	920	169	this work
Corchia	CC27 857,858	8.794	0.131	920	171	this work
Corchia	CC27 868	9.946	0.168	920	174	this work
Corchia	CC27 895	10.181	0.114	920	179	this work
Corchia	CC27 9	2.67	0.02	920	2	this work
Corchia	CC27-1000-1002	18.897	0.130	920	200	this work
Corchia	CC27-1045-1046	11.292	0.118	920	209	this work
Corchia	CC27-1135-1138	10.178	0.081	920	227	this work
Corchia	CC27-118	3.451	0.053	920	24	Isola et al., 2018
Corchia	CC27-220	4.125	0.035	920	44	Isola et al., 2018
Corchia	CC27-492	5.393	0.039	920	98	Isola et al., 2018
Corchia	CC27-608	5.809	0.054	920	122	Isola et al., 2018
Corchia	CC7-303/305	4.928	0.301	920	61	this work
Corchia	CC27-502/503	5.324	0.21	920	100	Isola et al., 2018
Corchia	CC27-809	7.200	0.112	920	122	Isola et al., 2018
Corchia	CC22 97-101	79.139	0.557	930	10	this work
Corchia	CC22 722	81.862	0.613	930	62	this work
Corchia	CC22 464	80.944	0.634	930	37	this work
Corchia	CC22 207-211	80.753	0.774	930	21	this work
Corchia	CC22 1325-1328	94.574	0.709	930	116	this work
Corchia	CC22 1280-1282	91.933	1.436	930	112	this work
Corchia	CC22 1157	88.177	0.667	930	99	this work
Corchia	CC22 1136-1139	84.109	0.637	930	97	this work
Corchia	CD20-1	1.233	0.147	940	2.00	this work
Corchia	CD20-2	7.530	0.163	940	2.7	this work
Corchia	CD20-3	10.002	0.103	940	3.8	this work
Corchia	CD20-4	12.755	0.145	940	4.3	this work
Corchia	CD20-5	99.702	1.112	940	5.0	this work
Corchia	CD20-6	117.398	1.631	940	5.4	this work
Corchia	CD20-7	129.286	1.566	940	7.0	this work
Corchia	CD20-8	151.382	2.126	940	7.9	this work
Corchia	CC53-A	0.478	0.052	950	1	this work
Corchia	CC53-6	1.106	0.054	950	6	this work
Corchia	CC53-15	1.668	0.07	950	15	this work
Corchia	CC53-B	2.092	0.035	950	40	this work
Corchia	CC53-65	2.665	0.036	950	65	this work
Corchia	CC53-C	3.147	0.035	950	87	this work
Corchia	CC53-112	4.133	0.125	950	112	this work
Corchia	CC53-114	4.306	0.055	950	114	this work
Corchia	CC53-123	4.544	0.054	950	123	this work
Corchia	CC53-154	5.175	0.108	950	154	this work
Corchia	CC53-156	5.466	0.127	950	156	this work
Corchia	CC53-D	5.249	0.055	950	160	this work
Corchia	CC53-170	5.557	0.114	950	170	this work

Corchia	CC53-186	6.229	0.095	950	186	this work
Corchia	CC4-1	5.971	0.057	960		this work
Corchia	CC4-A	9.731	0.156	960	319	this work
Corchia	CC4-B	8.421	0.154	960	202	this work
Corchia	CC4-C	7.341	0.226	960	113	this work
Corchia	CC4-D	6.577	0.128	960	91	this work
Corchia	CC4-E	4.706	0.199	960	41	this work
Corchia	CC4-F	3.257	0.165	960	8	this work
Corchia	CC4-23	4.040	0.071	960	23	this work
Corchia	CC4-39	4.960	0.077	960	39	this work
Corchia	CC4-60	5.864	0.070	960	60	this work
Corchia	CC4-78	6.370	0.055	960	78	this work
Corchia	CC4-84	6.516	0.072	960	84	this work
Corchia	CC4-139	7.484	0.074	960	139	this work
Corchia	CC4-186	8.108	0.058	960	186	this work
Grotta del vento	GV1-83_C	6.66	0.96	670	83	Piccini et al., 2003
Grotta del vento	GV1-142_B	7.15	0.96	670	142	Piccini et al., 2006
Grotta del vento	GV1-169_C	7.78	1.72	670	169	Piccini et al., 2007
Grotta del vento	GV1-264_C	9.08	3.9	670	264	Piccini et al., 2009
Grotta del vento	GV3-35_C	6.03	2.42	670	39	Piccini et al., 2010
Grotta del vento	GV3-95_C	4.45	2.02	670	107	Piccini et al., 2011
Grotta del vento	GV3-Base_C	11.46	1.32	670	133	Piccini et al., 2012
Tana che Urla	TCUD3E	111.826	5.5	640	313	Regattieri et al., 2014
Tana che Urla	TCUD4-102.5A	120.44	5.36	640	103	Regattieri et al., 2014
Tana che Urla	TCUD4-102.5B	122.15	4.68	640	102	Regattieri et al., 2014
Tana che Urla	TCUD3C	119.164	4.16	640	459	Regattieri et al., 2014
Tana che Urla	TCU.D3B_e	144.1	3.98	640	510	Regattieri et al., 2014
Tana che Urla	TCUD4-77.5	80.52	3.56	640	78	Regattieri et al., 2014
Tana che Urla	TCUD4-2	155.3	3.12	640	288	Regattieri et al., 2014
Tana che Urla	TCUD3Abis.b	100.25	2.97	640	281	Regattieri et al., 2014
Tana che Urla	TCUD4-1	152.83	2.94	640	310	Regattieri et al., 2014
Tana che Urla	TCUD4-263.5	146.38	2.91	640	264	Regattieri et al., 2014
Tana che Urla	TCUD4-244.5	139.44	2.89	640	245	Regattieri et al., 2014
Tana che Urla	TCUD4-90.5	112.55	2.77	640	91	Regattieri et al., 2014
Tana che Urla	TCUD4-70.5	81.12	2.61	640	71	Regattieri et al., 2014
Tana che Urla	TCUD4-212.5	133.73	2.17	640	213	Regattieri et al., 2014
Tana che Urla	TCUD4-3	131.23	2.01	640	226	Regattieri et al., 2014
Tana che Urla	TCUD4-181.5	129.24	1.98	640	182	Regattieri et al., 2014
Tana che Urla	TCUD4-4	128.1	1.98	640	157	Regattieri et al., 2014
Tana che Urla	TCUD4-A	159.08	1.3	640	335	Regattieri et al., 2014
Tana che Urla	TCUD4-C	124.3	1.16	640	124	Regattieri et al., 2014
Tana che Urla	TCUD4-B	129.21	1.1	640	208	Regattieri et al., 2014
Tana che Urla	TCUD4-46.5	75.03	0.78	640	47	Regattieri et al., 2014
Tana che Urla	TCUD4-24.5	12.61	0.65	640	25	Regattieri et al., 2014
Tana che Urla	TCUD4-D	7.79	0.28	640	9	Regattieri et al., 2014
Renella	RL4-2	1.77	0.77	275	15	Zhornyak et al., 2011
Renella	RL4-13	4.66	0.44	275	112	Zhornyak et al., 2011
Renella	RL4-8	6.87	0.43	275	153	Zhornyak et al., 2011
Renella	RL18-6	8.96	0.32	275	23	Zhornyak et al., 2011
Renella	RL13-8	9.13	0.3	275	39	Zhornyak et al., 2011
Renella	RL4-7	5.94	0.28	275	136	Zhornyak et al., 2011
Renella	RL13-2	9.26	0.19	275	43	Zhornyak et al., 2011
Renella	RL18-5	8.29	0.18	275	2	Zhornyak et al., 2011
Renella	RL13-7	8.68	0.17	275	36	Zhornyak et al., 2011
Renella	RL18-8	12.53	0.17	275	69	Zhornyak et al., 2011

Renella	RL13-3	4.57	0.16	275	34	Zhornyak et al., 2011
Renella	RL4-9	2.09	0.16	275	26	Zhornyak et al., 2011
Renella	RL18-4	11.85	0.15	275	60	Zhornyak et al., 2011
Renella	RL18-7	9.7	0.15	275	42	Zhornyak et al., 2011
Renella	RL13-6	9.72	0.14	275	41	Zhornyak et al., 2011
Renella	RL13-1	10.61	0.12	275	57	Zhornyak et al., 2011
Renella	Rl4-6	5.44	0.11	275	120	Zhornyak et al., 2011
Renella	RL13-4	3.8	0.1	275	20	Zhornyak et al., 2011
Renella	RL18-2	12.54	0.1	275	84	Zhornyak et al., 2011
Renella	RL4-11	3.63	0.1	275	77	Zhornyak et al., 2011
Renella	RL4-5	5.35	0.1	275	117	Zhornyak et al., 2011
Renella	RL4-10	3.11	0.09	275	56	Zhornyak et al., 2011
Renella	RL4-12	4.21	0.09	275	104	Zhornyak et al., 2011
Renella	RL18-3	8.86	0.08	275	10	Zhornyak et al., 2011
Renella	RL4-4	3.62	0.07	275	86	Zhornyak et al., 2011
Renella	RL13-5	0.9	0.05	275	3	Zhornyak et al., 2011
Renella	RL4-1	1.27	0.05	275	2	Zhornyak et al., 2011
Renella	RL4-3	2.28	0.05	275	31	Zhornyak et al., 2011
Buca Cava dell'Onice	A	83.76	1.06	700	14	this work
Buca Cava dell'Onice	B	104.25	2.28	700	23	this work
Buca Cava dell'Onice	C	107.29	1.25	700	28	this work
Buca Cava dell'Onice	J	109.89	0.93	700	69	this work
Buca Cava dell'Onice	D	122.88	1.45	700	78	this work
Buca Cava dell'Onice	E	122.93	1.53	700	99	this work
Buca Cava dell'Onice	F	145.48	2.88	700	110	this work

The activity ratios are standardized to the HU-1 secular equilibrium, and ages calculated using decay constants of 9.195_10_6 (230Th) and 2.835_10_6 (234U). 2 σ errors (column F) are the 95% uncertainties. See text and or the original papers for further information, references in the last column.

Table 2 Elevation used to to estimate the MAAT in the speleothem catchment areas

CAVE	Elevation (m, a.s.l.)		
	Sampling Site	C1	C2
Corchia Cave (CC)	840	1240	1460
Grotta Del Vento (GDV)	670	650	1230
Tana Che Urla (TCU)	640	650	1250
Renella (REN)	275	340	1045

Elevation of sampling sites in the cave (column B); the elevations of surface above the sampling site (C1); mean elevation values between the surface above sampling site and the maximum elevation of the basin (C2). All values are in metres a.s.l.